SHRP-A-649

Fluorometric Characterization of Asphalts

Gareth Mitchell
Alan Davis

Coal and Organic Petrology Laboratories
The Pennsylvania State University

Strategic Highway Research Program
National Research Council
Washington, DC 1993

SHRP–A–649
Contract AIIR-04

Program Manager: *Edward T. Harrigan*
Project Manager: *Jack Youtcheff*
Production Editor: *Cara J. Tate*
Program Area Secretary: *Juliet Narsiah*

June 1993

key words:
asphalt binders
asphalt oxidation
fluorescence intensity
fluorescence microscopy
fluorescence spectra
in-situ asphalt characterization

Strategic Highway Research Program
National Academy of Sciences
2101 Constitution Avenue N.W.
Washington, DC 20418

(202) 334-3774

350/NAP/693

Acknowledgments

The research described herein was supported by the Strategic Highway Research Program (SHRP). SHRP is a unit of the National Research Council that was authorized by section 128 of the Surface Transportation and Uniform Relocation Assistance Act of 1987.

TABLE OF CONTENTS

LIST OF TABLES

LIST OF TABLES (continued)

LIST OF FIGURES

LIST OF FIGURES (continued)

LIST OF FIGURES (continued)

ABSTRACT

Fluorescence microphotometry was evaluated as a technique for characterizing asphalt binder quality and the deterioration of asphalt cements. The technique employed optical microscopy to differentiate asphalt binder from aggregate materials in asphalt pavements, thereby eliminating the need to solvent extract the binder for evaluation. It may also obviate the possibility of solvent interaction or interference with the physical and chemical properties of asphalt binders that have developed in service.

In this research effort new techniques for the uniform measurement of fluorescence intensity and spectra were developed and applied to the characterization of thirteen raw asphalts. Analytical techniques and some of the factors which influence asphalt fluorescence were considered. With this small sample set, relationships were found between fluorescence intensity values and viscosity as measured in original and laboratory-aged asphalts. As viscosity increased, the fluorescence intensity decreased, a relationship thought to be due to the dependence of both these properties upon oxidation and/or molecular structuring. Fluorescence intensity also decreased significantly upon the mixing of aggregate materials with asphalt, the magnitude of the change being influenced more by the asphalt binder than the aggregate. As observed for raw asphalts, the fluorescence intensity of asphalt binders in contact with different aggregate materials decreased with curing/aging time.

Results of this investigation have demonstrated that fluorometric measurement of asphalt intensity has a great potential for use in monitoring asphalt oxidation occurring at the hot-mix plant and during lay-down, as well as a technique to monitor the deterioration of asphalt pavements that are in service.

EXECUTIVE SUMMARY

The objective of this research effort was the development of simple quantitative fluorescence microphotometric techniques for the measurement of asphalt quality and deterioration. Ideally, these techniques would allow us to probe those aspects of the molecular structure of asphalts bearing directly on performance characteristics such as rheology, viscosity, durability, oxidation and response to UV irradiation. The tasks involved were to develop simple means of preparing samples; the development of procedures for measuring characteristic fluorescence emissions (at selected wavelengths as well as complete spectra) which are both reproducible and significant in terms of asphalt chemistry and behavior; and to apply these techniques to the characterization of raw asphalts and asphalt-aggregate mixtures.

During the course of this research project, we have developed a simple, reproducible, empirical microphotometric fluorescence technique for the characterization of raw asphalts and asphalt/aggregate mixtures. Using this technique, thirteen SHRP asphalts were evaluated along with twelve asphalt chemical fractions from ion-exchange chromatography (IEC) and size-exclusion chromatography (SEC). The influence of storage, handling, laboratory oxidation, and aggregates on asphalt fluorescence properties have been studied. Results from these investigations demonstrate that fluorometric analysis can be employed to monitor asphalt quality, the effects of plant processing, oxidation/aging and setting characteristics of raw asphalts as well as asphalt binders in asphalt/aggregate mixtures.

Initial work performed under this project resulted in the development of a standard fluorometric technique capable of providing mean fluorescence intensity values that are unique for individual asphalts. The technique employed blue-light excitation (390-490 nm) generated from a xenon irradiation source and measured the intensity of fluorescence emissions (at 600 nm) calibrated against a uranyl glass standard. To prevent photo-oxidation, it was found that these measurements had to be made under a dry nitrogen atmosphere. Under these conditions, repeatability was determined to be less than 0.1%.

From a preliminary evaluation of fluorescence intensity with the initial physical and chemical properties of our set of asphalts, a weak correlation with viscosity (at 140°F) was observed, namely, as viscosity increased fluorescence intensity decreased. This relationship was independently supported from two sets of observations made from asphalt samples that had been oxidized or aged. First, a comparison of three asphalts from the same petroleum source (AAA-1, AAA-2 and AAE) but which were manufactured differently, showed that by air-blowing an asphalt (AAE) fluorescence intensity was significantly reduced. Air-blowing is a technique used to stiffen an asphalt, and is

generally accompanied by a rather large increase in viscosity as well as volatile loss and, presumably, oxidation. Second, laboratory aging of asphalts to different levels of severity and resulting in the formation of sulfoxide and carbonyl groups was accompanied by large increases in viscosity. We also observed a steady decrease in fluorescence intensity with this progressive oxidation.

The relationship between fluorescence intensity and asphalt viscosity may not represent a direct cause-and-effect relationship, but may be due to the fact that the chemical changes occurring as a result of asphalt oxidation or structuring influence both measurements. For example, during our investigations we found that measurement of fluorescence emissions in air resulted in the photochemical oxidation of the asphalt surface which in turn significantly reduced fluorescence intensity. However, surficial oxidation may not be exclusively responsible for these effects. Studies were undertaken to compare the fluorescence properties of asphalts exposed to room conditions (but protected from light) with those stored under argon in a refrigerator over the same time period. When the surface layer of asphalt exposed to the atmosphere was removed, the new surface also showed a large and progressive decrease in intensity with time. In most cases asphalt samples that had been stored in argon under refrigeration showed no change in fluorescence intensity. However, in one case an asphalt (AAH) was found to be susceptible to structuring at low temperature (-5°C). These results clearly showed that chemical structuring may influence asphalt fluorescence just as dramatically as oxidation.

Another goal of this project was the use of spectral fluorescence to study the raw and aged asphalt samples previously discussed as well as being employed in studies of asphalt chemical fractions and asphalt/aggregate mixtures (mastics). Spectral fluorescence was performed using a microscope system similar to that used in fluorometric analysis. Asphalt samples were irradiated with blue light (390-490 nm) using a mercury-arc source. Fluorescence emissions were directed through the same optical train used in fluorometric analysis to a double-grating monochromator and a photomultiplier having a broader and more consistent range of responsivity (250-850 nm). However, we relinquished our ability to measure accurate intensity values for a better measurement of spectral distribution. Thus, using this technique the relative intensities within the wavelength range from ≈510 - ≈760 nm were measured.

Spectral analysis of raw asphalts showed that most (90%) had broad and fairly uniform emissions between ≈510 and ≈760 nm when irradiated with blue light. About 70% of the asphalts had peak fluorescence values between 664 nm and 672 nm, whereas the other 30% had peak values at lower wavelengths (544 - 640 nm).

The effects of asphalt oxidation resulting from manufacturing upon spectral distribution were found to be very

similar to those due to laboratory aging. In both cases a narrowing of the distribution was observed in comparison to the parent asphalt spectra. Upon severe laboratory aging, three of the four asphalts tested showed a decrease (blue shift) in the peak wavelength.

To shed some light on the chemical changes which may be occurring to the fluorophoric centers during asphalt oxidation and aging, chromatographic fractions separated by polarity and by molecular size from three different asphalts were characterized. Those fractions which possessed greater concentrations of heteroatoms and having greater molecular weights and higher aromaticity demonstrated lower fluorescence intensities at 600 nm by one or two orders of magnitude. Thus, as the molecular weight and aromaticity of the IEC neutrals fraction increased between AAD-1 and AAG-1, fluorescence intensities were relatively high and the spectral distributions were similar. However, when the neutral fractions became dominated by aromatic compounds of high molecular weight (AAM-1), fluorescence intensity decreased and the peak wavelength shifted toward the red. When the asphalt fraction also included a fairly high concentration of heteroatoms and polar centers (SEC I, non-fluorescing fraction), fluorescence intensity was again reduced, but here the peak wavelength shifted toward the blue. From this, quenching mechanisms associated with a condensed molecular structure were assumed to be responsible for lower fluorescence intensity, and that the polar centers may provide a dominant fluorescence at lower wavelength. These observations appeared to be consistent with what was observed during asphalt oxidation/aging, in that an increase in polar centers resulted in a decrease in fluorescence intensity and in peak wavelength.

An additional objective was to investigate the influence of aggregate materials on asphalt binder fluorescence. The study of asphalt/aggregate mixtures was accomplished by evaluating mastics prepared from four aggregates (-74 μm) in combination with four asphalts. Findings from our study of mastics showed that there was a very rapid decrease in fluorescence intensity and a narrowing of the spectral distribution upon mixing asphalt with aggregate. Additional curing/aging time of the mastic samples when exposed to room conditions (protected from light) resulted in a further significant decrease in intensity. However, we were unable to detect any significant influence on asphalt fluorescence due to the presence of various aggregates. Instead, the specific asphalt used appeared to exert a greater influence on the final fluorescence properties of the mastic binder. No consistent results were observed from measurement of spectral distribution; with the addition of aggregate, peak wavelength decreased for two of the mastic sets and increased for the other two sets, again suggesting that it was the properties of the asphalt that controls fluorescence properties of the mastic and not the aggregate materials.

DEVELOPMENT OF FLUOROMETRIC TECHNIQUES

Introduction

The problem being addressed in this research concerned the need for an effective means of characterizing asphalt binder quality and deterioration, for both the raw product as well as cores from in situ cements and pavements. Current techniques used in the paving industry for measuring pavement deterioration first require that the asphalt binder be recovered by solvent extraction (1). Although asphalts can be effectively recovered, the technique may disrupt the molecular structuring developed during aging and which may be largely responsible for changes in their physical and chemical properties (2). Therefore, fluorescence microphotometry has been investigated as a non-destructive quantitative technique that may provide sensitive indices of the molecular structures of asphalts and which could be informative concerning their thermoplastic behavior and aging susceptibility.

The research presented in this section describes the initial development of the technique employed, the fluorometric characteristics of raw asphalts and some preliminary findings regarding the deterioration of asphalt fluorescence during storage and laboratory aging tests. All of this information has been reported previously (3-6), but is recounted here to provide a comprehensive final report.

Background

Fluorescence microphotometry, as employed in this investigation, is a technique that utilizes an optical microscope photometric system to measure the intensity of fluorescence emissions from fluorophoric materials (7). Fluorescence is the result of a rapid emission of light energy as excited electrons of an atom or molecule return to the ground state following their promotion to higher energy orbitals by absorption of light energy; the energy difference between the two states is related directly by the Einstein-Planck equation. Fluorescence emissions occur within about 10^{-9} seconds after excitation because of a variety of radiationless internal energy transfers, including re-absorption of emitted energy, formation of excimers, interaction of molecules of the same species, or interaction with molecular oxygen. Because of internal conversion, during which part of the absorbed energy is dissipated, fluorescence emission spectra occur at longer wavelengths than the excitation spectra.

Examples of the types of organic compounds or functional groups that have the potential to fluoresce (i.e., fluorophors) are those containing π-electrons (most aromatic compounds and conjugated aliphatic polyenes) and those containing heteroatoms of oxygen (carbonyl groups associated with carboxylic acids,

ketones and aldehydes) and nitrogen (particularly amines like quinoline). All of these groups are contained in varying concentrations in asphalts. Their relative concentrations and the way in which they interact to form a structured molecular network upon aging will influence the measured intensity of fluorescence emissions. Other factors which may effect the fluorescence properties of asphalts include oxidation and loss by volatilization of low molecular weight saturates so that the relative concentration of the remaining fluorophoric materials is changed.

Experimental

A Leitz MPV-II microscope photometer forms the basis of the system used in this investigation. Light energy from either an ultra-high pressure mercury-arc or xenon lamp was passed through a heat filter (suppressing red and infrared wavelengths) and then through a series of interference filters which defined the appropriate excitation and measuring wavelengths. The filter combination selected provided an excitation wavelength between 390-490 nm, or blue-light irradiation. The excitation light was reflected by a 510 nm reflection short-pass dichromatic beam splitter and condensed onto the sample through a 50X NPL FLUOTAR air objective. The total magnification of the optical system was 625 times. Part of the absorbed excitation energy was released as fluorescence emission, which was of longer wavelength than the absorbed light. Fluorescence emission (and part of the reflected excitation light) passed back through the dichromatic beam splitter; a 515 nm long-pass barrier filter blocked any reflected low-wavelength light. The light then passed through the measurement filter which was centered around 600 nm (570-630 nm). The optical signal(s) were transformed into electronic signals by an EMI 9558 photomultiplier and amplified (further details given in Appendix A).

For this initial study, twelve asphalts were obtained from the Materials Reference Library (MRL, 8). Some of the chemical and physical properties of these asphalts, as provided by MRL, are given in Table 1. Following the recommended protocol, asphalts were divided into subsamples suitable for microscopy. Each asphalt was heated in a controlled atmosphere oven in a flow of air at 137°C for 2h. Although a number of different types of subsamples were prepared, the plug-mount sample shown in Figure 1 was favored for microscopy. This sample type was prepared from a 2.5 cm diameter and 2.5 cm high clear epoxy-based cylinder which had both ends cut, ground and polished to form flat, level surfaces. A 0.95 cm diameter by 1.9 cm deep hole was drilled into one end which was then filled with ≈1.5 g of hot asphalt. About 30 plug mounts were made for each asphalt. Following a cool-down period (1h), one such preparation was analyzed and then the remaining subsamples were sealed in multilaminate foil bags in an argon atmosphere and refrigerated at -5°C.

Table 1. Summary of Properties of Materials Reference Library Asphalts

Test	Asphalt Codes												
	AAA-1	AAA-2	AAB-1	AAC-1	AAD-1	AAE	AAF-1	ABD	AAG-1	AAH	AAJ	AAK-1	AAM-1
Asphalt Grade	150/200	200/300	AC-10	AC-8	AR-4000	150/200	AC-20	AR-4000	AR-4000	--	--	AC-30	AC-20
ORIGINAL ASPHALT													
Viscosity													
140°F, poise	864	363	1029	419	1055	3634	1872	2112	1862	1058	1765	3256	1992
275°F, cSt	283	189	289	179	309	560	327	241	243	298	415	562	569
Penetration, 0.1 mm													
(77°F, 100 g, 5s)	160	291	98	133	135	73	55	47	53	95	67	70	64
(39.2°F, 100 g, 5s)	15	27	6	7	9	7	0	1	2	7	0	2	4
Ductility													
39.2°F, 1 cm/min, cm	150+	150+	40.1	137.0	150+	32.5	7.6	0	0	18.8	14.7	27.8	4.6
Softening Point, °F	112	102	118	109	118	125	122	120	120	114	118	121	125
Component Analysis, %													
Asphaltenes	18.3	16.2	18.2	11.0	23.0	23.7	14.7	7.0	5.8	16.2	11.1	21.1	3.9
Polar Aromatics	37.3	36.0	38.3	37.4	41.3	30.5	38.3	52.7	51.2	41.4	41.5	41.8	50.3
Naphthene Aromatics	31.8	36.1	33.4	37.1	25.1	31.6	37.7	28.4	32.5	28.6	35.9	30.0	41.9
Saturates	10.6	11.4	8.6	12.9	8.6	12.7	9.6	10.4	8.5	13.5	10.9	5.1	1.9
Elemental Analysis													
Nitrogen, %	0.50	0.50	0.50	0.42	0.90	0.39	0.23	1.05	1.10	0.48	0.51	0.80	0.50
Sulfur, %	7.30	6.00	5.60	2.74	8.60	7.89	4.52	1.45	2.00	5.85	3.69	6.60	2.40
Vanadium, ppm	158	138	186	71	293	129	68	63	32	80	133	1427	60
Nickel, ppm	78	77	45	40	145	47	27	164	71	32	43	128	29
THIN FILM OVEN TEST													
Mass change, %	-0.3115	-0.5370	-0.0362	-0.2590	-0.8102	-0.2888	-0.0921	-0.1208	-0.1799	-0.4524	+0.0260	-0.5483	+0.0516
Viscosity													
140°F, poise	1901	869	2380	1014	3420	11589	4579	3800	3253	2809	4021	9708	3947
275°F, cst	393	270	393	239	511	914	472	321	304	441	550	930	744
Viscosity Ratio (140°F)	2.20	2.39	2.31	2.42	3.24	3.19	2.45	1.79	1.75	2.66	2.28	2.98	1.98
Identification	Loydminster	Loydminster	Wyoming High Sulfur	Redwater	California Coastal	Loydminster (Air Blown)	West Texas Sour	California Valley	California Valley w/Lime	Rangely	Oklahoma Mix (SDA)*	Boscan	West Texas Intermediate (SDA)

*SDA = Solvent de-asphalted

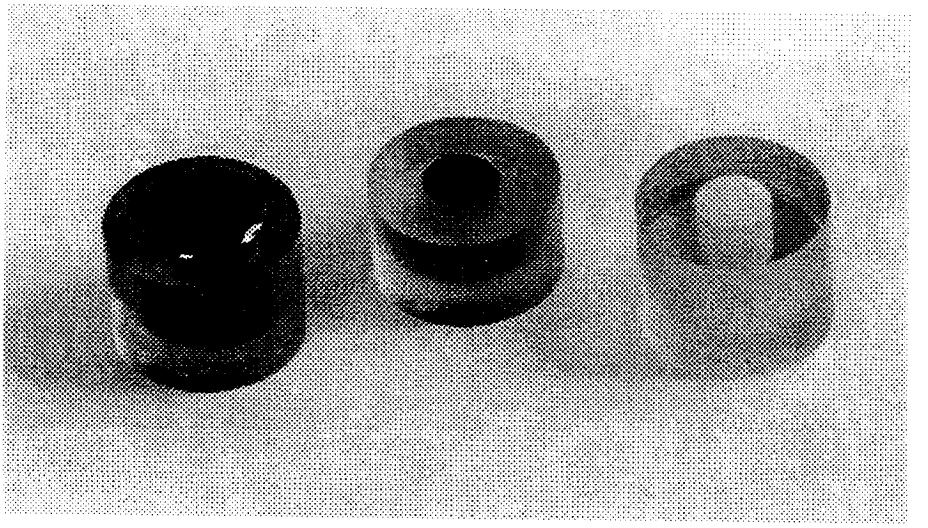

Figure 1. Plug Mount Samples before (right) and after (left) Filling with Asphalt and a Cut Surface Used for Microscopy (center)

Two different fluorometric measurements were performed on each asphalt, one to determine the mean fluorescence intensity and the other to determine the alteration of fluorescence intensity with increasing irradiation time. Measurements of fluorescence intensity were performed by first standardizing the photoelectric system using a masked uranyl glass plate (area of fluorescence ≈115 μm^2) and adjusting the digital photomultiplier reading to an arbitrary 1.000% ±0.002. A limiting aperture of 8 μm diameter was used to provide an effective measuring area of ≈50 μm^2 to the photomultiplier. An asphalt surface was brought into focus using white-light illumination, then, while all light was blocked from the surface, the appropriate filters and the illumination source (mercury-arc or xenon) were positioned in the light path. At the precise time that irradiation of the sample commenced, a fluorescence intensity reading was recorded. This procedure was repeated on unexposed areas of asphalt until a statistically significant number of readings were taken. The mean fluorescence intensity of 50 readings was found to be sufficient when measurements were made in air, whereas 10 readings were sufficient when intensity was measured in a nitrogen atmosphere (see below).

Alteration of fluorescence intensity occurs with most organic materials and may be represented by a change of fluorescence emission occurring as the time of exposure to the excitation source increases. Following system standardization, alteration was measured by taking photometric readings at regular intervals during a period of constant irradiation. For asphalts, alteration patterns were determined by recording intensity readings every 6 sec over a period of 2 min. During long exposures the asphalt surface becomes pitted, discolored and deformed when irradiated in air. To reduce this affect, the field diaphragm of the optical microscope should be reduced to the lowest effective diameter (≈50 μm), thereby limiting the amount of light energy affecting the surface. However, we found that these surface alterations could be eliminated by irradiating asphalts in a nitrogen atmosphere. To do this, a latex sleeve was attached between the microscope objective and the sample; fine-diameter plastic tubing was used as an inlet for nitrogen and a hole on the opposite side allowed excess nitrogen to escape (9). The chamber was purged with nitrogen for at least 5 min before analysis.

To investigate the influence of asphalt structuring and oxidative deterioration on fluorescence properties, a number of sets of plug-mount samples for three asphalts (AAH, AAB-1 and AAA-1) were exposed to air at room conditions (but protected from light) and compared with samples refrigerated under argon. Fluorometric analyses of exposed and refrigerated samples were conducted at random time intervals in an effort to separate the effects of molecular structuring from that of oxidation.

To study the influence of oxidation on fluorometric properties thin-film oven test (TFOT) residues (asphalts heated

for 5h at 163°C in air) and TFOT residues subjected to additional aging for 400h at 60°C in air at 300 psig (TFOT-PAV) were obtained from Western Research Institute (Dr. J. Branthaver). In addition, several TFOT residues were generated in our laboratory both in a sweep of air as well as in nitrogen. These studies were designed to separate the affects of oxidation from other processes that may occur during heating of an asphalt that could lead to "aging" or increased viscosity.

Results and Discussion

The alteration of fluorescence intensity with irradiation time and mean fluorescence intensity values were generated under four test conditions using mercury-arc or xenon illumination and air or nitrogen atmospheres. Using the information in Table 1, twelve asphalts were selected for study based upon the distribution of chemical fractions that might contribute to their fluorescence properties. [Asphalt ABD was not used in this initial investigation, but has been included in Table 1 for reference elsewhere in this report.] Groups of asphalts were chosen with high (50%), medium (40%) and low (30%) polar aromatic contents. Within each group, further selections were based upon asphaltene and heteroatom concentrations.

Fluorescence Alteration of Asphalts

The alteration of fluorescence intensity with time of exposure to the excitation source was studied as a means of characterizing asphalt deterioration due to oxidation. Our experience with the fluorescence alteration of coals has shown that patterns of alteration were characteristic and unique (9). For example, as coal rank increases from lignite through high volatile to medium volatile bituminous, the pattern of alteration undergoes change. For lignites, fluorescence alteration steadily increases with time of irradiation (positive), whereas for high volatile coals alteration shows a dual response, i.e., first decreasing then increasing. As coal rank increases through the high volatile rank range, the time required to reach a minimum value increases. For medium volatile coals, alteration remains negative through an extended period of irradiation. The alteration patterns for freshly mined coals, therefore, are seen to be characteristic of coal rank. However, when coal becomes weathered or oxidized and loses its thermoplastic properties, its pattern of alteration changes; coals giving a dual alteration pattern when fresh develop a positive alteration. On the basis of coal behavior, it was hypothesized that when asphalts become weathered and oxidized they too might demonstrate significant and characteristic changes in their patterns of alteration.

Fluorescence alteration tests were conducted on all asphalts shortly after heating using the mercury-arc and xenon illumination systems. Figures 2 and 3 summarize the alteration

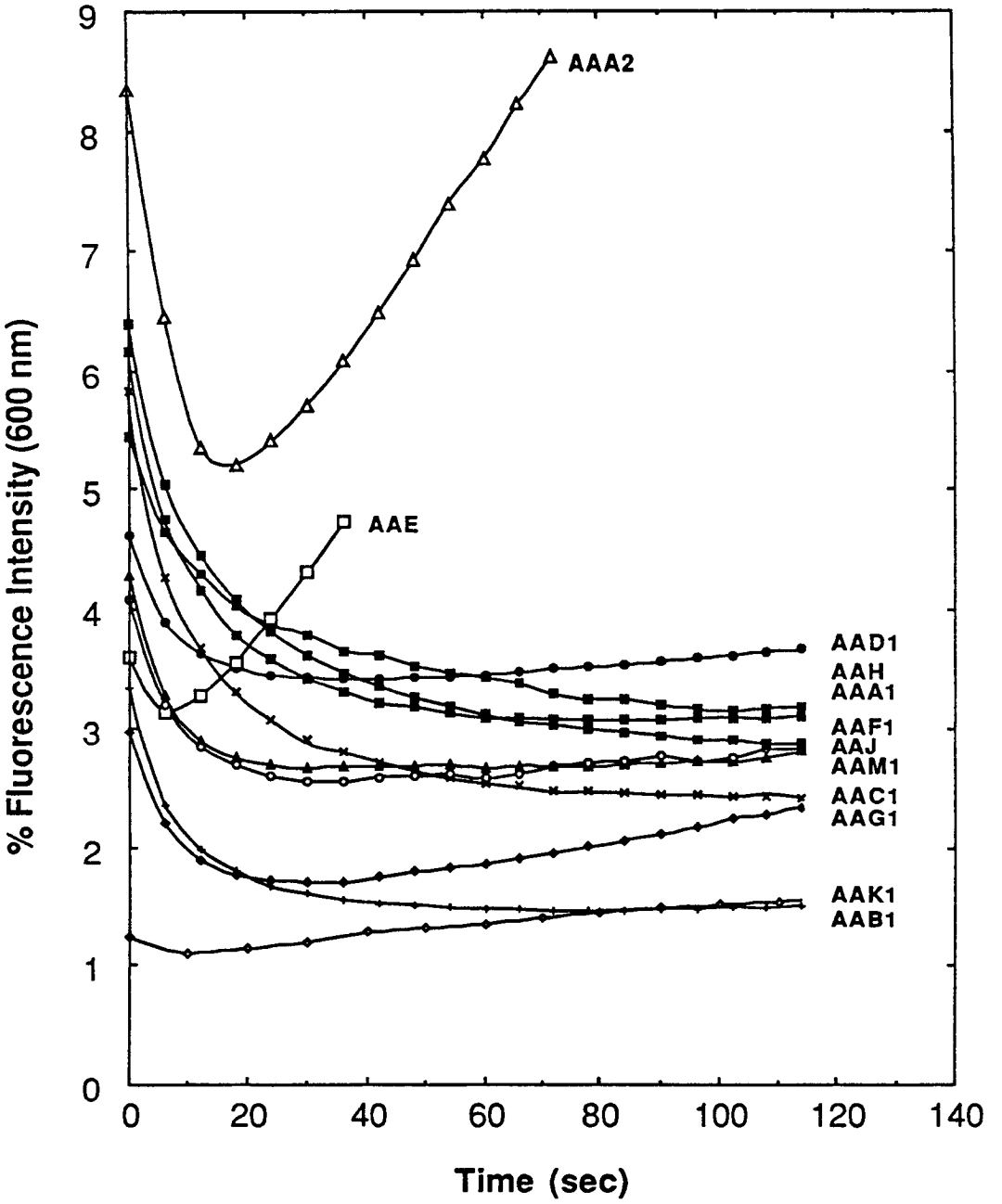

Figure 2. Comparison of Fluorescence Alteration Patterns of Different Asphalts in Air Using Mercury-Arc Illumination

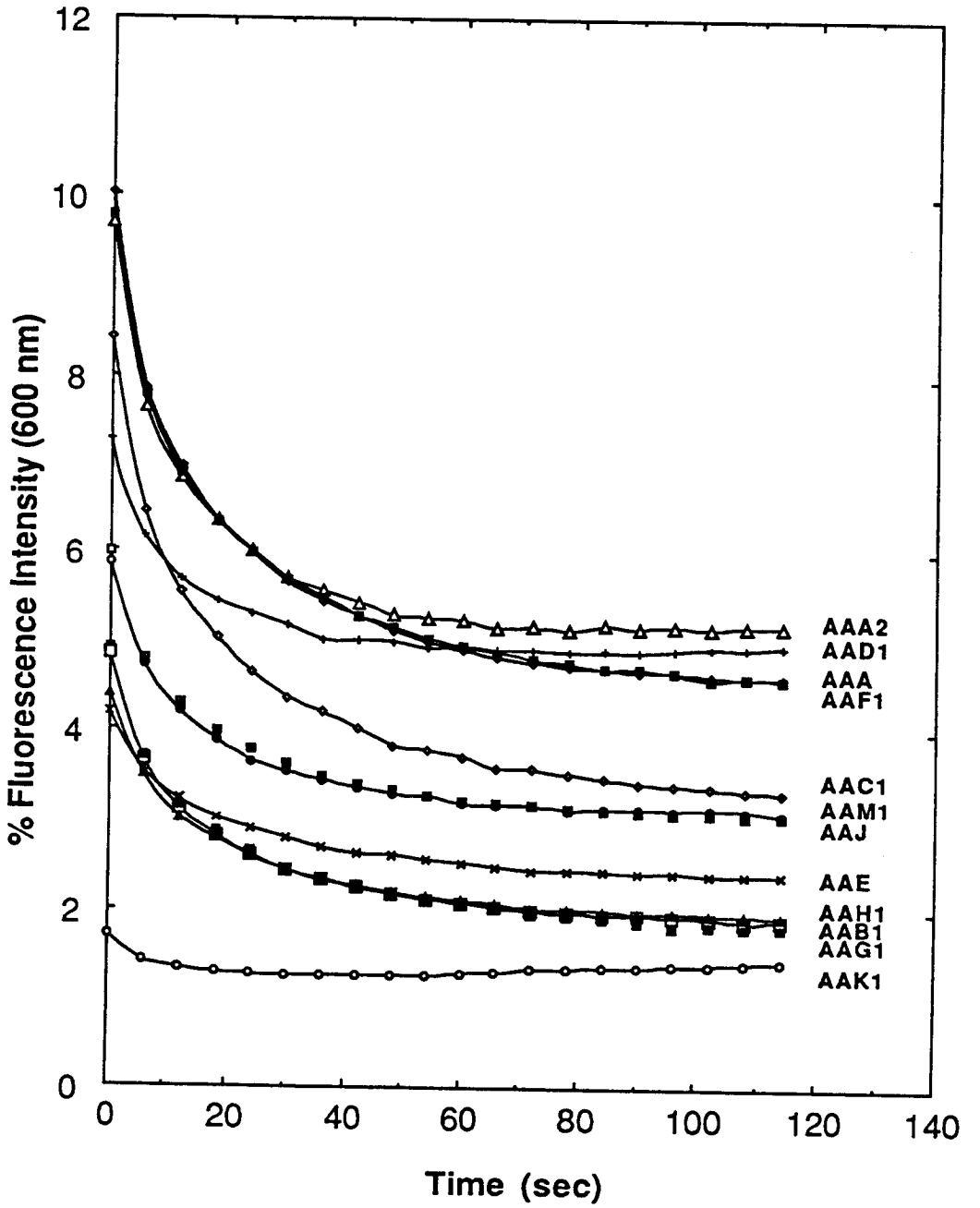

Figure 3. Comparison of Fluorescence Alteration Patterns of Different Asphalts in Air Using Xenon Illumination

patterns derived from 12 asphalts measured in air using the different excitation sources. The graphs clearly show the dual alteration observed for the mercury arc compared with the negative alteration obtained with the xenon system. The major difference between these illumination systems that may account for different alteration patterns was the absolute output of the excitation energy. Comparison of the spectral radiance of the two lamps given by Oriel Corporation (10) showed that there can be more than a two-fold difference in the 390 - 490 nm region (5.0-82.0 microwatts/cm^2-nm for mercury-arc versus 0.9-2.05 microwatts/cm^2-nm for xenon). These spectral differences alone do not translate into a large thermal output from either system. However, qualitative observation of interaction of the fluorescent beam with asphalt demonstrated that the mercury-arc system leads to far greater deformation (melting) than the xenon system when measurements were made in air.

The dual alteration patterns observed for asphalts when irradiation was performed in air using the mercury-arc system were more informative than when using xenon. As shown in Figure 2, the negative and positive components of each asphalt were different. Some have a small negative component that continued for less than 20 sec (AAE, AAA-2, AAK-1), whereas others required more time for intensity to rebound. The rates of increase of the positive component were similar for all of the asphalts except in the case of the AAE and AAA-2 asphalts. These asphalt samples were from the same petroleum source; AAA-2 was the raw asphalt, whereas AAE was air blown during its manufacture. The chemical effect of air blowing the AAA-2 asphalt was a reduction in polar (5.5%) and naphthenic (4.5%) aromatics and an increase in asphaltenes (7.5%) and saturates (1.3%) fractions in the AAE asphalt (Table 1). The change in concentration of these chemical fractions, the potential loss of volatiles, and partial oxidation of the asphalt during air blowing not only reduced fluorescence intensity but also diminished the negative component of the alteration pattern.

As illustrated in Figure 4, irradiation of asphalt in an inert atmosphere basically eliminated alteration of the fluorescence emission; the physical pitting of the asphalt surface was also diminished. However, when air was subsequently introduced to the surface there was an immediate alteration that mimicked the original alteration pattern obtained in air (see Figure 2). Figure 4 shows very effectively that it was not the thermal energy from the excitation source that was responsible for the alteration, but the presence of molecular oxygen. The alteration patterns for eight of the asphalts in nitrogen are given in Figure 5 and show that after the first 10 sec fluorescence emissions become relatively stable. Note also that the initial fluorescence intensities (at time zero) were mostly higher for each asphalt than when measured in air (compare Figures 2 and 5).

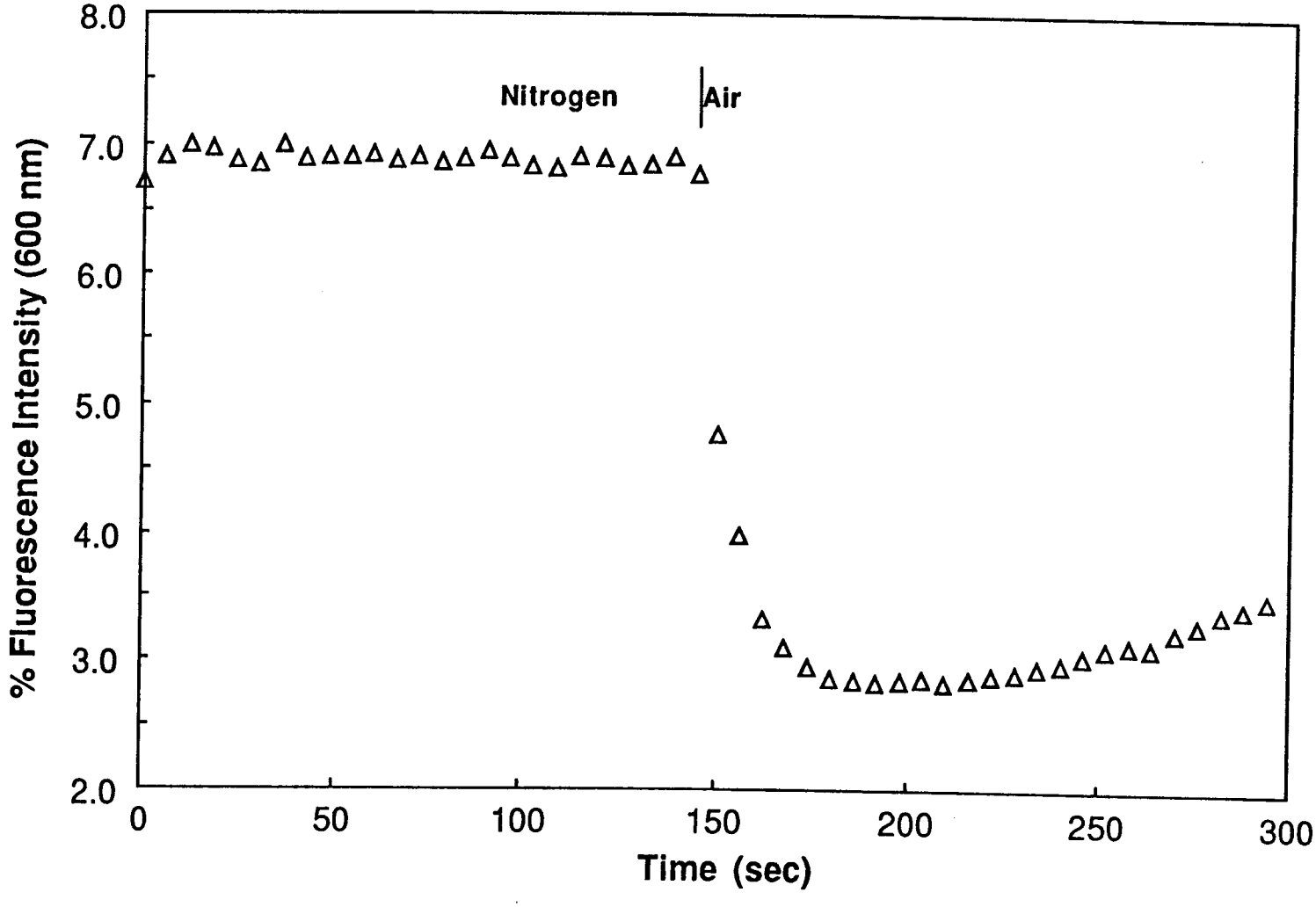

Figure 4. Fluorescence Alteration of the AAM-1 Asphalt Sequentially in Nitrogen and Air Atmospheres Using Mercury-Arc Illumination

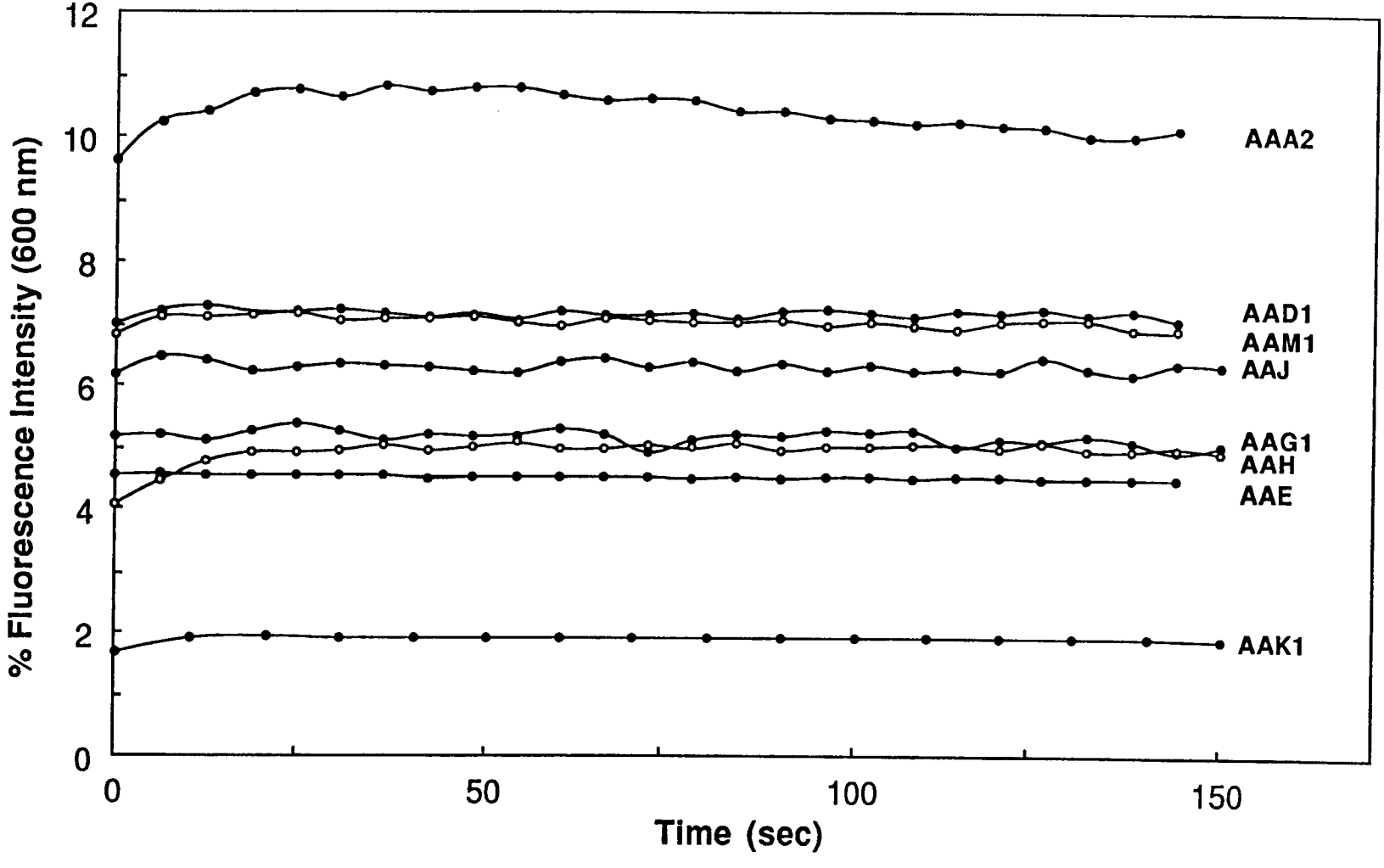

Figure 5. Fluorescence Alteration of Asphalt in Nitrogen Atmosphere Using Mercury-Arc Illumination

The uniformity of fluorescence emissions when measured in an inert atmosphere means that we have established a technique to generate precise intensity values. However, it is important to observe that the photochemical alteration effect may be valuable in providing interpretable information regarding asphalt chemistries. As seen with the AAA-2 - AAE asphalt pair (Figure 2) there are significant differences in the fluorescence intensities and in the photo-oxidation properties of these asphalts that can be directly related to their manufacture and petroleum source.

Fluorescence Intensity

The mean fluorescence intensity values determined using the four test conditions (xenon-air, xenon-N_2, mercury arc-air and mercury arc-N_2) are given in Table 2. With respect to each analytical method, in all but one case (AAH) intensity was highest when measured with the xenon source under nitrogen. Following this, progression from highest to lowest fluorescence intensity was about evenly split between xenon-N_2 > xenon-air > Hg-N_2 > Hg-air (AAA-1, AAB-1, AAC-1, AAF-1 and AAM-1) and xenon-N_2 > Hg-N_2 > xenon-air > Hg-air (AAA-2, AAD-1, AAE, AAG-1, AAJ and AAK-1). Some of the values given in Table 2 were obtained from samples refrigerated in argon (AAH, AAK-1, AAA-2 and AAM-1) and, therefore may not accurately represent the values that would have been obtained immediately after heating. For example, values reported for the AAH asphalt will be shown later to have changed significantly during storage.

A correlation coefficient matrix was generated among fluorescence intensities determined in nitrogen using both excitation sources and all of the original asphalt properties listed in Table 1. This exercise indicated that there may be a relationship between fluorescence intensity values and asphalt viscosity (Figure 6). Some of the scatter in the xenon data could have resulted from the delay in performing fluorometric measurements in nitrogen. No other significant correlations were observed with this data set.

Storage Deterioration of Asphalts

Molecular structuring may be partially responsible for the flow behavior of asphalts and is a phenomenon that develops slowly (over days or years) at ambient temperature and that can be reversed by heating (2). With this in mind, a study was undertaken to determine whether asphalt fluorescence intensity might change with the type and duration of storage being employed in this investigation. Using the AAH asphalt, a special series of plug mounts were prepared for microscopy shortly after heating. Half of these samples were refrigerated under argon and the other half were exposed to air at room temperature, but protected from light. Figure 7 shows that during 33 days of

Table 2. Fluorescence Intensity of Asphalts Measured at 600 nm

Asphalt Codes	Irradiation Source and Atmosphere			
	Xenon Air	Xenon N_2	Mercury-Arc Air	Mercury-Arc N_2
AAA-1	10.21	11.49	6.35	8.06
AAA-2	9.53	11.51*	8.27	10.43
AAB-1	5.09	6.50	3.16	4.64
AAC-1	8.65	10.74	5.72	8.00
AAD-1	7.00	10.06	4.61	7.20
AAE	4.05	4.94	3.76	4.44
AAF-1	10.40	11.58	6.77	8.26
AAG-1	4.93	5.83	3.00	5.19
AAH	4.99*	5.01*	5.23	5.30
AAJ	5.62	7.25	4.03	6.32
AAK-1	1.76*	2.20*	1.32	1.94
AAM-1	7.05	7.20*	4.04	6.92

*Analyses performed on samples refrigerated under argon; all remaining analyses performed immediately after heating.

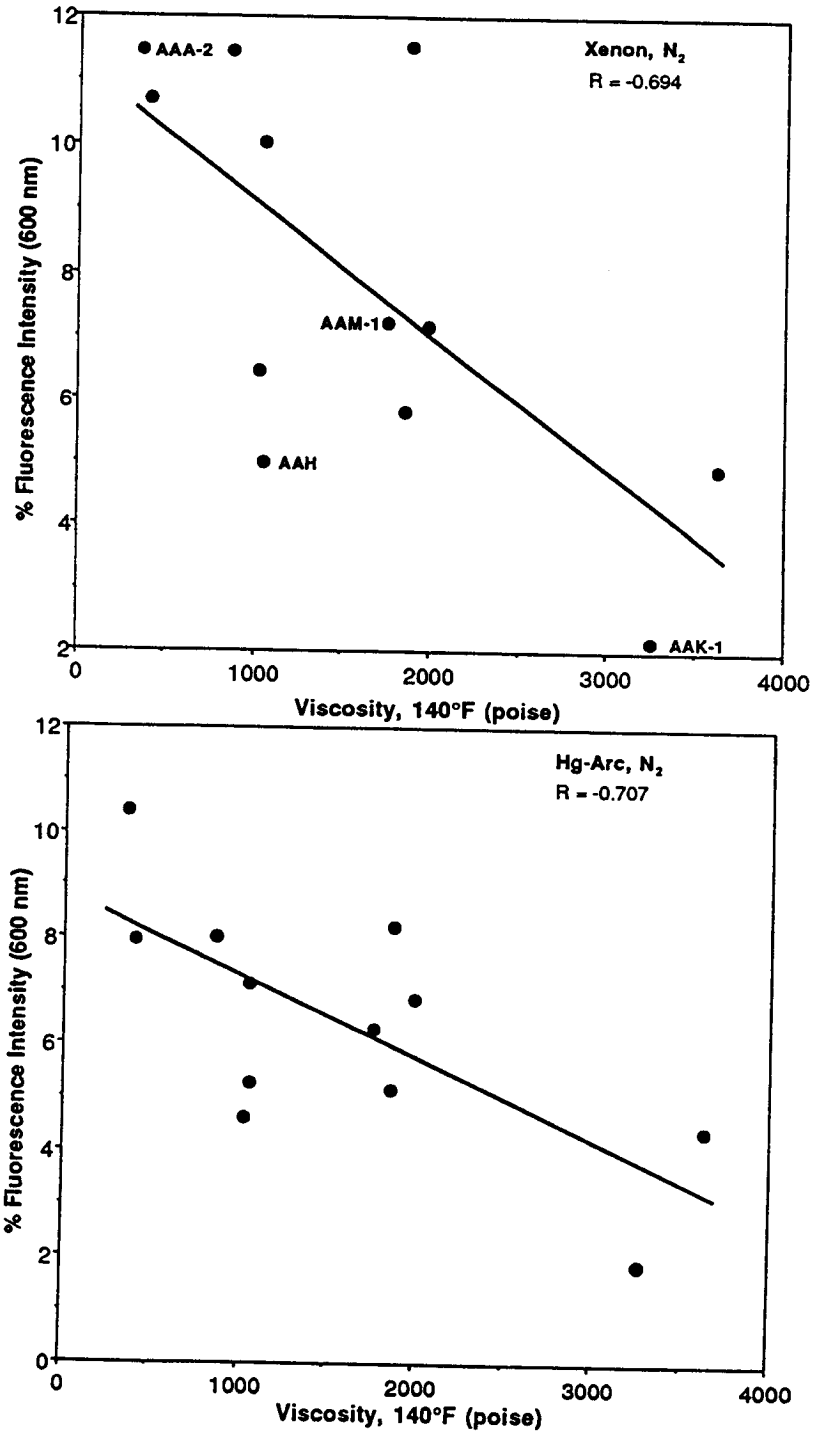

Figure 6. Relationship between Fluorescence Intensity and Original Viscosity of Asphalts Measured in Nitrogen Using Xenon and Mercury-Arc Illumination

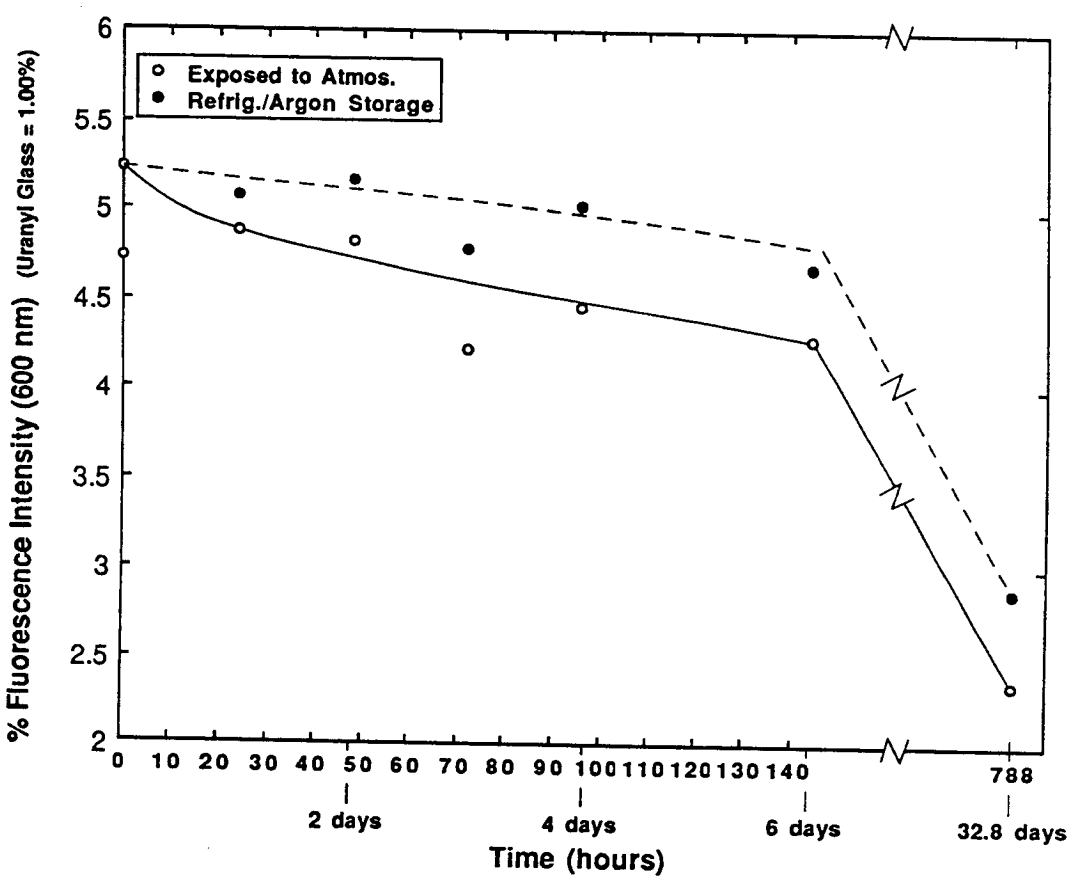

Figure 7. Change of Fluorescence Intensity as Measured in Air with Mercury-Arc Illumination with Duration of Storage of AAH Asphalt

storage there was a progressive decrease in fluorescence intensity which appeared to be slightly greater for exposed samples than for those stored in a refrigerator under an inert atmosphere. A further analysis of the exposed and refrigerated AAH asphalt after 149 days of storage showed no additional decrease in fluorescence intensity (i.e., 2.71% vs 3.29%, respectively). The difference in intensity observed between refrigerated (argon) and exposed (air) samples probably resulted from surface oxidation, whereas the progressive decrease in intensity with time may result from molecular structuring. This suggests that molecular structuring more strongly affects fluorescence emissions than short-term oxidation for the AAH asphalt. It also implies that fluorescence intensity may be a sensitive measure of the processes that cause molecular structuring of asphalts.

Alteration patterns were also generated during the study of the influence of duration of storage upon fluorescence characteristics using mercury-arc illumination in air. Figure 8 demonstrates that as storage time of the AAH asphalt increased, fluorescence alteration became more dual and the time to reach a minimum decreased. After 3570h (149 days) of exposure the alteration pattern resembled the initial analysis (init), but at a much lower fluorescence intensity. These tests were performed on asphalt which had been exposed to air at room temperature, but similar results (not shown) were found for those asphalt samples refrigerated in argon. These results suggest that the propensity for photochemical oxidation during blue-light irradiation may have changed as a result of molecular ordering within the surface layers of asphalt rather than from chemical oxidation.

As a further test of storage deterioration, fluorometric analyses of two additional asphalts (AAB-1 and AAA-1) were performed using the four analytical conditions. This effort was initiated to determine if other asphalts structure and/or oxidize in a manner similar to the AAH asphalt. Tables 3 and 4 provide fluorescence intensity values generated with time for the AAB-1 and AAA-1 asphalts, respectively. Considering the intensity values determined using the xenon excitation source in nitrogen, little change was observed after 2784h (AAB-1) or 1656h (AAA-1) refrigerated storage in argon compared with the initial values. However, in each case a significant decrease in intensity occurred following the same period of exposure under room conditions. Because all analyses were performed on freshly cut surfaces (where about 0.5 mm of asphalt was removed with a razor blade), we believe that the influence of surface oxidation or skin development were removed. Therefore, the implication being that molecular structuring occurred at higher temperatures (e.g. > -5°C) for the AAB-1 and AAA-1 asphalts than was observed for AAH.

Another important observation can be made from Tables 3 and 4 regarding the analytical techniques employing the different

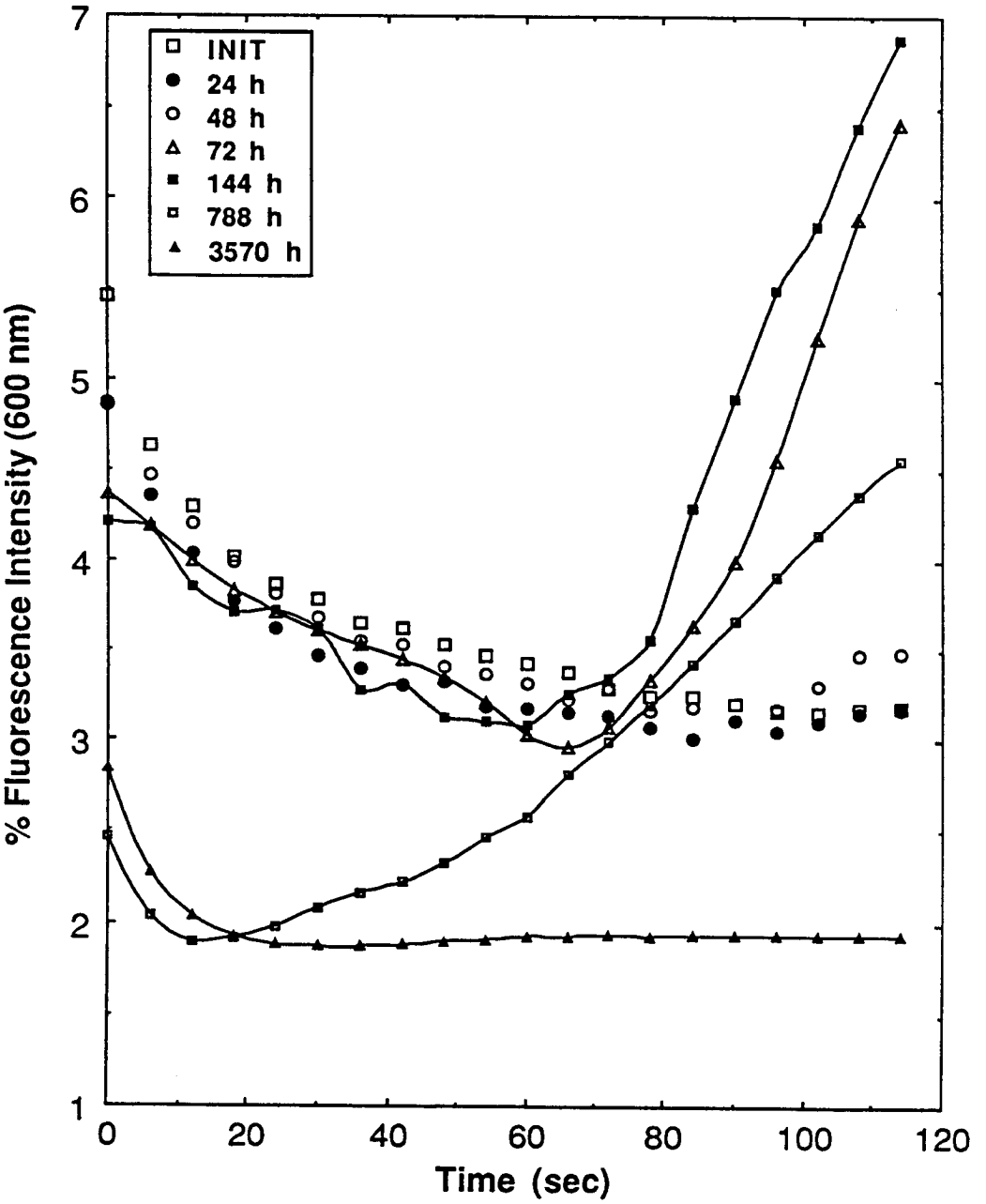

Figure 8. Change in Fluorescence Alteration of the AAH Asphalt with Duration of Exposure to Air

Table 3. Influence of Storage Time and Method and Analytical Technique on Fluorescence Intensity of the AAB-1 Asphalt

Elapsed Time, hr	Storage	% Fluorescence Intensity (600 nm)			
		Hg-Air	Hg-N_2	Xenon-Air	Xenon-N_2
0	Initial	3.16	4.64	5.09	6.50
70	RA-Stored	3.43	4.61	5.02	6.40
166	RA-Stored	3.34	4.62	4.88	6.36
1848	RA-Stored	3.70	4.59	5.38	6.48
2784	RA-Stored	3.23	4.47	5.00	6.42
	$\bar{x} \pm \sigma$	3.42 ± 0.20	4.57 ± 0.07	5.07 ± 0.22	6.42 ± 0.05
70	Exposed	3.39	4.51	4.83	6.40
166	Exposed	3.50	4.26	4.49	6.59
1848	Exposed	3.03	3.59	4.49	4.64
2784	Exposed	2.71	3.49	4.16	4.90
TFOT-Air	Initial	2.64	3.77	3.79	4.60
TFOT-N_2	Initial	2.96	4.17	4.15	5.07

RA-Stored = Refrigerated Storage in Argon; Exposed = Exposed to Atmosphere at Room Temperature, but Protected From Light.

Table 4. Influence of Storage Time and Method and Analytical Technique on Fluorescence Intensity of the AAA-1 Asphalt

Elapsed Time, hr	Storage	% Fluorescence Intensity (600 nm)			
		Hg-Air	Hg-N_2	Xenon-Air	Xenon-N_2
0	Initial	6.35	8.06	10.21	11.49
720	RA-Stored	5.89	8.82	9.72	11.33
1656	RA-Stored	6.18	9.30	9.02	11.29
	$\bar{x} \pm \sigma$	6.14 ± 0.23	8.73 ± 0.62	9.65 ± 0.60	11.37 ± 0.11
720	Exposed	5.22	8.35	8.60	9.78
1656	Exposed	5.24	7.75	7.82	9.32
TFOT-Air	Initial	3.88	4.34	6.38	7.08
TFOT-N_2	Initial	5.07	6.46	8.71	10.61

excitation sources and atmospheres. Because very little change in fluorescence intensity was observed during refrigerated storage, these data provide a means of measuring precision. Measurements made in nitrogen had a lower standard deviation (σ) than those made in air owing to the elimination of fluorescence alteration effects. Furthermore, measurements made using the xenon excitation source in nitrogen were more reproducible. Consequently, a xenon source and a nitrogen atmosphere should be employed as the standard method for measuring the fluorescence intensity of asphalts.

Influence of Asphalt Aging On Fluorescence

A number of experiments were performed to determine the influence of laboratory (thermal) aging on fluorometric parameters. Initially, we wanted to determine whether changes in fluorescence intensity during aging could be used to differentiate oxidation from thermal effects (loss of volatiles). Two types of TFOT tests were conducted with the AAB-1 and AAA-1 asphalts; one using a sweep of air during the 5h heating program and the other using a sweep of nitrogen.

Data from these experiments collected using the four analytical techniques are given in Tables 3 and 4 for the AAB-1 and AAA-1 asphalts, respectively. Fluorescence intensities were higher for the TFOT-N_2 test with both asphalts than for the TFOT conducted using air. However, the magnitude of change in fluorescence intensity was much different for each asphalt. A 29% reduction in intensity was seen for the AAB-1 asphalt compared with a 38% reduction for AAA-1 when the TFOT was performed in air. Using a nitrogen atmosphere during the TFOT, fluorescence intensity diminished significantly for the AAB-1 asphalt (22% or 75% of the change that occurred in air), whereas AAA-1 was influenced much less (8% or 20% of the change that occurred in air).

These large differences in the change of fluorescence intensity suggest some fundamental difference in the response of these two asphalts to heating and oxidation. Based on fluorescence intensity information, the AAA-1 asphalt was more severely altered by laboratory aging (TFOT-Air) than the AAB-1 asphalt. Also, if no oxygen was present during heating under the sweep of nitrogen, it could be concluded that most of the change in fluorescence intensity occurred as a result of oxidation for the AAA-1 asphalt and most occurred by the influence of heating for the AAB-1 asphalt. Unfortunately, it is likely that a small but significant (less than 2%) amount of oxygen may have been present during the nitrogen sweep experiments, thereby contributing to a reduction in fluorescence intensity by oxidation. Because our analytical procedure was the same for both experiments, fluorescence intensity of the AAA-1 asphalt may not have been as severely influenced by low levels of oxygen during heating (at 163°C) as the AAB-1 asphalt.

To further develop the relationship between asphalt aging and fluorometric analyses, another series of experiments was planned using TFOT and TFOT-PAV aged asphalts obtained from the Western Research Institute (WRI). Generally, as aging time and severity progressed, asphalt viscosity increased (11). Analyses of TFOT residues performed in-house also were included so that aging/fluorometric information would be available for a broader range of asphalts. These results are given in Table 5. Except for the AAG-1 asphalt, fluorescence intensity decreased significantly from initial asphalt to TFOT residues whether they were generated by WRI or PSU. In comparison, the AAM-1, AAB-1, AAA-1, AAF-1 and AAC-1 asphalts lost between 29 and 38% of their fluorescence intensity, whereas AAK-1 lost the least (16%) and AAD-1 lost the most (52%) following TFOT aging. As aging severity increased (TFOT to TFOT-PAV) for the AAD-1, AAK-1 and AAM-1 asphalts, fluorescence intensity decreased further. Considering the fact that asphalt viscosity increased by several orders of magnitude with the severity of aging (11), it appears that the chemical changes that were responsible also result in the quenching of fluorescence emissions. Fluorescence quenching can accompany an increase in the concentration of adsorption centers (i.e., increased heteroatom concentration) and/or an increase in molecular size such as that associated with an increase in the size of a polynuclear aromatic network.

The AAG-1 asphalt exhibited anomalous behavior with respect to the other seven core asphalts. Fluorescence intensity of AAG-1 increased 92% from initial (freshly heated at PSU) to the TFOT (WRI) sample. As seen in Table 5, we were able to duplicate the intensity value obtained from the WRI TFOT sample, thus eliminating potential analytical error. As a further test, a TFOT treatment was performed using a subsample of our original AAG-1 asphalt which had been refrigerated in argon. Fluorescence analysis of this sample (last column Table 5) showed a decrease (16%) instead of an increase in intensity. These results suggest that our original AAG-1 asphalt may be significantly different from those being used and evaluated by other SHRP contractors. In fact, analysis of a new AAG-1 sample acquired for our work with mastics (asphalt/aggregate mixtures) showed that our original AAG-1 sample must have been incorrectly identified.

Conclusions

From this initial investigation, a preliminary fluorometric technique for the characterization of raw asphalts has been developed that provides mean fluorescence intensity values that are unique for individual asphalts. Four analytical techniques using two illumination sources (mercury-arc and xenon) and two atmospheres (air and nitrogen) were evaluated during this study. Evaluation of these techniques showed that measurement of intensity using xenon illumination in a nitrogen atmosphere provided the most reproducible data.

Table 5. Fluorescence Intensity of Aged Asphalts from WRI and Produced at PSU

	Intensity, Xenon-N_2, 600 nm								
	Samples from WRI				TFOT Performed In-house				
Type of Aging	AAD-1	AAK-1	AAG-1	AAM-1	AAB-1	AAA-1	AAF-1	AAC-1	AAG-1
Initial Intensity	10.06	2.20	5.83	7.20	6.50	11.49	11.58	10.74	5.83
TFOT - 163°C/5 hrs	4.85	1.77	11.20*	4.72	4.60	7.08	7.47	6.64	4.92
TFOT - PAV	3.14	1.10	5.22	2.70	--	--	--	--	--

*Mean of duplicate analyses 11.04% and 11.37%.

Fluorometric analyses have been performed on twelve asphalts that were selected based on the concentrations of polar aromatics, asphaltenes and heteroatoms. However, the lack of correlation between concentration of these components and fluorescence intensity suggests that a better understanding of asphalt fluorescence may be obtained by determining the fluorescence properties of separate chemical fractions derived from asphalts. Further analysis of this data set did reveal a negative correlation between initial asphalt viscosity and fluorescence intensity.

The alteration of fluorescence intensity of asphalts with time of exposure to blue excitation light in air has been demonstrated to be a photochemical reaction with oxygen. The dual alteration patterns that are measured when using mercury-arc illumination in air appear to be characteristic of individual asphalts and change with asphalt composition and oxidation, i.e., either induced by air blowing the asphalt during manufacturing (AAE asphalt) or as they were exposed to air during storage (AAH). Fluorescence intensity and alteration patterns of the AAH asphalts stored in an inert atmosphere changed with storage duration in a manner similar to subsamples of the asphalt exposed to air at room temperature, thereby suggesting that fluorometric analysis may be a sensitive measure of molecular structuring in asphalts. Analysis of two additional asphalts (AAB-1 and AAA-1) did not show comparable changes in intensity between exposed and stored samples, suggesting that the AAH asphalt may be more sensitive to molecular structuring at lower temperatures than the AAB-1 or AAA-1 asphalts.

Finally, a relationship has been developed between fluorescence intensity measurements and asphalts that have been aged in the laboratory using the TFOT and TFOT-PAV techniques. In all but one case, as the severity of aging increased fluorescence intensity decreased. Because the laboratory aging procedures result in increased asphalt viscosity, the relationship between fluorescence intensity and asphalt viscosity observed for original asphalt properties is strengthened. The anomalous behavior of the AAG-1 asphalt which showed a large increase in intensity following the TFOT perhaps may be explained by incorrect identification of the sample.

From the foregoing it appears that fluorometric analysis has potential applications for determining the quality of refined asphalts, establishing the quality of asphalts after plant mixing, and for defining the rate of or state of deterioration of raw asphalts.

References

1. Welborn, J.Y. (1979). National Cooperative Highway Research Program, Synthesis, 59, Washington, D.C., 34 pp.

2. Petersen, J.C. (1984). Proc. 63rd Annual Meeting of the Transportation Research Board, 42 pp.

3. Davis, A. and Mitchell G.D. (1990). Fluorescence Characterization of Asphalts, Phase I Report, SHRP 88-AIIR-04.

4. Davis, A. and Mitchell G.D. (1990). Fluorescence Characterization of Asphalts, Phase II Report, SHRP 88-AIIR-04.

5. Mitchell, G.D. and Davis A. (1990). The Fluorescence Characterization of Asphalts, Am. Chem. Soc. Preprint, 35(3): pp. 469-475.

6. Mitchell, G.D. and Davis A. (1992). The Fluorescence Characterization of Asphalts, Fuel Sci. Tech. Internat., 10(4-6), pp. 909.

7. Lin, R. and A. Davis. (1988). The Chemistry of Coal Maceral Fluorescence: With Special Reference to the Huminite/Vitrinite Group, Spec. Research Report SR-122, Energy and Fuels Research Center, 278 pp.

8. Materials Reference Library. (1988). Section 5, Rev. 11-1-88, University of Texas at Austin.

9. Davis, A., R.F. Rathbone, R. Lin and J.C. Quick. (1990). Observations Concerning the Nature of Maceral Fluorescence Alteration with Time, Advances in Organic Geochemistry, 16, pp. 897-906.

10. Oriel Corporation. (1985). Light Sources, Monochromators, Detection Systems, II: pp. 42.

11. SHRP A-002A. (1990). Binder Characterization and Evaluation, Quarterly Report, June.

SPECTRAL FLUORESCENCE TECHNIQUES

CHARACTERIZATION OF ASPHALTS AND ASPHALT FRACTIONS

Introduction

The research described in this section principally involves the measurement of spectral emissions from raw asphalts and asphalt chemical fractions following irradiation in blue-light (390-490 nm) and dry nitrogen using mercury-arc illumination. However, fluorometric analyses were completed on one new asphalt (ABD) and duplicate analyses were performed on three additional asphalt subsamples (AAA-1, AAG-1 and AAM-1) obtained for the evaluation of asphalt-aggregate mixtures. Fluorescence spectra were collected on the complete set of thirteen asphalts, which were maintained in refrigerated storage under argon during the course of the project. Further, fluorometric and spectral analyses were performed on twelve asphalt chemical fractions separated via ion exchange chromatography (IEC, neutral and strong acid fractions) and size exclusion chromatography [SEC, non-fluorescing (SEC-I) and fluorescing (SEC-II) fractions].

The use of spectral fluorescence was advised, because during our initial, qualitative evaluation of the asphalt chemical fractions broad spectral differences were observed in the ion-exchange chromatography (IEC) neutrals fractions of different asphalts (1). The neutrals fractions of the AAD-1 and AAG-1 asphalts fluoresced yellow-green (≈550-590 nm), whereas that of the AAM-1 neutrals fraction fluoresced reddish-green (≈600-640 nm). The apparent red shift of the AAM-1 asphalt could partially be explained by its greater aromatic content compared with the other asphalts. It also suggested that spectral fluorescence may be a useful technique for the characterization of π-bond concentrations in asphalt fractions and perhaps in raw asphalts. Furthermore, some of the differences in fluorescence intensity measured at 600 nm among the different raw asphalts may result from a shift in the peak wavelength with respect to 600 nm. For these reasons collection of spectral fluorescence information has become an important consideration in the development of our fluorometric technique.

Experimental

Fluorometric evaluation of new raw asphalts and asphalt chemical fraction samples were performed in accordance with the technique presented in the previous section of this report. The only experimental change in the technique was to employ a desiccant to dry the nitrogen before it entered the environmental chamber during fluorescence intensity measurements; otherwise the standard set-up was used, e.g., measurement of emissions at 600 nm using blue-light irradiation induced by xenon excitation under a nitrogen atmosphere.

Spectral fluorescence was performed with a Leitz MPV-II microscope using a 100-watt high-pressure mercury lamp (instead of xenon) at 625 total magnification using a 50X NPL FLUOTAR air objective. Analyses were performed using blue-light excitation with the Ploemopak 2 vertical illuminator fitted with an H2 filter combination (395-490 nm excitation; 510 nm dichromatic beam splitter; 515 nm long-pass barrier filter). Fluorescence emissions were passed through a motor-driven Kratos GM200 double-grating monochromator with 20 nm bandwidth, and then to a RCA C31034A water-cooled photomultiplier for measurement (see Appendix A). Synchronization of the photomultiplier readings with the appropriate monochromator wavelength was controlled initially by adjusting the speed of the monochromator motor-drive and finally by computer software. Raw data was directed to a Swan 386SX computer having a math coprocessor and a Microtech PC Diadac-1 A/D control board.

Monochromator synchronization was adjusted and monitored using a uranyl glass standard with a peak fluorescence at 530 nm. Several light-emitting diodes with peak fluorescence intensities at 590 and 705 nm also were used to check a greater portion of the spectral range. An example of our initial synchronization is shown in Figure 9. Spectral information on these standards was collected several times during each session so that, if necessary, asphalt spectra could be adjusted. In addition, all spectra were corrected with respect to a quartz halogen lamp with a measured color temperature at 3400°K for the microscope equipment described above (2).

Spectral information on asphalt and asphalt fractions was gathered under a blanket of dry nitrogen. Data on all the raw asphalts were collected during two sessions over a period of 24h using a fresh mercury-arc lamp. Likewise, data on all of the asphalt chemical fractions were collected on the same day during an 8h period. Five separate spectra were collected on different areas of each sample and the mean values determined and used for the graphical representations which follow. In addition to collecting relative intensity values at 1 nm intervals from ≈490 to ≈780 nm, the computer software determined the peak wavelength as well as chromaticity values compared with various standard illuminants, i.e., E_e (equal energy, pure white light), E_a (illuminant A, tungsten filament lamp at color temperature 2854°K), E_b (illuminant B, average noon sunlight) and E_c (illuminant C, lighting provided by an overcast sky).

For some of the asphalt chemical fractions (IEC neutrals and SEC-II fluorescing fractions) that exhibited extremely high fluorescence intensity, neutral density filters were used to reduce the measured fluorescence emissions into the voltage range of the photomultiplier, i.e., ND#48 and #918 with percentage transmittance of 9.33% and 8.71%, respectively. The ND#48 was used for the SEC-II fluorescing fraction, whereas the ND#48 and #918 were used in combination for the IEC neutrals fraction.

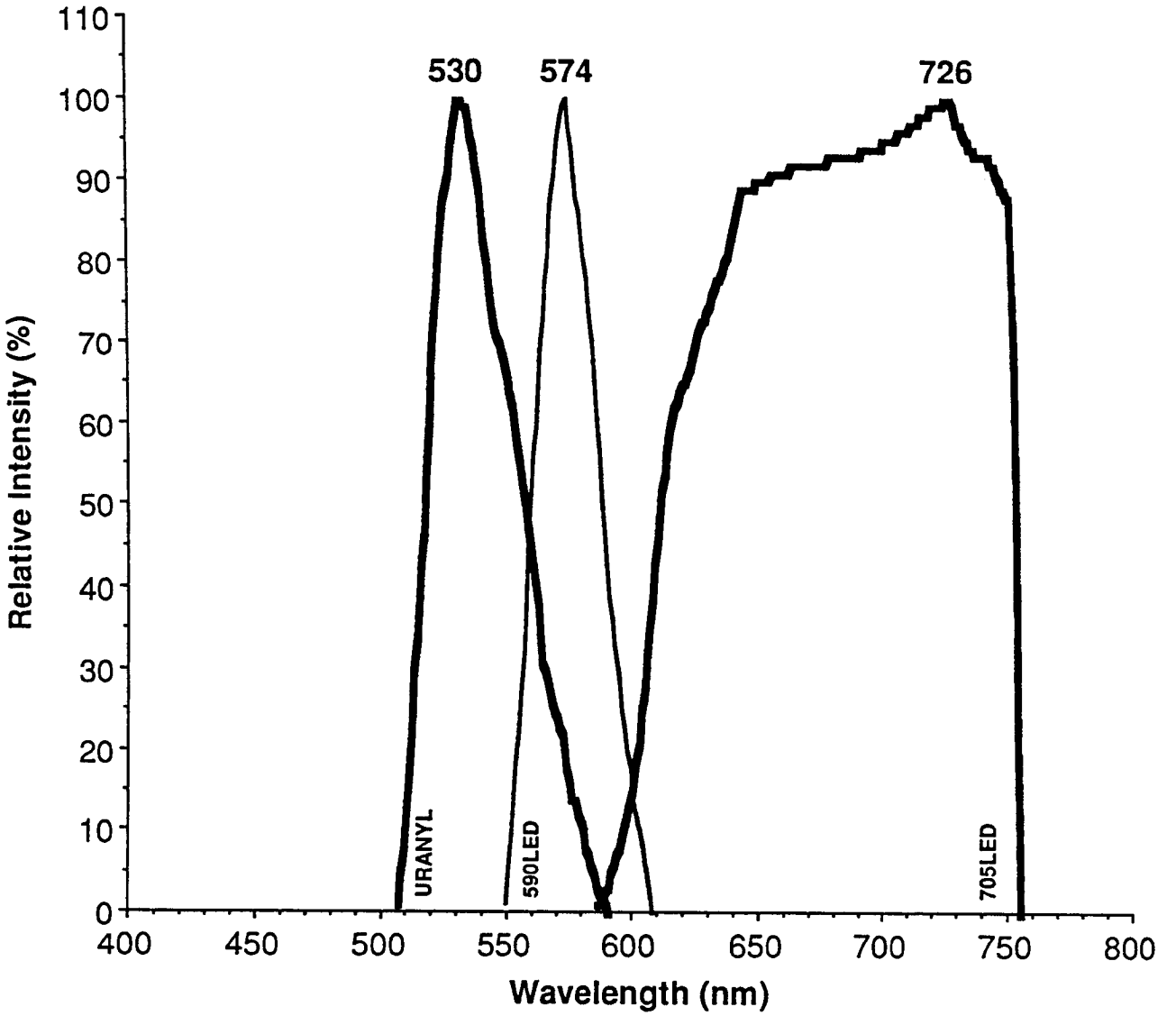

Figure 9. Spectral Distribution of the Uranyl Glass (529nm) and the 590nm and 705nm LEDs After Synchronization of the Monochromator Using Blue-Light Irradiation

All chemical fractions were obtained from WRI and included IEC neutrals and strong acid fractions and the SEC-II fluorescing and SEC-I non-fluorescing fractions from core asphalts AAD-1, AAG-1 and AAM-1. Fractions from these asphalts were selected because of the reported differences in aromaticity of the IEC neutrals fraction and decreasing amounts of the IEC strong acids fraction separated from the raw asphalts. Therefore, the sample set would provide a means of investigating the influence of decreasing London dispersion forces versus increasing π-bond interactions on the fluorometric and spectral properties of the "solvent phase" (neutrals) of different asphalts. The SEC-II fluorescing fraction which contained much of the IEC neutrals, weak acid and weak base fractions were used to determine the influence of molecular species which tend to associate (during structuring) on the overall fluorometric properties of asphalt.

Approximately 100 mg of each sample was received and immediately sealed in foil multilaminate bags under an argon atmosphere and refrigerated until analyzed. Special 2.5 cm diameter plug-mount samples were prepared by mounting the bottom end cut from a 10x75 mm pyrex test tube in a clear epoxy cylinder, thus forming a small cup. Both ends of the cylinder were cut, ground and polished to form flat level surfaces needed for microscopy. The cup produced by the tip of the test tube had an average estimated volume of <0.1 cm^3.

At room temperature, the IEC neutrals fraction was a viscous liquid and could easily be transferred to the sample containers just described. The IEC strong acid and the SEC-I fractions were brittle solids. To minimize handling and interaction with solvents, the largest particles having flat or uniform surfaces were selected. These particles were fixed into the sample holders by pushing them into small particles of modelling clay. Consequently, measurements of fluorometric intensity and spectral distribution were performed on as-received surfaces for these samples.

Results and Discussion

Spectral Analysis of Raw Asphalts

Table 6 summarizes the information obtained from spectra of the thirteen raw asphalts shown in Figures 10 through 13. Peak fluorescence intensity of 70% of the raw asphalts fall between 664 and 672 nm, two asphalts (AAD-1 and AAE) had slightly lower peaks at about 640 nm, whereas the ABD and AAK-1 asphalts had significantly lower peak wavelengths at 600 nm and 544 nm, respectively. Generally, all of the spectra showed a very rapid rise in fluorescence intensity in the range of 500-530 nm and then gently increased to their respective peak values. Most of the asphalts showed a gentle decline in intensity for the 70-100 nm following the peak value and then rapidly declined to zero between 730-760 nm. However, four of the asphalts (AAE, AAG-1,

Table 6. Peak Fluorescence and Mean Chromaticity of Raw Asphalts and Asphalt Chemical Fractions

Asphalt Code	Chromaticity E_e x	E_e y	E_a x	E_a y	E_b x	E_b y	E_c x	E_c y	Intensity Xenon N_2	Primary Peak Fluorescence nm	Intensity at Peak Wavelength	Minor Fluorescence Peaks (P) or Shoulders (S) nm
AAA-1	0.483	0.501	0.528	0.461	0.487	0.498	0.472	0.511	11.49	663	12.2	720P
AAA-2	0.481	0.502	0.527	0.462	0.486	0.498	0.470	0.512	11.51	668	12.1	720P
AAB-1	0.490	0.497	0.533	0.459	0.493	0.494	0.478	0.508	6.50	668	6.9	--
AAC-1	0.485	0.500	0.530	0.460	0.489	0.496	0.473	0.510	10.74	668	11.5	749S
AAD-1	0.481	0.503	0.526	0.463	0.485	0.499	0.470	0.513	10.06	640	10.3	664P
AAE	0.488	0.499	0.531	0.460	0.492	0.496	0.477	0.509	4.94	641	5.3	652P
AAF-1	0.486	0.499	0.531	0.459	0.490	0.496	0.474	0.509	11.58	666	12.5	--
ABD	0.498	0.494	0.535	0.460	0.501	0.492	0.488	0.504	20.90	600	20.9	681P
AAG-1	0.490	0.497	0.533	0.459	0.494	0.494	0.479	0.508	5.83	672	6.4	--
AAH	0.494	0.494	0.537	0.456	0.498	0.491	0.483	0.504	5.01	672	5.5	--
AAJ	0.486	0.499	0.531	0.460	0.491	0.496	0.475	0.509	7.25	666	7.6	--
AAK-1	0.462	0.526	0.503	0.489	0.466	0.523	0.452	0.535	2.20	544	2.6	--
AAM-1	0.487	0.499	0.531	0.459	0.491	0.495	0.476	0.509	7.20	664	7.7	713S
Ion Exchange Chromatographic Fractions												
Neutrals												
AAD-1	0.409	0.566	0.452	0.531	0.414	0.563	0.400	0.574	288	535	417	568S 671S
AAG-1	0.452	0.527	0.498	0.488	0.456	0.524	0.440	0.537	472	544	514	582P 594P 680P
AAM-1	0.477	0.507	0.523	0.467	0.482	0.503	0.466	0.517	433	686	446	550P 572P
Strong Acids												
AAD-1	0.484	0.506	0.522	0.471	0.487	0.504	0.474	0.516	0.57	573	0.60	566P 581P 660S
AAG-1	0.507	0.485	0.543	0.452	0.509	0.483	0.496	0.496	0.47	596	0.47	646S
AAM-1	0.494	0.498	0.529	0.466	0.497	0.497	0.484	0.508	0.16	580	0.17	553P 660P
Size Exclusion Chromatographic Fractions												
Fluorescing Fraction												
AAD-1	0.475	0.507	0.521	0.467	0.480	0.504	0.464	0.518	90	668	92	676P 615P 600P
AAG-1	0.488	0.498	0.531	0.460	0.492	0.495	0.477	0.509	63	680	66	672P
AAM-1	0.499	0.491	0.539	0.454	0.502	0.488	0.488	0.502	39	694	44	--
Non-fluorescing Fraction												
AAD-1	0.487	0.504	0.524	0.470	0.490	0.502	0.477	0.514	0.47	581	0.50	666P
AAG-1	0.465	0.526	0.500	0.493	0.468	0.524	0.456	0.535	0.27	548	0.33	655S
AAM-1	0.495	0.496	0.532	0.462	0.498	0.494	0.485	0.506	0.81	585	0.82	644S

E_e = Equal Energy pure white light; E_a = Illuminant A -- tungsten filament; E_b = Illuminant B -- average noon sunlight; E_c = Illuminant C -- lighting provided by overcast sky

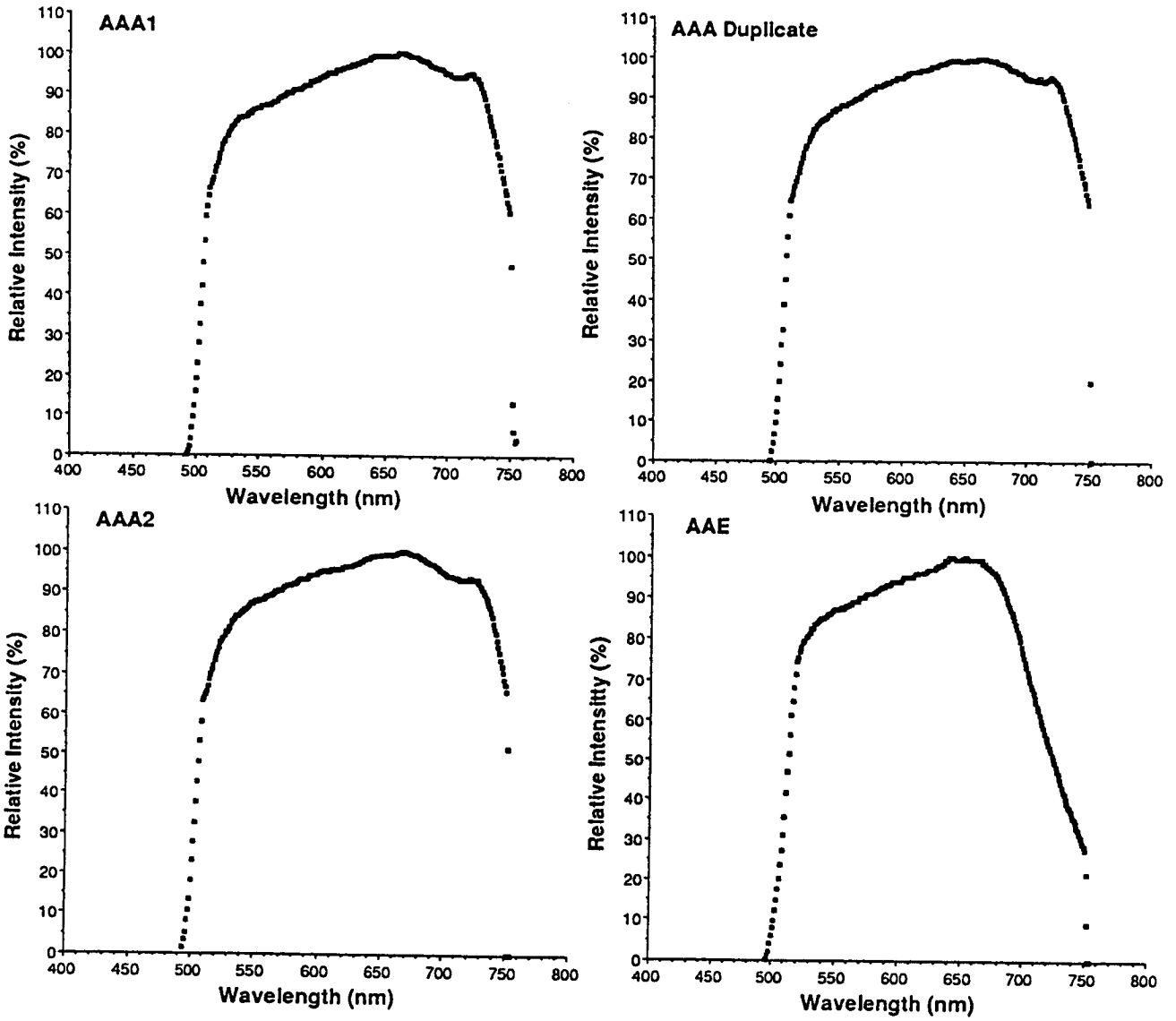

Figure 10. Fluorescence Spectra of Raw Asphalts Using Blue-Light Excitation and Mercury-Arc Illumination in Dry Nitrogen

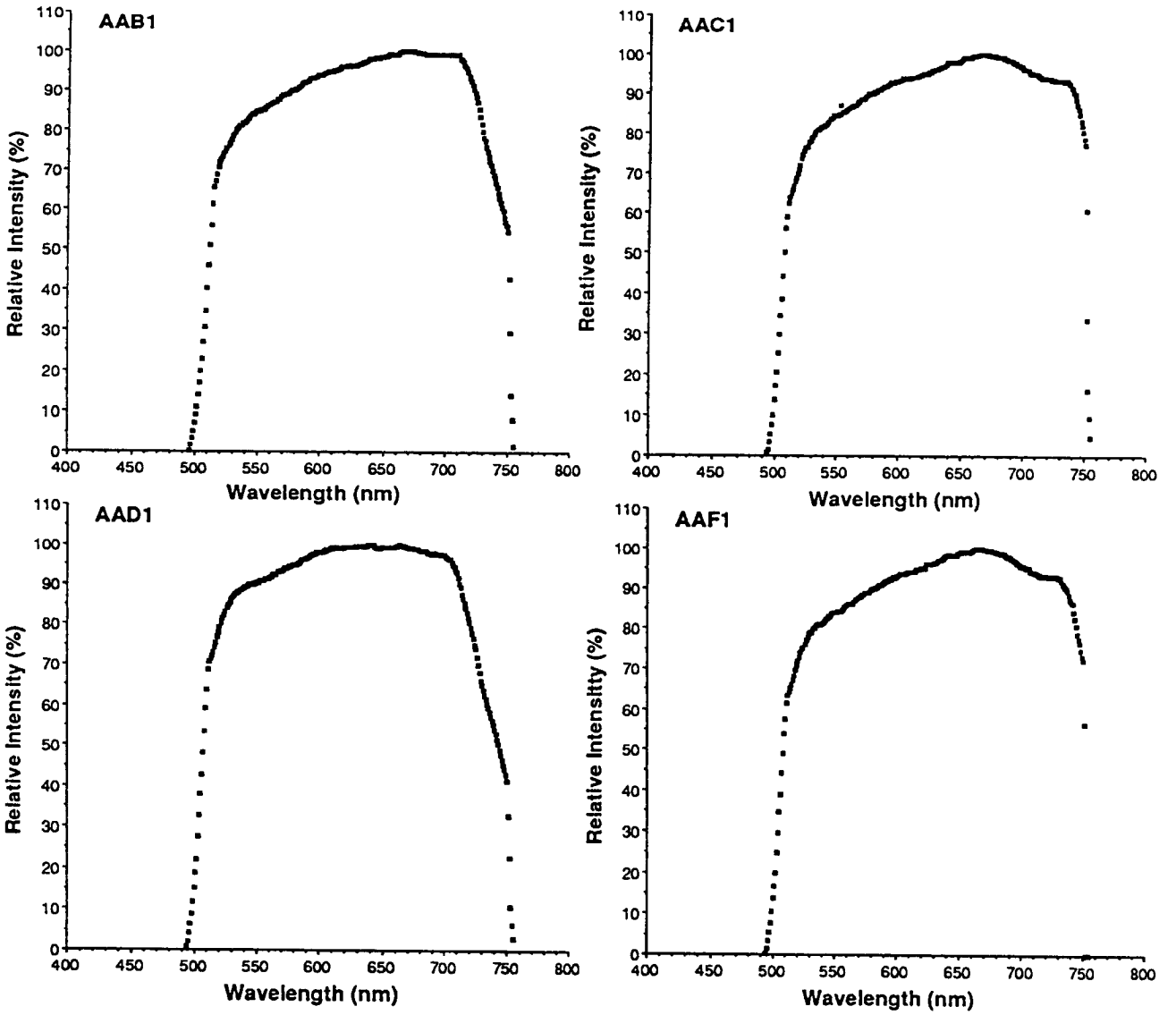

Figure 11. Fluorescence Spectra of Raw Asphalts Using Blue-Light Excitation and Mercury-Arc Illumination in Dry Nitrogen

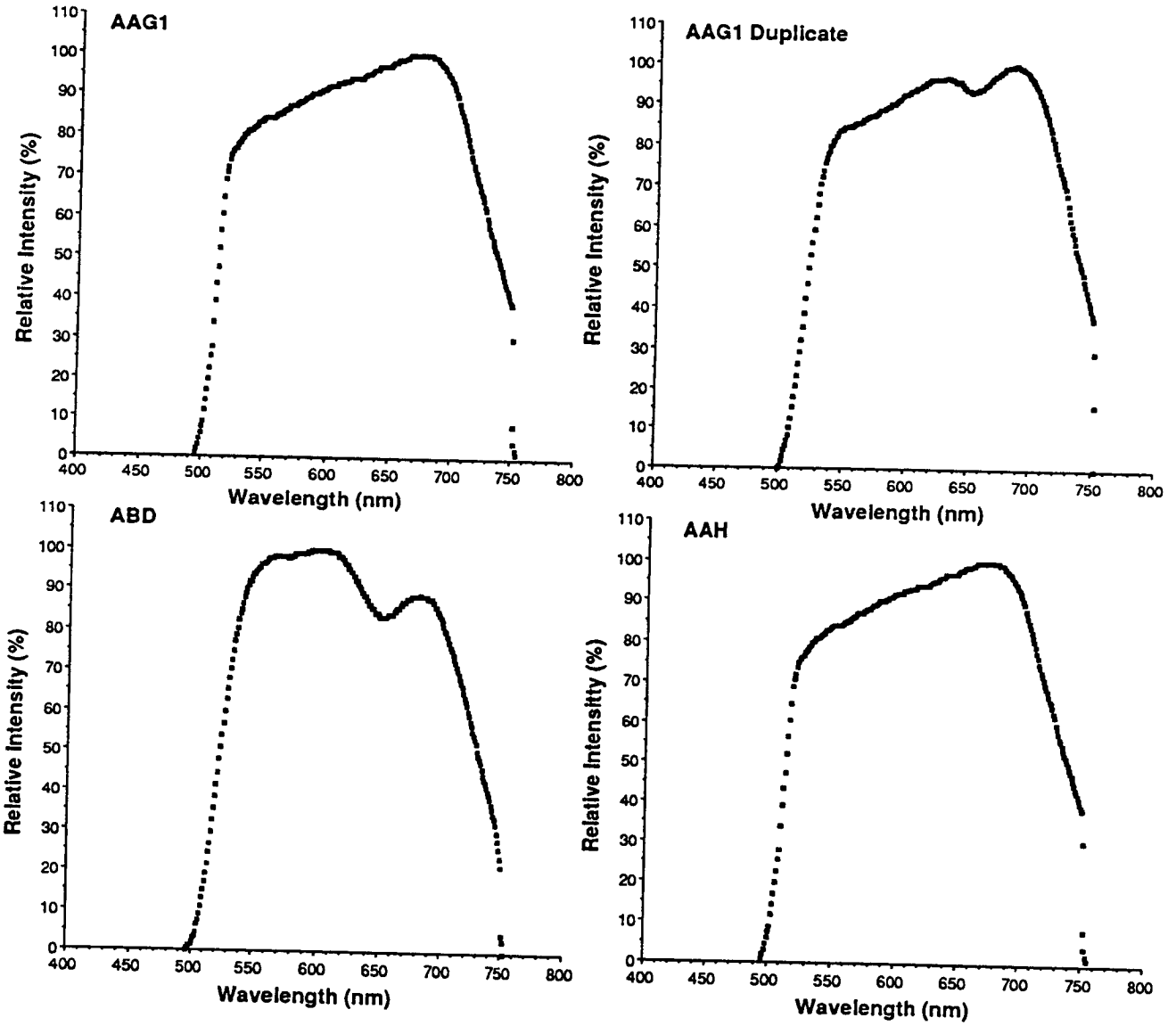

Figure 12. Fluorescence Spectra of Raw Asphalts Using Blue-Light Excitation and Mercury-Arc Illumination in Dry Nitrogen

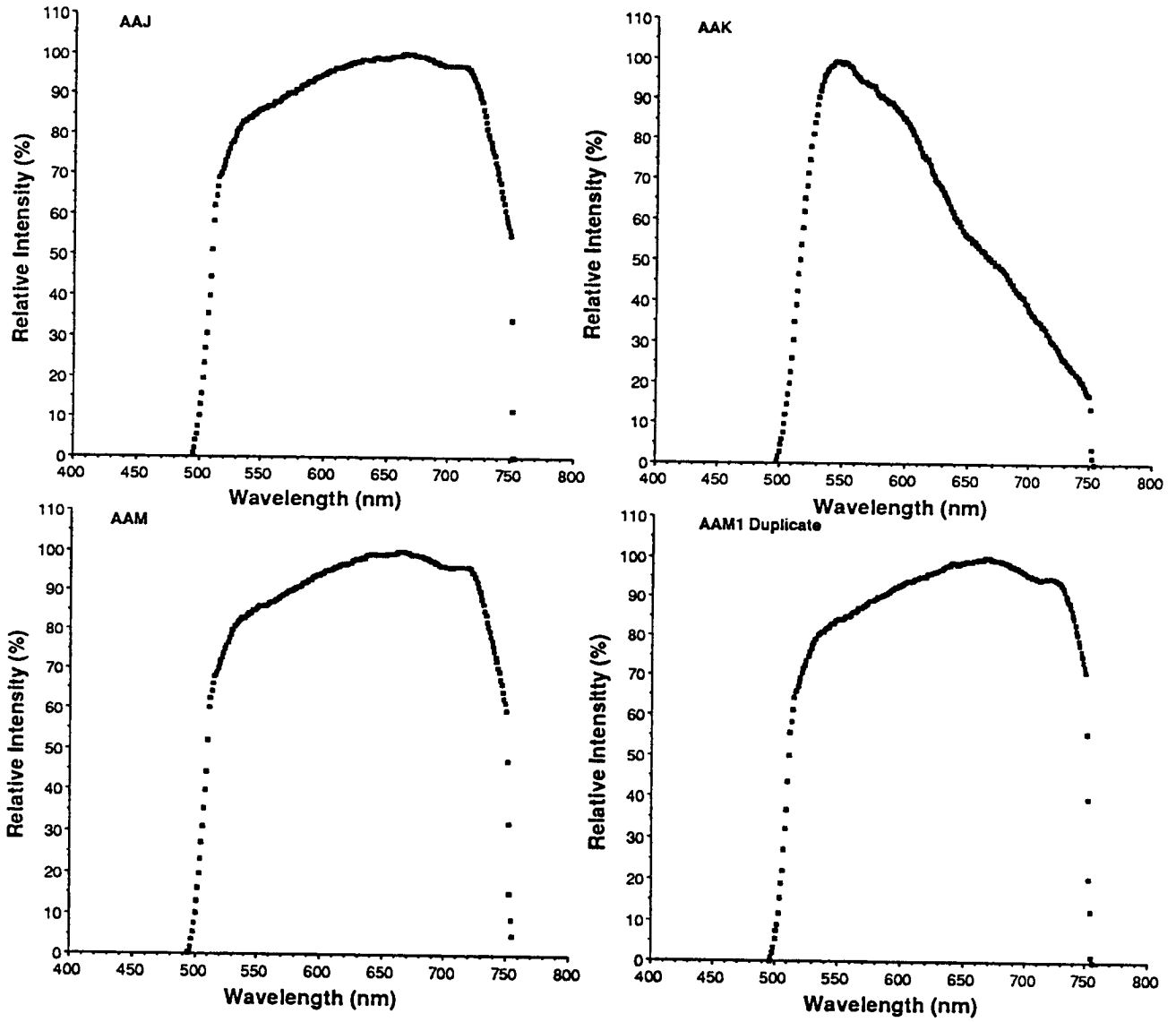

Figure 13. Fluorescence Spectra of Raw Asphalts Using Blue-Light Excitation and Mercury-Arc Illumination in Dry Nitrogen

AAH-1 and AAK-1) showed a more brisk decline in intensity following peak fluorescence. In addition, a number of soft peaks and/or shoulders were identified and are listed in Table 6. Most of these were very minor and all occurred at higher wavelengths than the main peak value. These observations show that a majority of the asphalts have very similar broad spectral emissions when irradiated in blue-light.

Fluorescence spectra also were collected on three newly acquired and freshly heated asphalts (AAA-1, AAG-1 and AAM-1) that had been evaluated previously. Spectra from the original samples that were stored under argon (refrigerated) and the new subsamples are shown together in Figures 10, 12 and 13 for each asphalt, respectively. For the AAA-1 and AAM-1 asphalts, spectra were reproduced fairly well between subsamples. However, a significant difference was found between subsamples of the AAG-1 asphalt, which may explain some of the ambiguous results obtained with this asphalt in the last section (see Table 5). As shown in Table 7 and Figure 12, the spectra obtained for the new AAG-1 subsample exhibited a peak fluorescence at a slightly higher wavelength than the original sample and it has a secondary minor peak at 631 nm. In comparison, a strong similarity exists between the new AAG-1 and the ABD spectra (Figure 12), except that the primary and secondary peak wavelengths for the two asphalts were approximately reversed (see Table 7). The ABD asphalt was from the same petroleum source as AAG-1, but was not treated with caustic. The spectral similarity suggests that the original AAG-1 sample may have been altered in some way prior to its receipt (see next section).

Fluorometric analyses completed on the new samples also are given in Table 7. These results showed that we were able to repeat the original intensity value of AAA-1 fairly closely, but significant differences were found for the AAM-1 and AAG-1 samples. Perhaps the 30% increase in the AAM-1 fluorescence intensity may be explained by the fact that the intensity measured using xenon irradiation for the original AAM-1 subsample was obtained from a sample that had been stored (refrigerated in argon) for several months. As discussed in the previous section, some asphalts (AAH) exhibited a decrease in intensity during storage. However, because our sample preparation techniques have been consistent throughout the project, the >400% increase in intensity for the AAG-1 sample can only be explained by differences in the original subsample. Specifically, it is suggested that the initial sample was severely oxidized (see following section). Note too that the intensity of the ABD asphalt, which had no caustic additive, was lower than that of the new AAG-1, thereby eliminating the additive as a direct cause of low intensity in the original AAG-1 sample.

The AAA-1, AAA-2 and AAE asphalts were derived from the same petroleum source, but each has different rheological and chemical properties resulting from refining procedures. Comparison of the spectra in Figure 10 showed that AAA-1 and AAA-2 (different

Table 7. Comparison of Intensity and Peak Fluorescence between Different Subsamples of Core Asphalts

Asphalt Code	Intensity, Xenon, N_2 at 600 nm	Primary Peak Fluorescence nm	Minor Peaks nm
AAA-1-Orig.	11.49	663	--
AAA-1-new	11.72	664	--
AAG-1-Orig.	5.83	672	--
AAG-1-New	29.90	686	631
ABD	20.90	600	681
AAM-1-Orig.	7.20	664	--
AAM-1-New	9.55	668	--

grades of the parent asphalt) were nearly the same, whereas AAE (air blown asphalt) was significantly different. The AAE asphalt has lower intensity values between 700-754 nm than the other asphalts, showing that controlled oxidation of the asphalt by air-blowing results in a narrowing of the spectral emissions.

Chromaticity information obtained from the set of thirteen raw asphalts were surprisingly similar. As shown in Table 6 for example, except for the AAK-1 asphalt all of the coordinate values (x and y) for illuminant A (E_A) were very nearly the same. In comparison to the AAK-1 asphalt the mean x-coordinate values for the other twelve asphalts equaled 0.531 ±0.003 vs 0.503 for AAK-1; the corresponding y-coordinate values equaled 0.460 ±0.002 vs 0.489 for AAK-1. Similar comparisons can be made for the other illuminants, but as shown in Figure 14 for illuminant A twelve of the asphalts plotted in the yellow-orange region and AAK-1 plotted in the orange.

Spectral analysis of the raw asphalts showed that, for the most part, peak intensity values occur at higher wavelengths than 600 nm which was the wavelength selected for the fluorometric intensity analysis. If we assumed that intensity changes proportionally throughout the visible spectrum, then fluorescence intensity could be calculated for the peak wavelength using the value measured at 600 nm. These estimates given in the "Intensity at Peak Wavelength" column in Table 6 showed that intensity increased from the value measured at 600 nm by an average of 7.0% ranging from 0.0% (ABD) to 18.2% (AAK-1) for the raw asphalts. This exercise resulted in no changes in our interpretation of fluorometric data derived from the raw asphalts. Even correlation of viscosity with the intensity values determined at peak wavelength were about the same as those observed for intensities measured at 600 nm. The fact that the spectral distribution for most of the asphalts was fairly uniform in intensity between 530 and 700 nm may be the reason that no large variations were observed.

Asphalt Chemical Fractions

Fluorometric Analysis

Table 6 compares the fluorescence intensities obtained from each chemical fraction for the three different core asphalts. From these data, it appears that the IEC neutrals fraction contains much of the fluorescing material in the three asphalts studied. Intensities for this fraction were about two-orders of magnitude higher than the raw asphalts and three-fold higher than the intensities measured for the IEC strong acids fraction. The low fluorescence of the strong acids fractions was anticipated, as this material reportedly contained more of the polar aromatic compounds which are typically fluorophoric. However, because of a high concentration of fluorophors, measured intensities may be lowered as a result of concentration quenching.

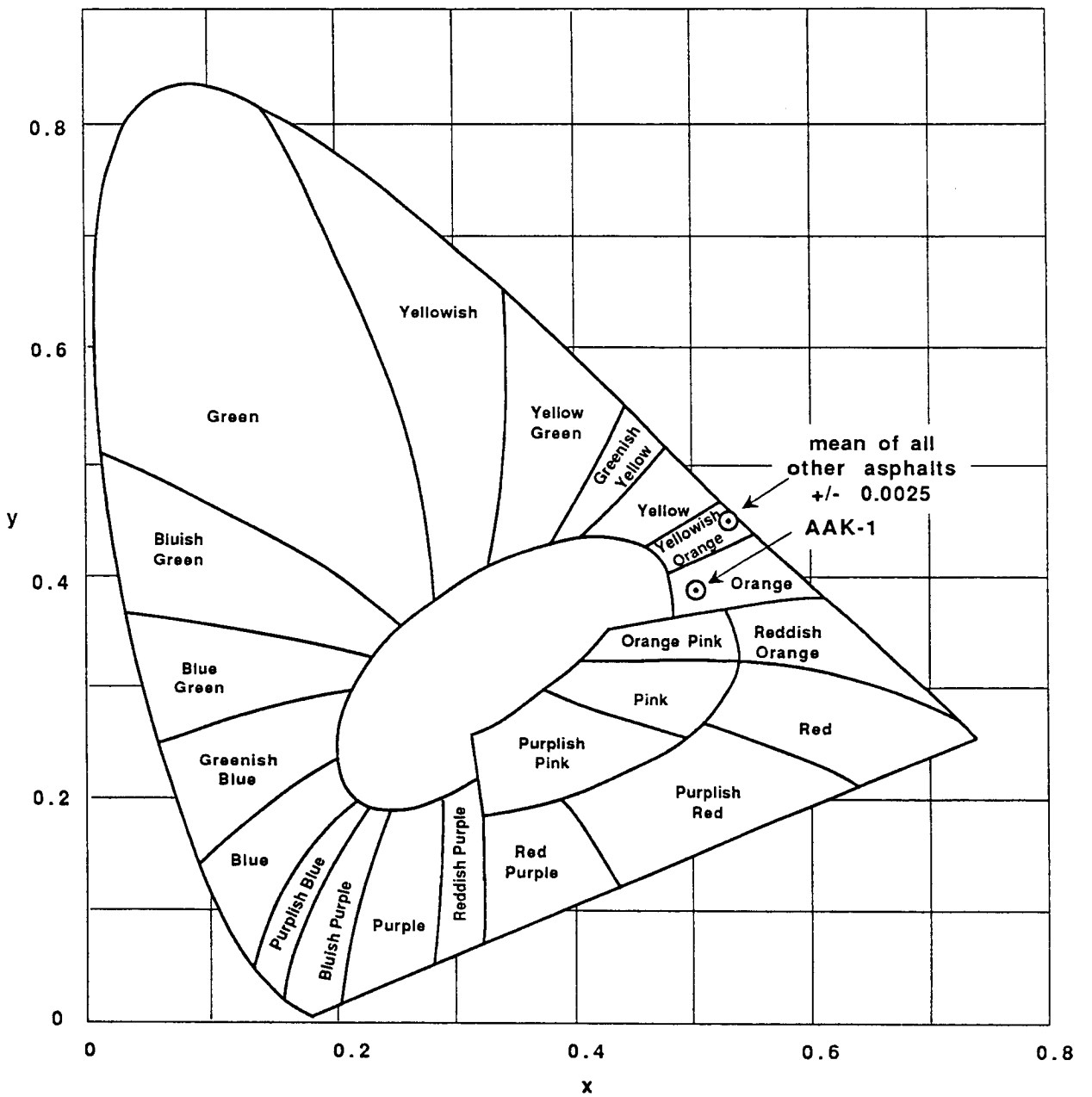

Figure 14. C.I.E. Chromaticity Diagram Comparing Illuminant A of 12 Asphalts; The Mean Value for 11 of the Asphalts and that of AAK-1 Were Significantly Different

Although there was a trend suggesting that the more aliphatic the neutrals fraction the lower the fluorescence intensity (e.g. AAD-1), the very high intensity observed for the neutrals fraction was not anticipated. As the fraction becomes more aromatic and dominated with π-bonds, fluorescence intensity increased to a maximum value for the AAG-1 asphalt. Qualitatively, fluorescence for both of these asphalts (AAD-1 and AAG-1) was yellowish-green (perhaps peaking around 550-590 nm). The AAM-1 neutrals fraction fluoresced distinctly reddish-orange (perhaps peaking 600-640 nm), signifying a red shift for this more aromatic fraction. Fluorescence intensity for the AAM-1 was found to be slightly lower than the AAG-1 neutrals fraction suggesting that the higher concentration of π-bonds (higher aromaticity) and larger molecules may result in some quenching.

The interrelationships among the fluorescence intensities and weight concentrations of the IEC neutrals and strong acids fractions compared with the fluorescence of the whole asphalts were not easily resolved with the current limited data. Without considering the influence of strong bases, weak acids, and weak bases, we can only tentatively conclude that the AAG-1 and AAM-1 were more similar to each other than to the AAD-1 asphalt. The neutrals fraction of the AAG-1 and AAM-1 asphalts had similar fluorescence intensities, they had relatively low weight percentages of strong acids (3,4), and as the concentration of these acids increased the fluorescence intensity of the whole asphalt decreased (Table 6). This suggested that as the concentration of molecular types that result in associative behavior in asphalts increased, fluorescence of the whole asphalt decreased. This tendency may be supported by the findings of our aging studies discussed in the next section.

Following the aforementioned logic, the AAD-1 whole asphalt should have had the lowest fluorescence intensity, because it had the greatest amount of strong acids and its neutrals fraction had the lowest fluorescence of the group. In fact, AAD-1 had the highest whole asphalt fluorescence (10.06%). This apparent ambiguity may be addressed by considering the types of associative behavior occurring in the different asphalts. For the AAD-1 asphalt, which was mostly aliphatic, the strong acids or polar molecules may be initially dispersed after heating, but then associate with each other in a solvent phase (neutrals) characterized by relatively weak London dispersion forces. Therefore, the AAD-1 asphalt may be thought of as a two phase system with clusters of highly associative molecules of low fluorescence intensity dispersed within a relatively inert highly fluorescent phase. This set of circumstances perhaps leads to a high whole asphalt fluorescence.

In asphalts for which the solvent phase was more aromatic, like AAM-1 and to some extent AAG-1, the polar phase may more readily associate with a solvent phase that may be characterized by stable dipoles, π-bonds, and hydrogen bonding. This type of molecular association may cause the solvent and dispersed phases

to behave as a single phase. Thus, during irradiation with blue-light this single phase may have a greater tendency to re-absorb fluorescence emissions, ultimately lowering the measured fluorescence intensity.

Table 6 shows that the fluorescence intensity of the SEC-II fluorescing fraction was intermediate between raw asphalt and the IEC neutrals fraction. This SEC fraction reportedly contained most of the IEC neutral, weak acid and base fractions. If so, this demonstrates the inhibition of neutrals fraction fluorescence when diluted with the relatively low concentration weak acid and base fractions. In the case of the SEC-II fluorescing fraction there was a tendency for reduced fluorescence with increasing aromaticity.

The fluorescence intensities of the SEC-I non-fluorescing fraction were low and variable ranging from 0.27 to 0.81 %. The variability may have resulted from the method by which they were recovered (3). In fact the SEC-I fraction of the AAM-1 asphalt was actually a two phased system; a highly fluorescent, micron-sized phase uniformly distributed in a matrix of very low fluorescing material. Because of the intimate mixture and particle size, individual intensity readings were not possible. Consequently, the AAM-1 non-fluorescing intensity value can be thought of as a resultant value of two phases.

Spectral Analysis

Spectral fluorescence and chromaticity information also was collected on the asphalt chemical fractions. Spectra are found in Figures 15 and 17 and chromaticity for illuminant A is found in Figures 18 and 19. Peak fluorescence values for the IEC neutrals and strong acids fractions of AAD-1, AAG-1 and AAM-1 are compared in Figure 15 and Table 6. The wavelength of maximum fluorescence intensity was lower for the AAD-1 and AAG-1 neutrals fraction compared with the strong acids, but this trend was reversed for the AAM-1 IEC fractions. Also, the AAM-1 neutrals fraction spectrum resembled that of the raw asphalt (Figure 13) and exhibited a higher peak wavelength than the strong acids fraction or the raw asphalt.

Estimation of the fluorescence intensity at peak wavelength instead of 600 nm profoundly influenced the intensity of the AAD-1 neutrals fraction. As shown in Table 6, its intensity value increased (from 288 to 417) into the range of values measured for the other two asphalt fractions. As reported by the A-002A contractor (3,4), the AAD-1 asphalt was found to be mostly aliphatic and of relatively low molecular weight, whereas AAM-1 was of higher molecular weight and aromaticity. AAG-1 was described as intermediate in aromaticity and molecular weight. Consideration of fluorescence intensities determined at peak wavelength has not modified our interpretations made from fluorometric analysis (1); that is, as the molecular weight and

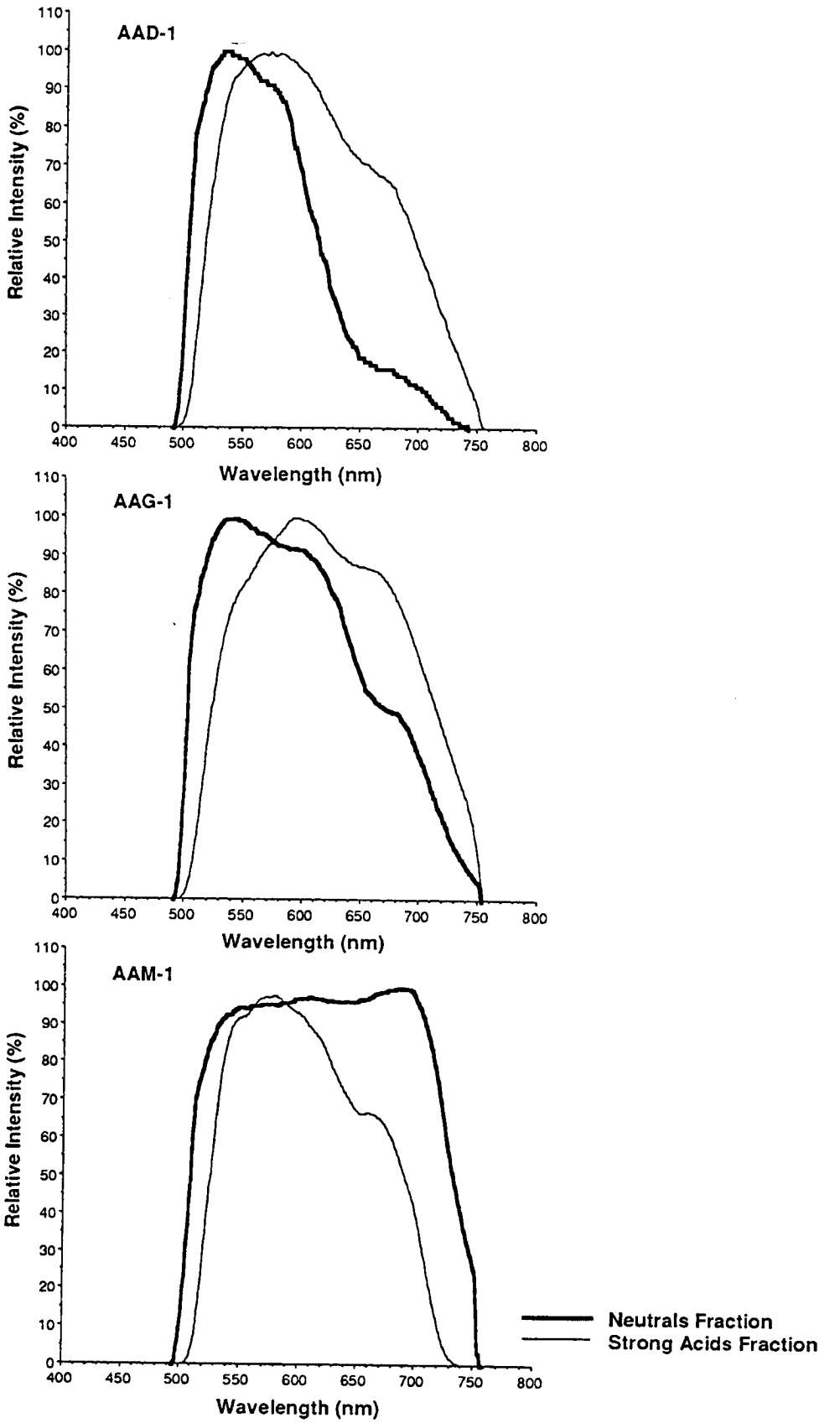

Figure 15. Fluorescence Spectra of the IEC Neutrals and Strong Acids Fractions of the AAD-1, AAG-1 and AAM-1 Asphalts Measured Using Blue-Light Excitation and Mercury-Arc Illumination in Dry Nitrogen

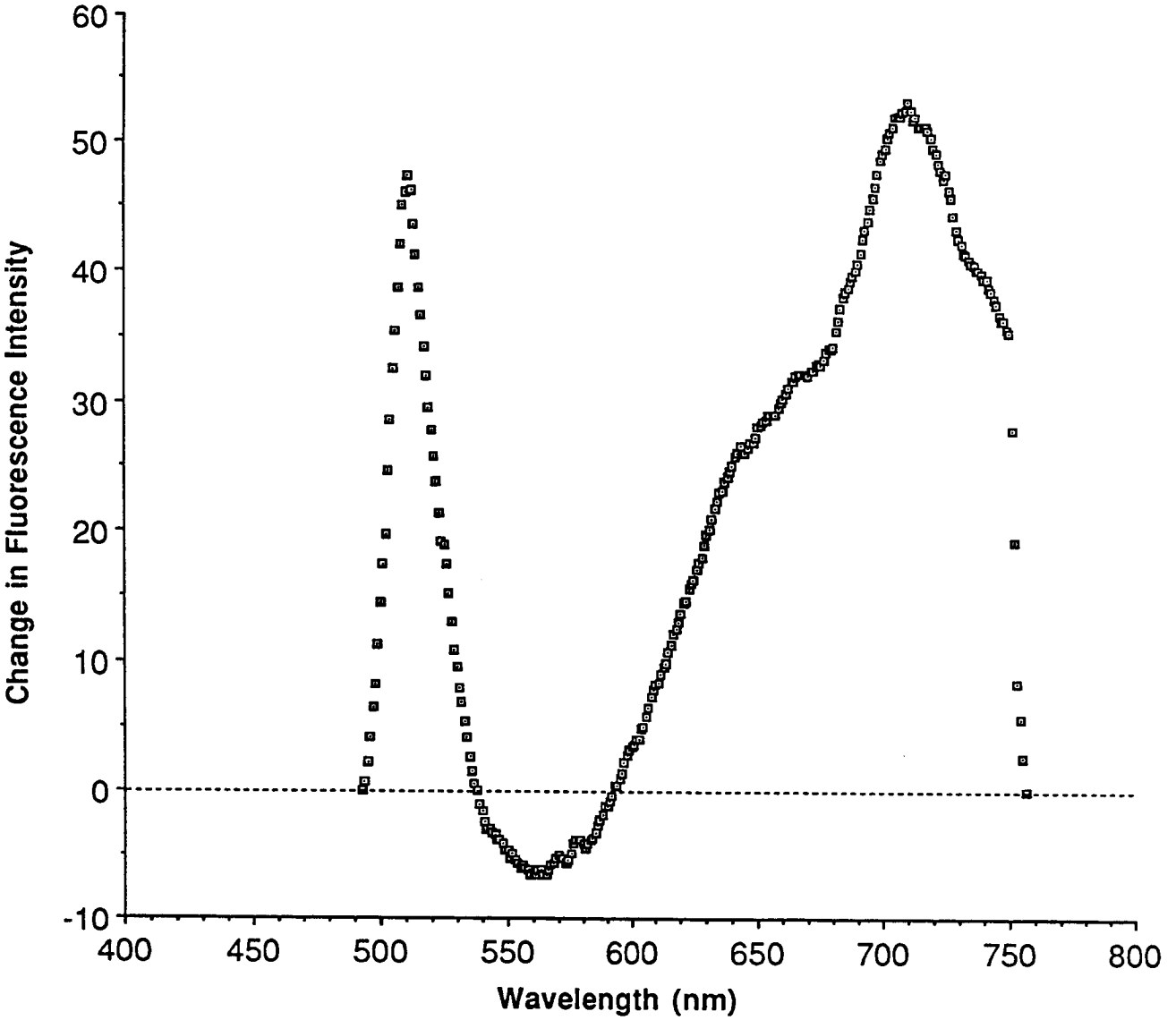

Figure 16. Difference Spectrum Generated by Subtraction of the AAD-1 IEC Strong Acids Spectrum from that of the AAD-1 Raw Asphalt

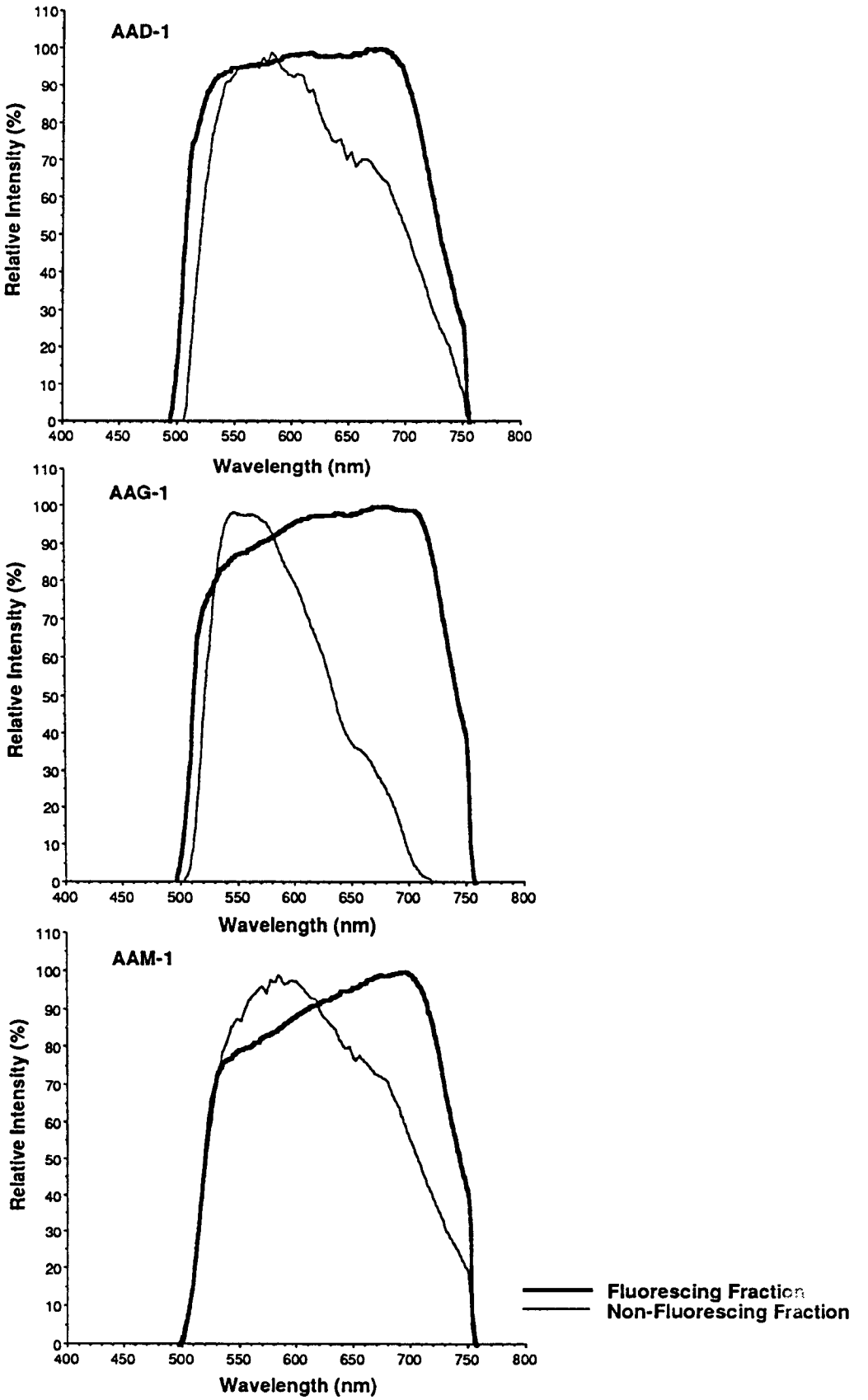

Figure 17. Fluorescence Spectra of the SEC Fluorescing and Non-Fluorescing Fractions of the AAD-1, AAG-1 and AAM-1 Asphalts Measured Using Blue-Light Excitation and Mercury-Arc Illumination in Dry Nitrogen

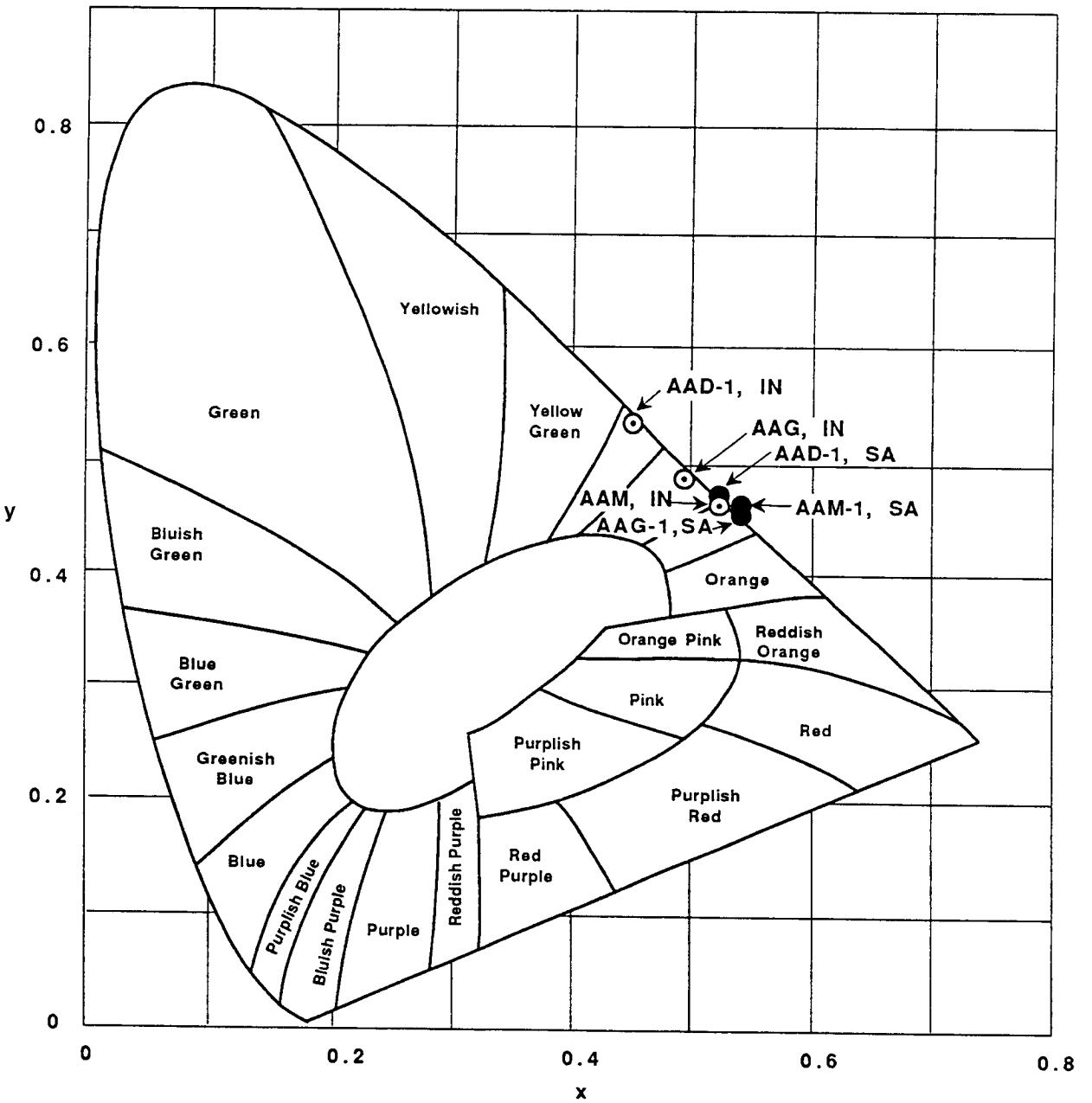

Figure 18. **C.I.E. Chromaticity Diagram Comparing Emissions for Ion Exchange Chromatography Neutrals (IN) and Strong Acids (SA) Fractions of the AAD-1, AAG-1 and AAM-1 Asphalts to Standard Illuminant A**

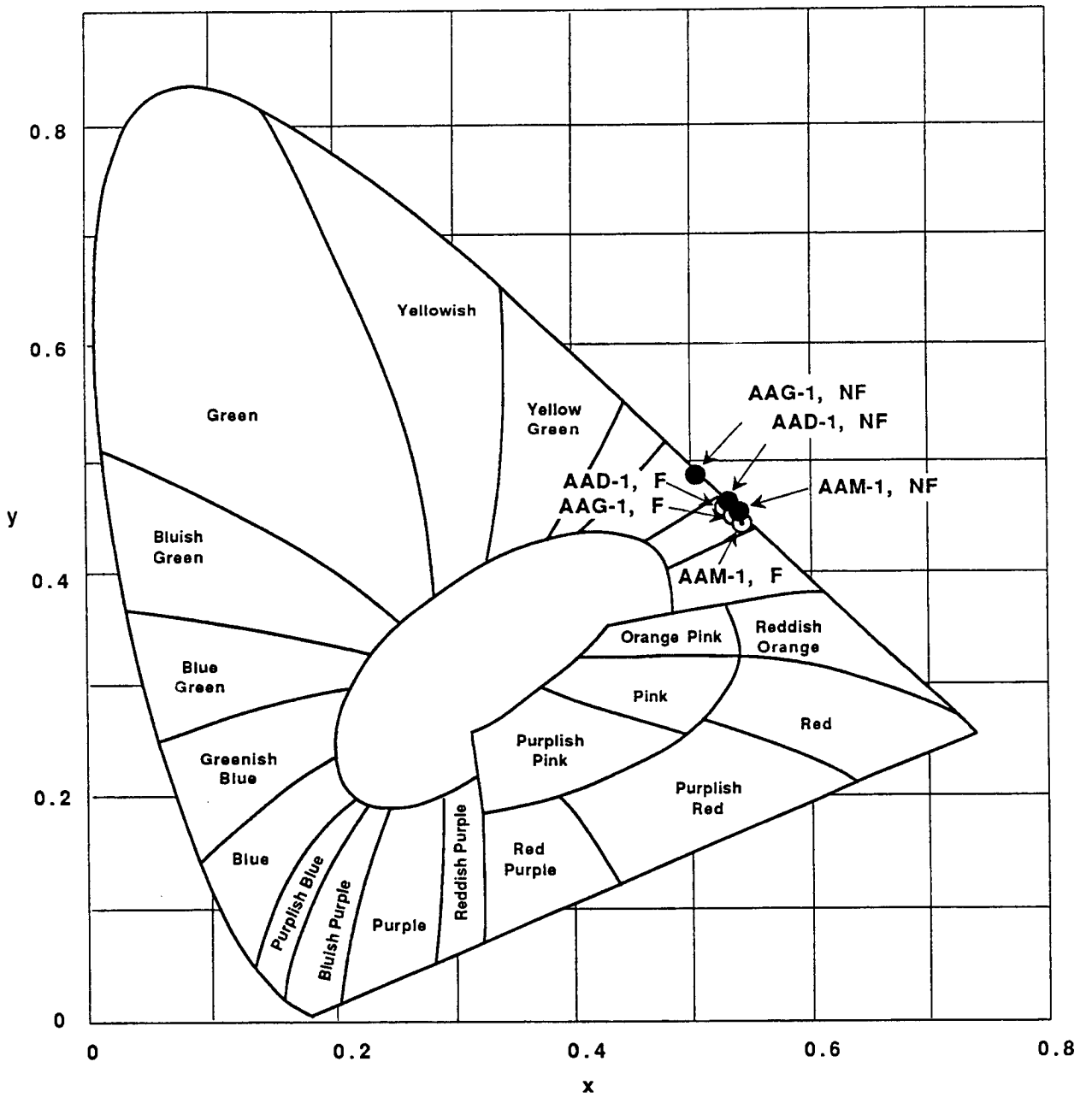

Figure 19. C.I.E. Chromaticity Diagram Comparing Emissions for Size Exclusion Chromatography Fluorescing (F) and Non-Fluorescing (NF) Fractions of the AAD-1, AAG-1 and AAM-1 Asphalts to Standard Illuminant A

aromaticity increased from AAD-1 to AAG-1, so the fluorescence intensity increased. As the neutrals fraction becomes dominated by aromatic compounds of high molecular weight (AAM-1), the higher concentration of π-bonds apparently results in some quenching of intensity and a shift of the peak wavelength toward the red. Intensity values of the IEC strong acids fraction were not greatly influenced by consideration of wavelength.

In an attempt to determine the extent to which the spectra of chemical fractions differed from those of their parent asphalt, a difference spectrum, like that depicted in Figure 16 was generated for each sample. The peak wavelength of these differences, their relative intensities and the percentage of the parent spectrum they represent are summarized in Table 8. In this table negative relative intensities represent those areas of the chemical fraction spectrum that were of higher intensity than the parent, whereas positive relative intensities represent areas where the chemical fraction spectrum were of lower intensity. In this and all subsequent characterizations only changes of ≥5% were considered significant. Thus, in Figure 16 there are three significant areas, two where intensities of the AAD-1 strong acids fraction were of lower intensity (positive) and one where it was higher (negative).

In general, the IEC neutrals fractions have greater relative intensities at lower wavelengths (509 nm) and much lower intensities at higher wavelengths (699-740 nm) compared with the parent spectrum. Of course this can readily be seen by simple observation of the spectra. However, in comparing the neutrals fractions from the three asphalts the data in Table 8 clearly showed that at lower wavelengths the AAG-1 neutrals fraction was three times more intensely fluorescent than the other samples (see percent of spectrum, Table 8), whereas at higher wavelengths half of the AAD-1, a quarter of the AAG-1, and 6% of the AAM-1 parent spectra were not accounted for by the neutrals fraction. In comparison, the IEC strong acids fraction exhibited three areas of difference; the strong acids spectra were slightly more intense in the 564-593 nm region and lower in the 511-530 nm and 710-731 nm regions compared with the respective parent spectra. These determinations suggest some similarities between the AAD-1 and AAM-1 strong acids fractions.

Spectral information derived from the SEC fluorescing and non-fluorescing fractions are compared in Table 6 and Figure 17. For these samples it was interesting to note that the fluorescing fractions all had peak fluorescence intensities at higher wavelengths than the non-fluorescing fractions. Particularly when considering that the fluorescing fractions were of relatively lower molecular weight and exhibited non-associated behavior. It was originally anticipated that the higher molecular weight fraction (non-fluorescing) would be more aromatic and would show peak fluorescence values at higher wavelengths because of a greater density of π-bonds. This was apparently not the case. The non-fluorescing fractions possess a

Table 8. Changes in Asphalt Fluorescence Intensity Resulting from Chromatographic Fractionation: Only Peak Intensity Differences >5% Are Noted

Asphalt Code	Area #1			Area #2			Area #3		
	Peak, nm	Relative Intensity, %	Percent of Spectrum	Peak, nm	Relative Intensity, %	Percent of Spectrum	Peak, nm	Relative Intensity, %	Percent of Spectrum
ION EXCHANGE CHROMATOGRAPHIC FRACTIONS									
AAD-1, Neutral	509	-18.8	3.2	699	86.4	50.0			
AAD-1, Strong Acid	511	47.2	4.3	564	- 6.6	1.0	710	53.0	22.4
AAG-1, Neutral	509	-65.2	11.2	710	59.2	28.7			
AAG-1, Strong Acid	530	9.8	1.1	593	- 8.0	1.4	710	33.2	12.3
AAM-1, Neutral	509	-18.8	3.4	740	48.0	5.9			
AAM-1, Strong Acid	514	50.8	4.4	568	- 9.8	1.8	731	90.8	31.2
SIZE EXCLUSION CHROMATOGRAPHIC FRACTIONS									
AAD-1, Fluor.	508	- 6.8	1.6	744	17.8	3.8			
AAD-1, Non-Fluor.	511	53.2	4.8	710	51.2	21.7			
AAG-1, Fluor.	514	-39.4	4.0	720	-12.4	2.0			
AAG-1, Non-Fluor.	512	6.6	0.4	546	-14.2	2.9	703	88.2	44.3
AAM-1, Fluor.	512	28.6	2.1	745	31.6	4.1			
AAM-1, Non-Fluor.	512	35.4	2.9	577	- 8.6	1.7	731	62.4	21.3

larger heteroatom content and most of the polar functional groups (IEC amphoteric fraction) compared with the fluorescing fractions. Therefore, it may be that the condensed π-bond network of the aromatic system served to reduce overall fluorescence intensity through quenching, but the heteroatoms and polar centers provided a dominant fluorescence at lower wavelengths.

The wavelength at maximum intensity for the SEC-fluorescing fractions compared closely with the mean value for a majority of the raw asphalts (Table 6). Also, the complete spectra were generally very similar to those of the raw asphalts. This may not be too surprising, when considering that this fraction comprised between 70-87% of the total asphalt and has been equated with the lower molecular weight solvent phase of asphalts which may be more aliphatic and contain less polar functionality. Thus, a lower concentration of fluorophoric material in this fraction may lead to less quenching, resulting in higher relative intensity values at a lower wavelength. Intensities at peak wavelength for the SEC fluorescing fractions (Table 6) change slightly and uniformly for all the asphalts compared with the intensity values measured at 600 nm, thus preserving the relationship of increasing intensity with aromaticity discussed during evaluation of the fluorometric data.

Information from difference spectra generated from the SEC fractions (Table 8) showed that the fluorescing fractions of AAD-1 and AAG-1 exhibited relatively more intensity at lower wavelengths (508-514 nm) compared with the parent spectra. At higher wavelengths (720-745 nm), only the fluorescing fraction of AAG-1 was more intense than the parent spectrum, AAD-1 and AAM-1 were both positive in this region. Overall, percentage differences between the SEC fluorescing fraction and the parent spectra were small. A greater difference was seen with the SEC non-fluorescing fraction. In these cases large differences were observed in the higher wavelengths (703-731 nm), with AAG-1 showing the greatest difference and AAD-1 and AAM-1 being very similar.

Chromaticity values for the IEC and SEC fractions are shown in Table 6 and values for illuminant A are plotted in Figures 18 and 19. Basically, all of these fractions fluoresced greenish-yellow, yellow or yellow-orange. The IEC strong acids and the SEC fluorescing fractions tended to plot at higher wavelengths (yellow-orange), whereas the IEC neutrals and SEC non-fluorescing fraction plotted at lower wavelengths. The reason for this separation and for the apparent similarity of the IEC neutral and the SEC non-fluorescing fractions may have resulted from their color purity. Color purity is a measure of color mixing and, in some respect, reflects the simplicity of the chemical system. Thus, these fractions have a relatively narrower spectrum as observed in Figures 15 and 17.

Conclusions

Spectral fluorescence analysis was completed on thirteen raw asphalts under blue-light irradiation using mercury-arc illumination. All but one of the asphalts (AAK-1) showed broad spectral emissions between ≈510 nm and ≈760 nm. In addition, the peak wavelength for 70% for the asphalts was found to lie between 664-672 nm with two having slightly lower peaks at 640 nm (AAD-1 and AAE) and two having significantly lower peaks (AAK-1 and ABD) at 544 nm and 600 nm. The fact that peak fluorescence wavelengths measured from spectral analyses were significantly different from the 600 nm used to measure asphalt intensity values, appeared to have little influence on our interpretation made from fluorometric analyses. This probably resulted from the broad and mostly uniform spectral emission within the 570-700 nm region for most of the asphalts. Spectral distributions collected on subsamples of different asphalts were highly reproducible.

The AAA-1, AAA-2 and AAE asphalts were from the same petroleum source but were of different grades as a result of processing. In particular, the AAE asphalt was air-blown during its manufacture, a technique used to increase the viscosity of an asphalt. The asphalt properties presumably result from oxidation and volatile loss. Spectral analysis of this set of asphalts showed that the AAE asphalt had a much narrower spectral distribution compared with spectra from AAA-1 and AAA-2 asphalt which were very similar. These results demonstrate that asphalt oxidation induced during manufacturing can be monitored by spectral fluorescence techniques.

Spectral analyses were performed on IEC and SEC chemical fractions to augment fluorometric analyses. Chromatographic fractions of three asphalts (AAD-1, AAG-1 and AAM-1) with markedly different properties were obtained from WRI. Fluorescence properties of the IEC neutrals fraction showed that as molecular weight and relative aromaticity of the fraction increased between AAD-1 and AAG-1, intensity values increased but the peak wavelength was similar. However, when the neutrals fraction became dominated by aromatic compounds of high molecular weight (AAM-1), the higher concentration of π-bonds resulted in some quenching of intensity and a red shift of the peak wavelength.

The SEC-I non-fluorescing fraction were reported to be of higher molecular weight, possess more heteroatoms and polar centers, and generally to exhibit associative behavior within an asphalt binder compared with the SEC-II fluorescing fraction. The SEC non-fluorescing fraction exhibited a much lower level of fluorescence intensity at 600 nm and had peak wavelengths that were typically lower than the fluorescing fraction. From this observation we suggest that the condensed π-bond network may be responsible for lower intensity values through quenching of the fluorescence emission, but that the higher concentration of polar centers may provide a dominant fluorescence at lower wavelengths.

References

1. Davis, A. and Mitchell, G.D. (1990). Fluorometric Characterization of Asphalts, Phase II Report, SHRP 88-AIIR-04.

2. Lin, R. and Davis, A. (1988). "The Chemistry of Coal Maceral Fluorescence: With Special Reference to the Huminite/ Vitrinite Group", Spec. Research Report SR-122, Energy and Fuels Research Center, The Pennsylvania State University, 278 pp.

3. SHRP A-002A (1989). Binder Characterization and Evaluation, Quarterly Report, December.

4. SHRP A-002A (1990). Binder Characterization and Evaluation, Quarterly Report, March.

CHARACTERIZATION OF AGED AND OXIDIZED ASPHALTS

Introduction

As discussed in previous sections, results from fluorometric analyses of laboratory aged/oxidized asphalts (Table 5) clearly showed that fluorescence intensity at 600 nm decreased with increasing level of aging. Furthermore, it has been shown that the influence of air-blowing the AAE asphalt on the fluorescence spectra was a narrowing of the distribution resulting from a loss of intensity at higher wavelengths (≈700-754 nm). This affect was attributed to oxidation and/or to loss of volatiles. The question remaining to be addressed was, "whether asphalt aging results in a significant and uniform change in the emission spectrum from blue-light irradiation"? Moreover, additional spectral and fluorometric analyses were conducted on SEC-I fractions separated from three aged asphalts and the issue of repeatability was addressed.

Thin-film oven test (TFOT) and TFOT-PAV residues of four asphalt (AAD-1, AAG-1, AAK-1 and AAM-1) representing short and long term field aging, respectively, were used. These samples were obtained from WRI and had remained in refrigerated storage under argon for several months prior to spectral analysis. Thus, in this section of the report, the spectral fluorescence characteristics of these aged asphalts was investigated. Further, to establish a chemical basis of asphalt aging on fluorescence properties, a series of SEC-I, non-fluorescing fraction residues from three asphalts (AAD-1, AAG-1 and AAM-1) were evaluated. These chemical fractions were obtained from TFOT-PAV (144h at 60°C) aged asphalts. It has been determined that pressure oxygen vessel (POV) aging of asphalts for 144h at 60°C was approximately equivalent to five years of field aging (1). Presumably, air oxidation for 144h in the pressure vessel (PAV) would be provide equivalent level of oxidation compared to the use of pure oxygen.

Experimental

The WRI aged samples were retrieved from refrigerated storage and allowed to warm to room temperature in a desiccator for two hours. Fluorescence spectral analyses were performed following the procedure outlined in the previous section. Duplicate fluorometric analyses were performed on these asphalts to establish the level of repeatability that could be anticipated from the quantitative fluorometric technique as well as to evaluate whether the samples may have deteriorated during storage. The SEC-I fraction samples of AAD-1, AAG-1 and AAM-1 were received as brittle solids and were mounted as individual particles as discussed previously.

Results and Discussion

Fluorescence spectra of the raw, TFOT aged and TFOT-PAV aged AAD-1, AAG-1, AAK-1 and AAM-1 asphalts are shown in Figures 20 through 23. The wavelengths of primary and minor peaks and the maximum intensity at 600 nm are given for each sample in Table 9. In comparison to the raw asphalts, these data showed that the wavelength of peak fluorescence for the AAD-1, AAG-1 and AAM-1 asphalts decreased when severely aged, whereas an increase in peak fluorescence was observed for the AAK-1 asphalt. Peak fluorescence for the short-term aged samples was more erratic and did not always follow the same trend observed for long-term aged samples.

As a possible explanation for change in peak fluorescence, the amounts of carbonyl and sulfoxide functional groups are given in Table 9 for each of the asphalts (2,3). As was evident during the evaluation of asphalt chromatographic fractions, the polar asphalt fraction (SEC-I, non-fluorescing) exhibited lower peak wavelengths. Therefore, as aging becomes more severe an increase in the polar functionality with an increased production of carbonyl and sulfoxides can be observed. Note that there was only a small increase in these functional groups during mild (TFOT) aging which could account for the more erratic shift in peak fluorescence. The increase in peak fluorescence observed for the severely aged AAK-1 asphalt may be a typical response for asphalts which naturally exhibit low peak fluorescence.

Estimations of maximum fluorescence intensity at the peak wavelength (from that measured at 600 nm) also are given in Table 9. These estimates show increased intensity by an average of 8.4% (ranging 2.3 to 18.2%). However, the resulting increase was found to be fairly uniform and does not alter our interpretation of decreasing intensity with increasing severity of aging.

Subtraction spectra, like that shown in Figure 16 were generated for each asphalt set. The change in intensity resulting from aging with respect to the parent asphalts are shown in Table 10. As was seen with the chemical fractions, the most significant spectral changes occurred at low (509-520 nm) and high (650-740 nm) wavelengths. However, the spectral changes observed from asphalt aging were not as great as those observed for chemical fractionation. For the AAD-1 and AAM-1 asphalts long-term aging tended to reduce emissions more significantly at higher wavelengths. For the AAG-1 and AAK-1 asphalts long-term aging resulted in an increase in emissions at higher wavelengths. In fact AAG-1 was different from the other asphalts in that there were three areas showing slightly increased emissions compared with its parent spectrum.

As discussed in previous sections, we suspected that the fluorometric intensity value of the original sample of AAG-1 was in error. As shown in Table 5 the initial value for AAG-1 (5.83% at 600 nm) was much lower than the TFOT residue fluorescence

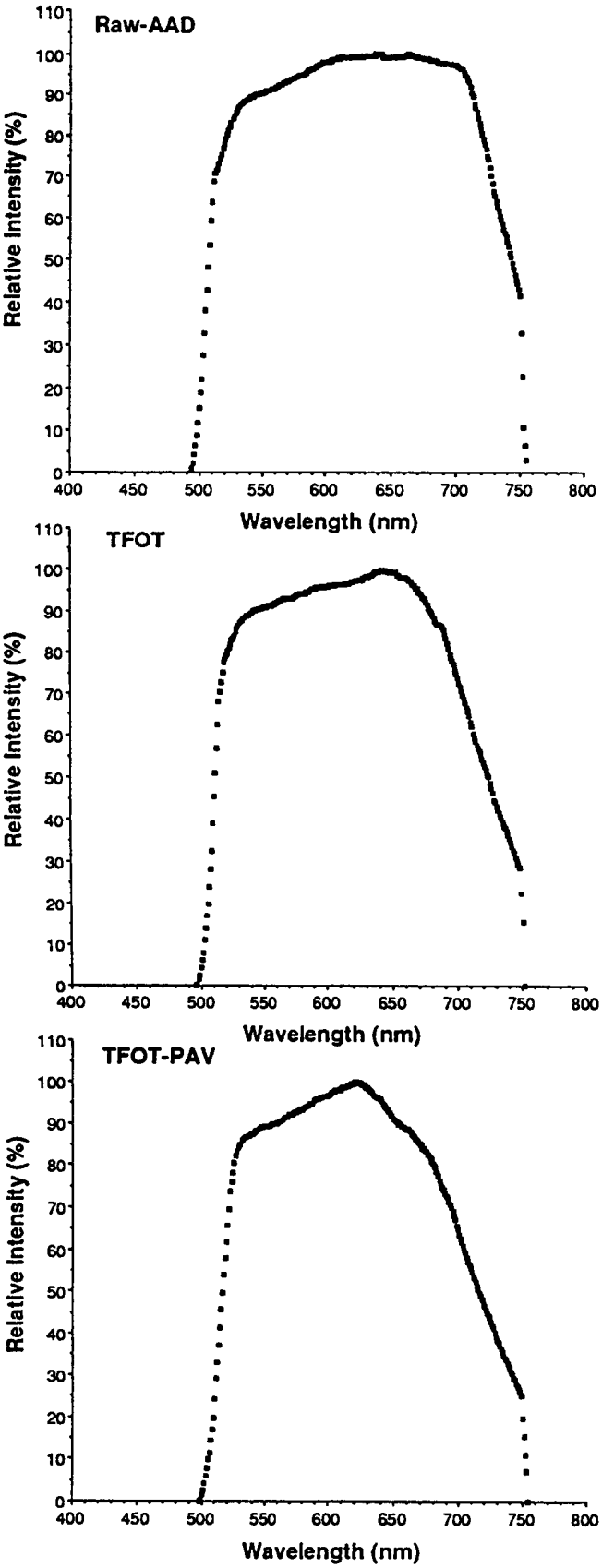

Figure 20. **Influence of Short (TFOT) and Long (TFOT-PAV) Aging on the Spectral Fluorescence of the AAD-1 Asphalt Using Blue-Light Excitation and Mercury-Arc Illumination in Dry Nitrogen**

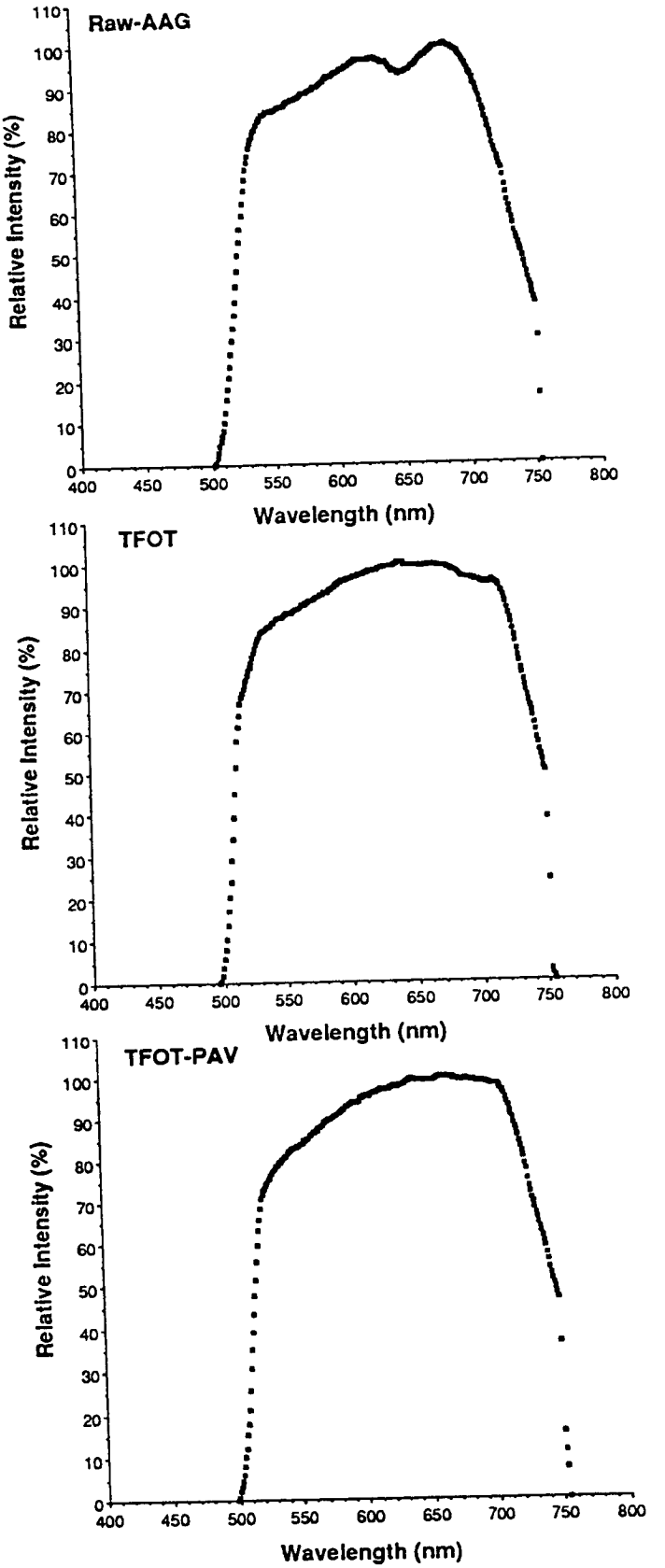

Figure 21. **Influence of Short (TFOT) and Long (TFOT-PAV) Aging on the Spectral Fluorescence of the AAG-1 Asphalt Using Blue-Light Excitation and Mercury-Arc Illumination in Dry Nitrogen**

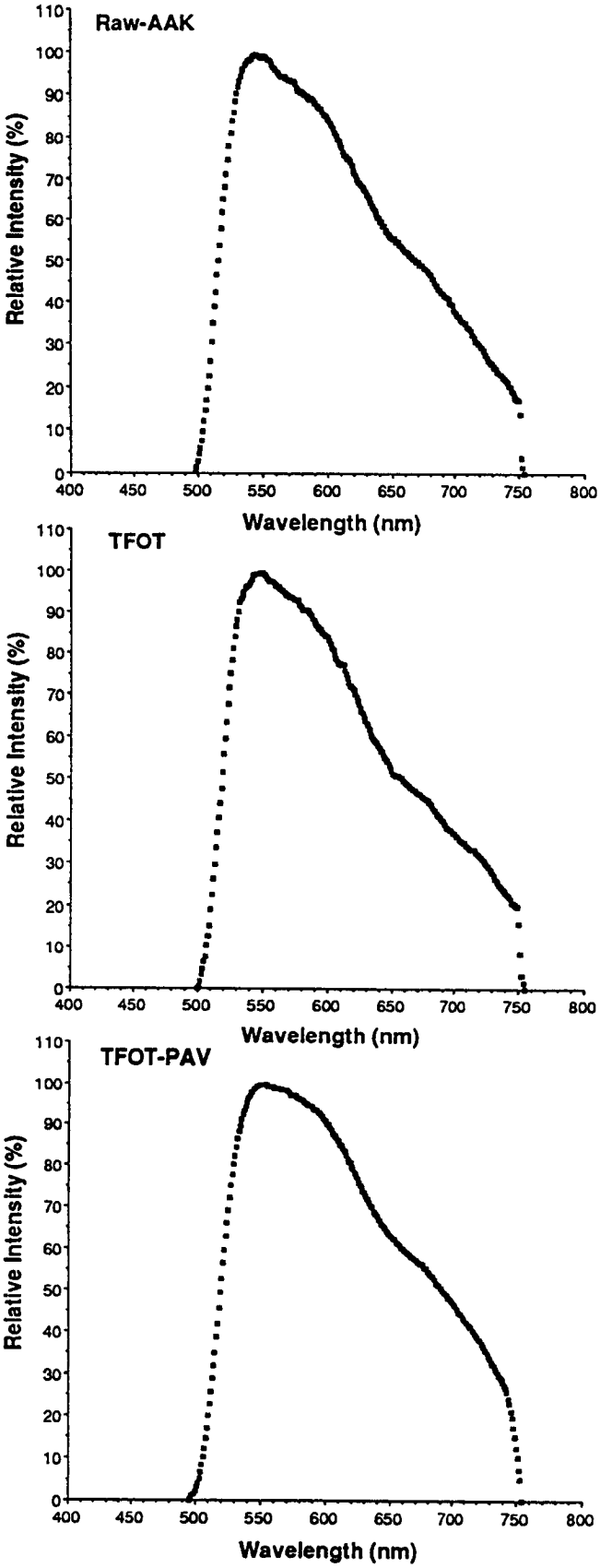

Figure 22. **Influence of Short (TFOT) and Long (TFOT-PAV) Aging on the Spectral Fluorescence of the AAK-1 Asphalt Using Blue-Light Excitation and Mercury-Arc Illumination in Dry Nitrogen**

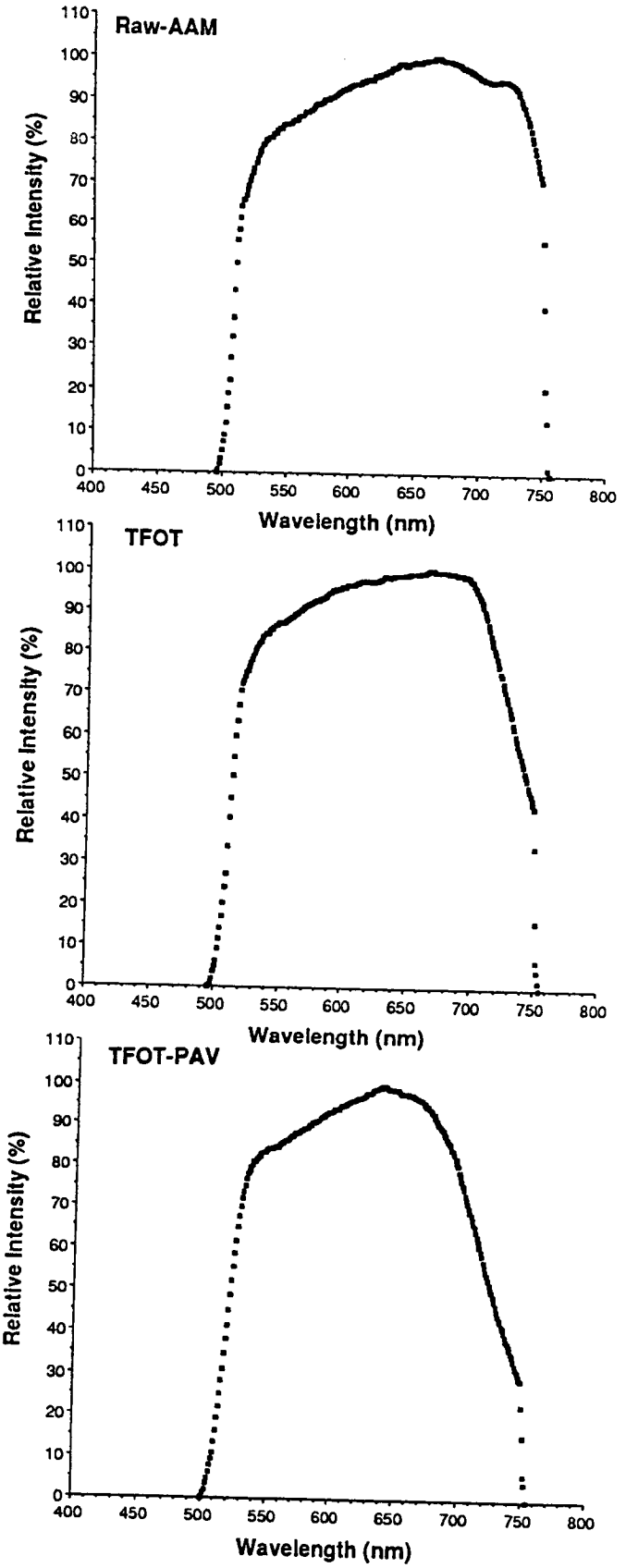

Figure 23. **Influence of Short (TFOT) and Long (TFOT-PAV) Aging on the Spectral Fluorescence of the AAM-1 Asphalt Using Blue-Light Excitation and Mercury-Arc Illumination in Dry Nitrogen**

Table 9. Peak Fluorescence and Intensity Changes with Aging

Asphalt Code	Fresh Asphalt					TFOT Aged 163°C/5 hr					TFOT-PAV Aging				
	Intensity at 600 nm Xenon, N_2		Primary (minor) Peaks, nm		Carbonyl, abs†	Sulfoxides, m/L†	Intensity at 600 nm Xenon, N_2		Primary (minor) Peaks, nm		Carbonyl, abs†	Sulfoxides, m/L†	Intensity at 600 nm Xenon, N_2		Primary (minor) Peaks, nm		Carbonyl, abs†	Sulfoxides, m/L†
AAD-1	10.06	(10.3)*	640	(664)	0.04	0.05	4.85	(5.1)	646		0.02	0.06	3.14	(3.3)	622	(661)	0.09	0.37
AAG-1	28.72	(29.9)	686		0.03	Trace	11.20	(11.7)	640	(710)	0.04	0.09	5.22	(5.5)	663		0.25	0.22
AAK-1	2.20	(2.6)	544		0.03	Trace	1.77	(2.1)	549		--	--	1.10	(1.2)	552		0.08	0.32
AAM-1	9.55	(10.3)	668		0.02	Trace	4.72	(4.9)	666		0.04	0.06	2.70	(2.9)	640		0.16	0.12

(*) Estimated Intensity at Peak Wavelength.

† Data from Ref. 3 and 4.

Table 10. Changes in Asphalt Fluorescence Spectral Intensity Resulting from Aging (Oxidation): Only Peak Intensity Differences >5% Are Noted

	Area #1			Area #2			Area #3		
Asphalt Code	Peak, nm	Relative Intensity, %	Percent of Spectrum	Peak, nm	Relative Intensity, %	Percent of Spectrum	Peak, nm	Relative Intensity, %	Percent of Spectrum
AAD-1, TFOT	509	26.6	1.48	713	29.0	7.11			
AAD-1, TFOT-PAV	511	39.8	2.90	710	38.6	11.31			
AAG-1, TFOT	514	-40.6	4.22	650	-6.2	0.97	736	-9.6	2.63
AAG-1, TFOT-PAV	519	-24.4	2.21	650	-5.8	0.85	735	-14.6	1.93
AAK-1, TFOT	518	10.2	1.41	650	4.4	1.91			
AAK-1, TFOT-PAV	520	12.4	1.97	717	-9.4	8.84			
AAM-1, TFOT	512	10.4	0.23	740	31.6	5.05			
AAM-1, TFOT-PAV	512	36.6	2.88	736	49.4	11.09			

value (11.20% at 600 nm). Because of this a new subsample of the AAG-1 asphalt was obtained from the SHRP Technical Assistance Contractor. Results for this sample given in Table 9 show that fluorescence intensity of the new subsample was nearly 400% greater than the original (i.e., 28.72 vs 5.83). With this change in fluorescence intensity, we can now say that asphalt aging (oxidation) uniformly results in a decrease fluorescence intensity. As shown in Figure 12, the fluorescence spectra from the two AAG-1 subsamples were also much different. Comparing the fluorescence spectrum from the original sample with those aged samples shown in Figure 21 and judging from the narrowing of the spectrum, it appears that the original asphalt was probably severely oxidized.

To establish confidence in the intensity analysis of aged asphalts, fluorometric analyses were repeated for the two sets of WRI samples. Intensity values for each sample are given in Table 11 along with the standard deviation calculated for the individual measurements. As can be seen, fluorescence intensity for the stored asphalts were slightly greater than the values initially measured (except for TFOT AAD-1 and AAK-1). Differences for the repeat analyses ranged from +0.01% to -0.23% and averaged 0.12%. This level of variation was significant with respect to the individual measurements, but was insignificant compared to the magnitude of the change in asphalt fluorescence resulting from aging.

Fluorescence spectra of the SEC-I fraction derived from fresh and TFOT-PAV aged AAD-1, AAG-1 and AAM-1 asphalts are compared in Figure 24 and the results summarized along with fluorometric intensity values in Table 12. Spectral distributions derived from the SEC-I fractions for the aged AAD-1 and AAM-1 asphalts were very similar to their fresh counterparts, whereas AAG-1 was much different. Spectral distributions were nearly unchanged for the AAD-1 and AAM-1 even though there was a substantial increase in MW and significant oxidation as shown from the sulfoxide and ketone concentrations. In the case of the AAM-1 SEC-I fraction the peak fluorescence appeared to decrease slightly, which is in response to the fact that under the optical microscope this SEC-I fraction was observed to be a two-phase system containing significant concentrations of the SEC-II fluorescing fraction. This observation also accounts for the increased fluorometric intensity measured for the AAM-1 SEC fraction, whereas intensity decreased for the fractions from the other two asphalts.

The spectral distribution of the AAG-1 asphalt was unique, in that in response to oxidation both major and minor peak intensity values increased to higher wavelengths. Thus, what had been a shoulder at 655 nm in the un-aged SEC fraction, became a major peak following aging. Normally we would associate this result with increased molecular weight and aromaticity, but for the aged AAG-1, SEC-I fraction MW was found to be lower (Table 12). When the AAG-1 asphalt becomes severely aged its SEC-I

Table 11. Repeat Fluorescence Intensity Analyses of Aged Asphalts from WRI

Type of Aging	Condition	Intensity, Xenon-N_2, 600 nm			
		AAD-1	AAK-1	AAG-1	AAM-1
Initial Intensity	Raw Asphalt	10.06 ± 0.02	2.20 ± 0.03	5.83 ± 0.01	7.20 ± 0.01
TFOT-163°C/5 hrs	Initial	4.85 ± 0.01	1.77 ± 0.01	11.20 ± 0.01	4.72 ± 0.01
	Stored	4.77 ± 0.02	1.76 ± 0.05	11.23 ± 0.03	4.95 ± 0.01
TFOT-PAV	Initial	3.14 ± 0.01	1.10 ± 0.01	5.22 ± 0.01	2.70 ± 0.01
	Stored	3.26 ± 0.01	1.19 ± 0.01	5.45 ± 0.01	2.89 ± 0.01

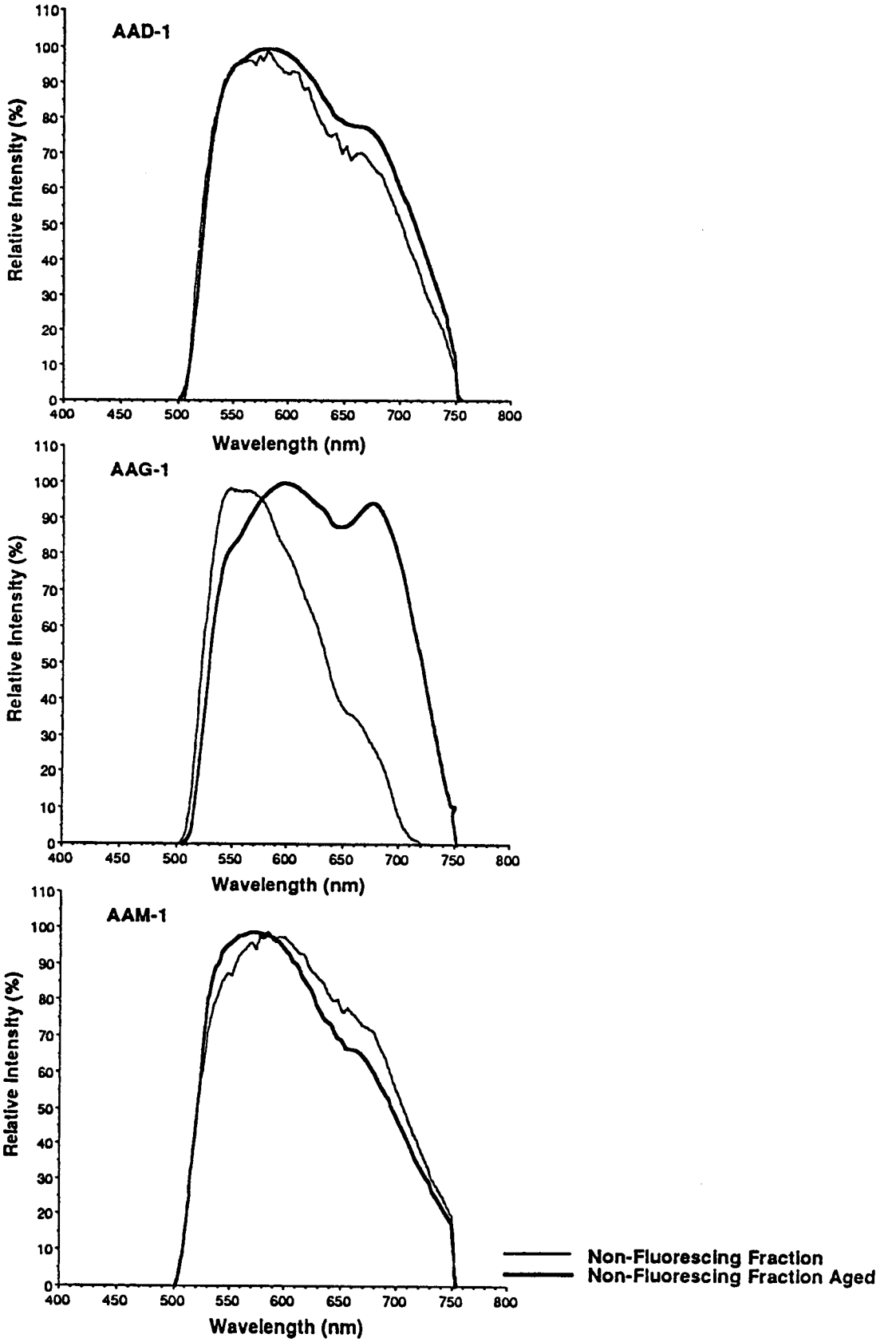

Figure 24. Fluorescence Spectra of the SEC-I Non-Fluorescing Fractions of the AAD-1, AAG-1 and AAM-1 Fresh and TFOT-PAV Aged Asphalts Measured Using Blue-Light Excitation and Mercury-Arc Illumination in Dry Nitrogen

Table 12. Comparison of SEC–I Non–fluorescing Fraction Samples from WRI, Separated from Fresh and TFOT–PAV Aged Asphalts

Asphalt Code	Chromaticity Ea x	Chromaticity Ea y	Measured Intensity Xenon, N_2	Primary Peak Fluor. nm	Minor Fluorescence Peaks (P) or Shoulders (S) nm	†wt%	†MW	†Sulfoxide Conc. (m/L)	†Ketone Conc. (m/L)
SEC–I, Non–fluorescing Fraction from Fresh Asphalts									
AAD–1	0.524	0.470	0.47	581	666P	23.4	7,000	–	–
AAG–1	0.500	0.493	0.27	548	655S	12.9	7,900	–	–
AAM–1*	0.532	0.462	0.81	585	644S	30.5	4,600	–	–
SEC–I, Non–fluorescing Fraction from TFOT–PAV Aged Asphalts 144h 60°C									
AAD–1	0.533	0.462	0.34	581	665S	27.4	13,710	0.56	0.09
AAG–1	0.550	0.446	0.23	598	676P	14.3	5,380	0.20	0.13
AAM–1*	0.523	0.470	1.12	574	660S	34.7	5,640	0.08	0.12

* Blend of non–fluorescing and fluorescing fractions

†Data from Ref. 4.

fraction begins to develop spectral similarity to its SEC-II fraction (see Figure 17). In terms of SEC separation, these results may suggest a higher component compatibility than the other asphalts studied.

Conclusions

A number of observations can be made regarding the influence of asphalt aging on their fluorescence properties. As the severity of aging increased fluorescence intensity at 600 nm decreased uniformly as viscosity and the amounts of carbonyl and sulfoxides increased. From repeat fluorometric analyses it appeared that the measured differences in asphalt fluorescence resulting from aging were significant. In terms of the spectral analysis, fluorescence spectra appeared to narrow and the primary peak decreased in wavelength for three out of the four asphalts (AAD-1, AAG-1 and AAM-1). The observed changes in fluorescence intensity and spectral distribution were consistent with an increase in the concentration of polar centers (as observed with the SEC-I non-fluorescing fraction) and asphalt oxidation (as observed from air-blowing of the AAE asphalt). Severe aging had only a minor influence on the spectral fluorescence of the SEC-I non-fluorescing fraction of three asphalts even though there was a significant increase in molecular weight as well as sulfoxide and ketone concentration. Evidence was found for a higher compatibility of the two SEC fraction upon aging. However, as seen previously for whole asphalts, increased heteroatom content resulted in decreased fluorescence intensity.

References

1. SHRP A-002A (1990). Binder Characterization and Evaluation, Quarterly Report, March.

2. SHRP A-002A (1990). Binder Characterization and Evaluation, Quarterly Report, June.

3. SHRP A-002A (1990). Binder Characterization and Evaluation, Quarterly Report, September.

4. SHRP A-002A (1991). Binder Characterization and Evaluation, Quarterly Report, March.

FLUORESCENCE PROPERTIES OF ASPHALT-AGGREGATE MIXTURES

Introduction

This portion of our research was designed to identify the degree and/or extent of absorption of asphalt binders when associated with different aggregate materials. Originally, we were to obtain a suite of some 15 asphalt/aggregate composites from the SHRP Technical Assistance Contractor for this evaluation. However, these samples were not forthcoming and alternative methods of evaluation were undertaken.

In a preliminary investigation (1), the influence of two different limestone aggregates on the fluorescence intensity of an asphalt binder (AAC-1) was studied. Asphalt/aggregate mixtures were prepared as mastics where the aggregate particle size was maintained below 74 μm and the volumetric blend was 50/50. These initial results showed that there was a 25-30% decrease in the fluorescence intensity of the AAC-1 asphalt shortly after it was mixed with either limestone aggregate. Although the limestone aggregates were of high and low absorption, no significant difference in fluorescence intensity was obtained. Also, no physical separation and/or sorption of the asphalt was observed for either aggregates. After a period of curing (<5 days), fluorescence intensity of the asphalt binders had decreased, but the decrease was not statistically significant compared with the initial values.

One conclusion that could be reached from this investigation, was that the observed decrease in fluorescence intensity may have resulted from an immediate interrelationship between the polar functional groups in the asphalt binder with the aggregate surface. Selective removal (by migration to the aggregate surface) of these fluorophoric functional groups from the binder may effectively reduce fluorescence intensity. An alternative interpretation was that the aggregate may be acting as a diluent which physically reduces fluorescence intensity by its presence.

With this in mind, the direction of our research was changed to employ mastics for the characterization of asphalt/aggregate mixtures. We also found it necessary to address the potential influence of dilution by measuring the effect on fluorescence of the introduction into the binder of particulate material with a fairly inactive surface (teflon).

Experimental

Four aggregates were obtained from the Technical Assistance Contractor (TAC), including RC (high absorption limestone), RD (low absorption limestone), RB (granite) and RJ (gravel). Table 13 provides some of the chemical, mineralogical and physical

Table 13. Summary of Properties of Materials Reference Library Aggregates

Test	RB* Granite	RC Limestone	RD Limestone	RJ Gravel
Major Oxides, %				
Silicon Dioxide	56.2	11.8	14.8	63.98
Aluminum Oxide	19.8	1.5	1.95	14.6
Ferric Oxide	6.49	0.89	0.96	4.54
Calcium Oxide	8.87	35.04	33.71	6.09
Magnesium Oxide	2.60	11.76	11.43	1.52
Sulfur Trioxide	--	0.48	0.43	0.10
Sodium Oxide	3.04	0.21	0.08	1.67
Potassium Oxide	0.44	0.51	2.00	3.31
Titanium Dioxide	0.51	0.18	0.21	0.41
Phosphorus Pentoxide	0.06	< 0.01	< 0.01	0.11
Manganic Oxide	0.12	0.03	0.02	0.13
Loss on Ignition	1.98	37.64	34.45	3.54
X-Ray Diffraction Major Minerals:	Quartz Feldspar Epidote	Calcite Dolomite Quartz	Calcite Dolomite Quartz	Quartz Potassium Cyanide Albite Sodium Acetate
Surface Area M^2/g:*	0.83	1.78	0.43	0.37
Porosity, ASTM D-4404				
Avg. Pore Dia. ($M \times 10^{-6}$)	--	0.0611	0.0111	0.0151
Total Pore Area (M^2/g)	--	2.548	1.465	1.888
L.A. Abrasion, AASHTOT-96, % Wear	29.7	39.1	23.4	29.5
% Water Absorption, AASHTOT-84, T-85	1.0	3.7	0.3	0.7
Specific Gravity, AASHTOT-84, T-85				
Bulk	2.742	2.536	2.704	2.625
Saturated Surface Dry	--	2.595	2.717	2.646
Apparent	2.281	2.682	2.739	2.680
Sand Equivalent, % (AASHTOT-176)	88	32	69	60
% Acid Insoluble Residue, (ASTM D-3042)	--	4.8	18.1	99.2

*Measurements made by Univ. of Cal., Berkeley. Other values by Southwestern Laboratories.

properties of the aggregates. Also, three of the four aggregates (RC, RD, and RJ) were SHRP core aggregates. One quart of each of these samples was received and found to be of variable particle size (<1 mm). Approximately one quarter of each aggregate was split from the head sample and stage-crushed to minimize the production of fines passing a 200 mesh (<74 μm) screen. In addition, four fresh asphalts were obtained from the TAC, these included samples of AAA-1, AAG-1, AAM-1 and ABD (which is the AAG-1 product without addition of caustic). These asphalts and aggregates were the basis of our fluorometric evaluation of asphalt/aggregate mixtures.

Mastics were prepared by forming a 50/50% volumetric mixture of each asphalt and aggregate following the same methodology. To do this, the density of each dry aggregate was determined at its specific particle size using the volume displacement method with methanol. The measured densities for each -74 μm aggregate compared with the bulk value obtained from the TAC in parentheses were as follows:

RB - 2.78 g/cm^3 (2.74)

RC - 3.22 g/cm^3 (2.54)

RD - 3.34 g/cm^3 (2.70)

RJ - 2.86 g/cm^3 (2.62)

About 50 g of each aggregate were measured into a steel can (≈550 cm^3) and dried in an oven at 150°C for 10h. A fresh subsample of asphalt was heated using our standard procedure (137°C for 2h with hourly stirring). When the asphalt was thoroughly heated and homogenized, each aggregate in turn was removed from the oven and while still hot an appropriate amount of asphalt was weighed into the aggregate. Depending upon the dry weight of each aggregate between 15.5 g and 18 g of asphalt was added. Asphalt-aggregate mixtures were stirred until aggregate particles were wetted with asphalt (≈5 min). As the mixture cooled it stiffened and in some cases the stirring became kneading. Subsamples of the mixture were then placed into preheated 2.5 cm diameter steel molds fitted with steel end caps and pressed under 4000 psi using a hydraulic press.

Two cylindrical samples of each mastic were prepared, one for fluorometric analysis and the other for spectral analysis. While still in their molds, samples were placed in multilaminate foil bags under argon and refrigerated (-5°C) overnight. The following day samples were pushed from their molds and the sides and one end were covered with masking tape and labelled, whereas the exposed end was lightly rubbed on 600 grit abrasive paper to reveal interfaces between asphalt and aggregate. Samples were allowed to warm to room temperature in a desiccator before analysis.

In addition to the aggregates, mastic-like samples were prepared at the same time using either glass beads or teflon boiling chips. It was hoped that these materials would provide relatively inert surfaces with regard to asphalt sorption such that we might be able to study the influence of dilution. Glass beads (≈0.8 mm dia.) were used initially during the preparation of the AAG-1 asphalt; however, the mixture did not produce a competent sample for microscopy. In subsequent preparations with the AAA-1, ABD and AAM-1 asphalts teflon boiling chips (<1 mm dia.) were used more effectively. Presumably, because the chips had a more irregular surface, asphalt/teflon mastics were competent. These samples were handled in the same manner as the aggregates.

Fluorometric and spectral analyses were performed on all mastics of a given asphalt on the day following preparation. Fluorescence intensity was determined using the standard procedure (e.g., measurement of emission at 600 nm following blue-light irradiation using xenon excitation in dry nitrogen). However, from our preliminary investigation it was found that a total of 50 readings were necessary to obtain repeatable mean fluorescence intensity values from the asphalt binder when aggregate materials were present. Spectral analyses were conducted using the technique described in previous sections of this report. Using both techniques, areas to be irradiated were selected using white-light illumination so as to minimize overlap with aggregate particles. However, in practice this was very difficult to achieve, especially for the spectral fluorescence which uses a very much larger measuring spot size. Test measurements were performed to determine whether asphalt binder areas could be selected in blue light before measurement without influencing the overall intensity of the reading. It was found that there was no measurable difference in fluorescence intensity using this approach when irradiated under a nitrogen atmosphere.

Repeat fluorometric analyses also were performed on two sets of mastics. For the AAA-1 mastic set an additional set of samples was prepared at the time of the original preparation. These samples, undisturbed in their steel molds, were refrigerated under argon for about 1500h before being removed and prepared for microscopy. In addition, one of the original sets of the AAA-1 mastic that had been exposed to air under room conditions (protected from light) for 1532h was analyzed to determine what influence short-term aging/curing might have on binder fluorescence intensity. A similar approach was used with the AAM-1 mastic set, except that the once-heated asphalt was reheated and a new set of mastics prepared. Fluorometric analyses of this set of samples was compared to an original set exposed to room conditions for 2420h. The exposed mastic samples were prepared for intensity measurements by cooling the sample and then removing the surface layer by gently rubbing the exposed surface on 600 grit abrasive paper.

Results and Discussion

Samples of each aggregate were prepared as standard petrographic cylindrical briquettes for reflected-light microscopy using a cold-setting epoxy resin. No strongly fluorescent minerals were observed during qualitative evaluation of these samples in white and blue light. However, some of the particles in the RC (limestone) aggregate had a very slight brown fluorescence, whereas particles in the RB (granite) and RJ (gravel) aggregates exhibited only a dull fluorescence which, in part, may result from the juxtaposition of the highly fluorescent epoxy with transparent quartz grains. Relative to the other aggregates, the RD (limestone) aggregate was observed to be non-fluorescent.

Close inspection of the asphalt/aggregate mixtures under blue light predominantly showed non-fluorescing, angular aggregate particles surrounded by the yellow-orange to orange fluorescing asphalt binder. Areas of binder that were free of aggregate particles were typically chosen for fluorometric or spectral measurement. However, a second fluorescing material was observed in some of the samples. This phase was distinguished by a bright green fluorescence, small particle size (<20 μm) and relatively low concentration (<0.5% visual estimated). About 60% of this material appeared to be isolated particles within the asphalt binder phase, whereas the remainder appeared to be associated with aggregate particle surfaces and fractures. Because of the particle size an accurate measurement of intensity or spectrum could not be obtained. Furthermore, no relationship was observed between aggregate type or asphalt and the presence of this green fluorescing phase. Although it appeared to be randomly distributed among mastic samples (including those made with teflon), it may very well be of importance in latter studies. The only reason for mentioning this phase is to point out that asphalt areas containing it were avoided and measurements in close proximity to the phase were rejected.

Intensity values measured using our fluorometric technique are given in Table 14 for each asphalt/aggregate mixture along with the primary and minor peak wavelengths obtained from spectral analysis. In addition, intensity values estimated for the peak wavelengths are provided for each sample. Generally, these data show that the addition of aggregate to a diversity of asphalt binders results in a rapid (within 17h) and significant decrease in fluorescence intensity at 600 nm. In comparison, a much smaller decrease in intensity was observed when teflon was used as the aggregate, suggesting that neutralization of fluorophoric emissions in asphalt binders may be limited in the presence of a relatively inactive surface like teflon.

Table 15 shows the percentage decrease in intensity for each asphalt/aggregate mixture tested. From this consideration, it appears that the asphalt binder exerts a greater influence on mastic fluorescence properties compared to the aggregates. That

Table 14. Peak Fluorescence of Raw Asphalt and Mastics and Intensity Values at 600 nm

Asphalt Code	% Intensity Values at 600 nm and Primary and Minor Peaks in nm											
	Raw		RB-Granite		RC-Limestone		RD-Limestone		RJ-Gravel		Teflon	
	Intensity	Peak (nm)	Intensity	Peak (nm)	Intensity	Peak (nm)	Intensity	Peak (nm)	Intensity	Peak (nm)	Intensity	Peak (nm)
AAA-1	11.72%	664	7.44%	665	7.85%	677	7.65%	670	7.72%	665	11.13%	664
	(12.3%)*	720 MP	(7.9%)	--	(8.4%)	--	(8.2%)	--	(8.2%)	--	(11.7%)	719 MP
ABD	20.90%	600	14.15%	556	13.50%	552	12.65%	553	12.86%	555	17.79%	598
	(20.9%)	681 MP	(15.5%)	682 MP	(14.9%)	683 MP	(14.3%)	685 MP	(14.4%)	686 MP	(17.8%)	682 MP
AAG-1	28.7%	686	16.18%	559	16.83%	555	16.61%	558	15.00%	556	Not Prepared	
	(29.9%)	631 MP	(16.9%)	681 MP	(18.0%)	681 MP	(17.7%)	684 MP	(16.3%)	682 MP		
AAM-1	9.55%	668	5.23%	607	5.62%	676	5.66%	665	5.40%	668	7.44%	668
	(10.3%)	720 MP	(5.3%)	--	(6.0%)	--	(6.0%)	--	(5.8%)	--	(8.0%)	716 MP

MP = Minor Peak

(*) Intensity at Peak Wavelength.

Table 15. The Percentage Decrease in Asphalt Binder Fluorescence Intensity Resulting from the Addition of Aggregates

Asphalt Code	% Change in Fluorescence Intensity					
	RB-Granite	RC-Limestone	RD-Limestone	RJ-Gravel	Average Decrease	Teflon
AAA-1	36.5	33.0	34.7	34.1	34.6	5.0
	(35.8)*	(31.7)	(33.3)	(33.3)	(33.5)	(4.9)
ABD	32.3	35.4	39.5	38.5	36.4	14.9
	(25.8)	(28.7)	(31.6)	(31.1)	(29.3)	(14.8)
AAG-1	43.6	41.4	42.1	47.7	43.7	--
	(43.5)	(39.8)	(40.8)	(45.5)	(42.4)	
AAM-1	45.2	41.2	40.7	43.4	42.6	22.1
	(48.5)	(41.7)	(41.7)	(43.7)	(43.9)	(22.3)

(*) Intensity at Peak Wavelength.

is, the average decrease in fluorescence intensity was different for each asphalt with AAA-1 (or ABD if peak intensity estimates are used) being the lowest and AAG-1 being the greatest. For each binder, the percentage change in intensity did not differ significantly from one aggregate to the next. Further there was no single aggregate that consistently showed a higher or lower intensity value. The AAA-1 and ABD mastics exhibited smaller decreases in intensity and were more similar compared with the AAG-1 and AAM-1 mastics which showed greater changes in intensity.

Within these two groups there were some minor relationships between intensity changes and aggregate types. For example, there were similarities in the percentage change in intensity between mastics made with RD and RJ in the AAA-1/ABD set, whereas there were minor similarities for the RC and RD mastics in the AAG-1/AAM-1 set. These similarities appear to hold up regardless of the intensity values used (intensity at 600 nm or the estimated intensity at peak wavelength). Unfortunately, in comparison with the physical and chemical properties of the aggregates reported in Table 13, no satisfactory explanation for these pairings can be offered.

Fluorometric intensity analyses were repeated for two of the mastic sets (AAA-1 and AAM-1) and the results are shown in Table 16. As discussed, different procedures were used to obtain new samples for testing. The results from these analyses are compared with other mastic samples that were aged/cured at room temperature. The AAA-1 set of mastics was used to study the influence of storage in argon under refrigeration. Analysis of the raw AAA-1 asphalt in Table 16 compare very closely with our earlier storage study of this asphalt reported in Table 4. For the asphalt/aggregate mixtures (AAA-1 set) a general increase in intensity ranging from 0.01% to 0.66% was observed. An average increase of 0.36% intensity was measured for the mastic samples (excluding teflon) following storage. This difference probably represents more analytical error than physical/chemical changes to the asphalt binder during storage. Thus, it appears that somewhat less than 3% of the 35% decrease in fluorescence intensity observed with the addition of inorganic aggregates to the AAA-1 asphalt may result from storage effects and/or measuring variation.

A slightly different response was observed by reheating the AAM-1 asphalt to prepare a third set of mastics. First, there was a relatively large decrease in the fluorescence intensity of the raw asphalt which may be a result of oxidation and/or volatile loss from the asphalt. Secondly, for the asphalt/aggregate mixtures there was mostly a decrease in fluorescence intensity ranging from 0.01% to 0.72% (AAM1-RC increased 0.01%). There was an average decrease of 0.22% intensity which could be attributed to mastic preparation or to analytical errors. Therefore, about 2% of the ≈43% decrease in

Table 16. Repeat Analyses and Influence of Aging/Curing of Raw Asphalt and Mastics on Fluorescence Intensity at 600 nm

Condition	Intensity, Xenon-N_2, 600 nm					
	Raw Asphalt	RB-Granite	RC-Limestone	RD-Limestone	RJ-Gravel	Teflon
AAA-1 Asphalt						
Original	11.72 ± 0.01	7.44 ± 0.06	7.85 ± 0.04	7.65 ± 0.05	7.72 ± 0.07	11.13 ± 0.04
RA-Stored (1508 hrs)	11.53 ± 0.01	7.86 ± 0.07	7.86 ± 0.03	8.02 ± 0.04	8.38 ± 0.06	10.94 ± 0.04
Exposed (1532 hrs)	7.56 ± 0.01	5.50 ± 0.04	5.73 ± 0.02	6.39 ± 0.03	6.10 ± 0.04	7.75 ± 0.06
AAM-1 Asphalt						
Original	9.55 ± 0.01	5.23 ± 0.05	5.62 ± 0.04	5.66 ± 0.04	5.40 ± 0.03	7.44 ± 0.04
Reheat (2396 hrs)	8.84 ± 0.01	5.08 ± 0.04	5.63 ± 0.04	4.94 ± 0.03	5.39 ± 0.04	7.07 ± 0.04
Exposed (2420 hrs)	5.66 ± 0.01	3.77 ± 0.02	3.99 ± 0.02	3.84 ± 0.02	3.99 ± 0.02	5.19 ± 0.02

intensity resulting from the addition of aggregates to the AAM-1 asphalt may be attributed to analytical errors.

When both sets of mastics were allowed to age/cure exposed to room conditions a significant decrease in fluorescence intensity was observed. On average the mastics made from AAA-1 lost slightly more intensity than those made with the AAM-1 asphalt, i.e., 1.74% vs 1.58%. Unfortunately the differences observed in measured intensity among the different mastics are not much greater than the variation found during the repeat analyses. Therefore, no conclusion can be reached regarding the influence of different aggregates on the setting characteristics of the asphalt/aggregate mixtures. From this it must again be concluded that the type of aggregate used in our mastic preparation has much less of an influence on changes in fluorescence properties compared with the type of asphalt used.

Comparison of fluorescence spectra are given for each asphalt and mastic in Figures 25 through 28. Primary and minor peak wavelengths have been determined from these spectra and appear in Table 14. The figures show that mastics made from asphalts AAA-1 and AAM-1 were more similar to each other than to ABD and AAG-1. In comparing the peak wavelengths of these sets there was perhaps a slight increase in peak fluorescence wavelength for the AAA-1/AAM-1 set with the addition of inorganic aggregate materials. However, the converse was found to be true for the ABD/AAG-1 set where a consistent and significant decrease in peak wavelength was observed following aggregate addition. Note that in each case the use of teflon in the mastic preparation had little significant influence on peak wavelength compared with the spectra of the raw asphalt.

Table 17 provides the relative change in the fluorescence spectra by wavelength for each mastic compared with the parent asphalt. As discussed in previous sections, most of the spectral changes occurred at the lower (509-553 nm) and higher (665-737 nm) wavelengths. Also, changes observed in spectral distribution (percentage of spectrum) were relatively small compared with changes observed from chromatographic fractionation or from asphalt aging. As with the peak wavelength, spectral changes resulting from aggregate addition showed that the AAA-1/AAM-1 and the ABD/AAG-1 sets exhibit similarities. Further, there did not appear to be an overwhelming influence of any one aggregate on spectral changes. The AAA-1/AAM-1 set showed more variability among the aggregates, but generally displayed a consistent loss in intensity at shorter and longer wavelengths with that between 729-737 nm being more significant. For the ABD/AAG-1 set, addition of aggregate resulted in a slight increase in intensity at shorter wavelengths (532-553 nm) and a decrease at longer wavelengths. Therefore, for both sets of mastics a blue shift was observed that appeared to be more meaningful for the ABD/AAG-1 set.

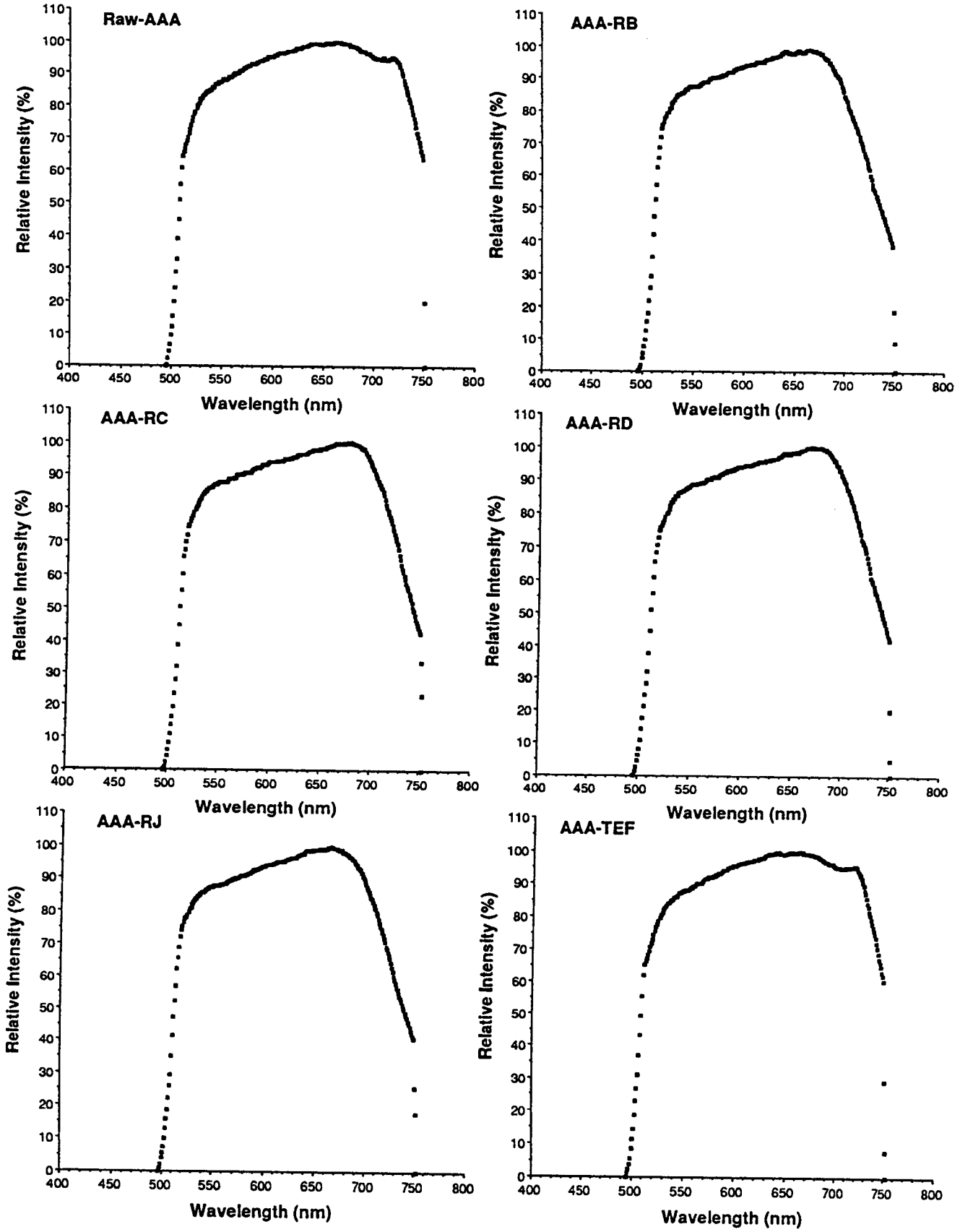

Figure 25. Fluorescence Spectra of Raw AAA-1 Asphalt and Mastics Using Blue-Light Excitation and Mercury-Arc Illumination in Dry Nitrogen

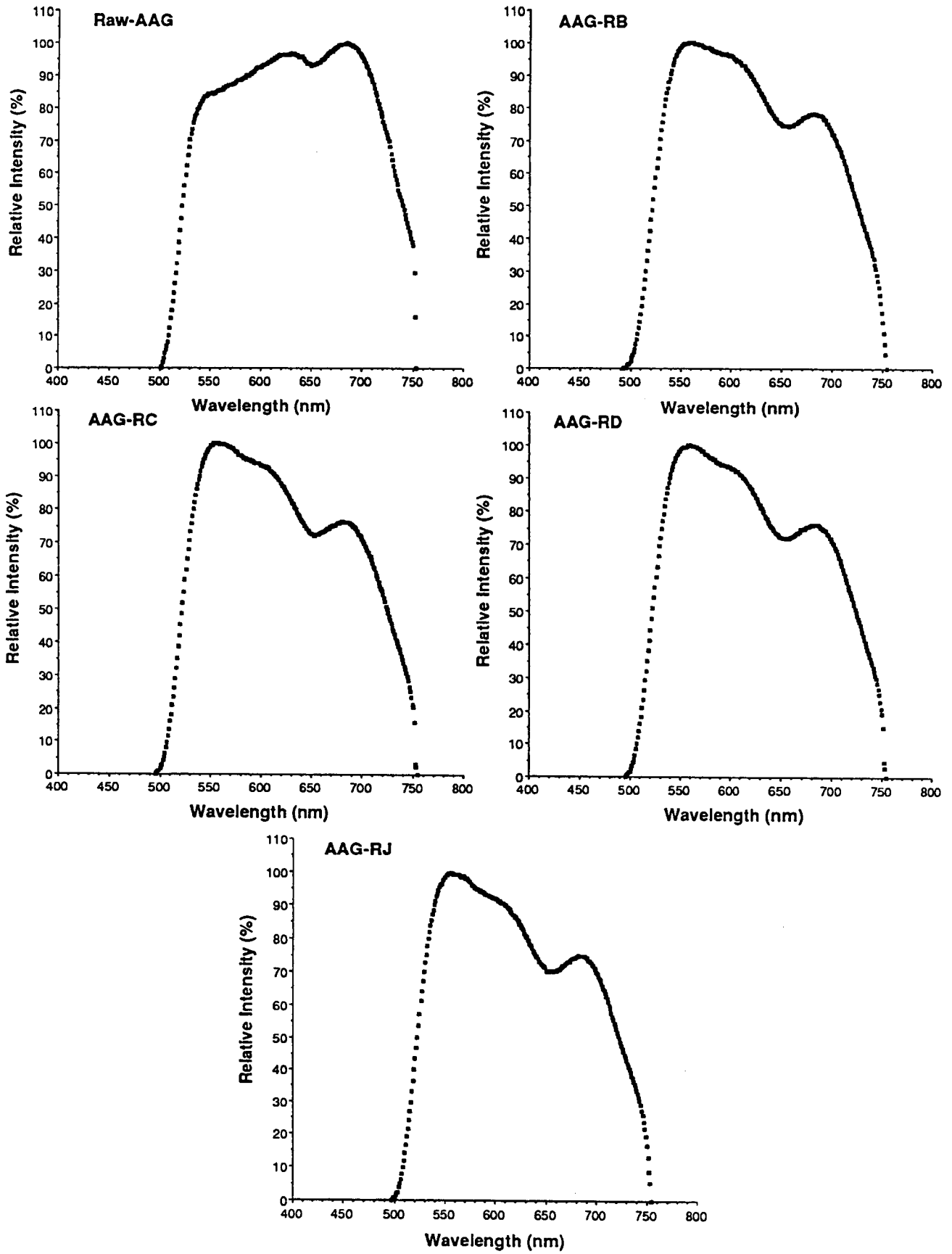

Figure 26. Fluorescence Spectra of Raw AAG-1 Asphalt and Mastics Using Blue-Light Excitation and Mercury-Arc Illumination in Dry Nitrogen

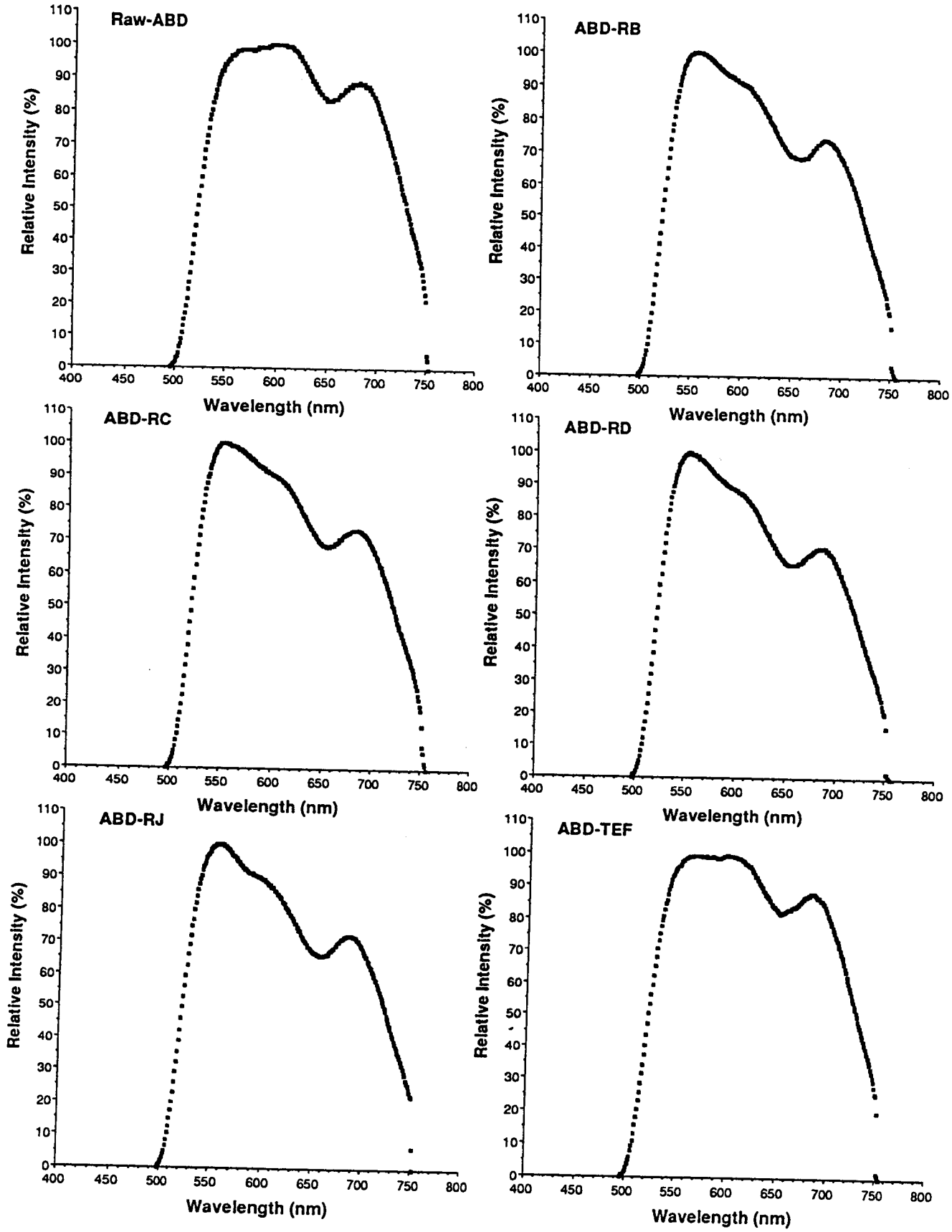

Figure 27. Fluorescence Spectra of Raw ABD Asphalt and Mastics Using Blue-Light Excitation and Mercury-Arc Illumination in Dry Nitrogen

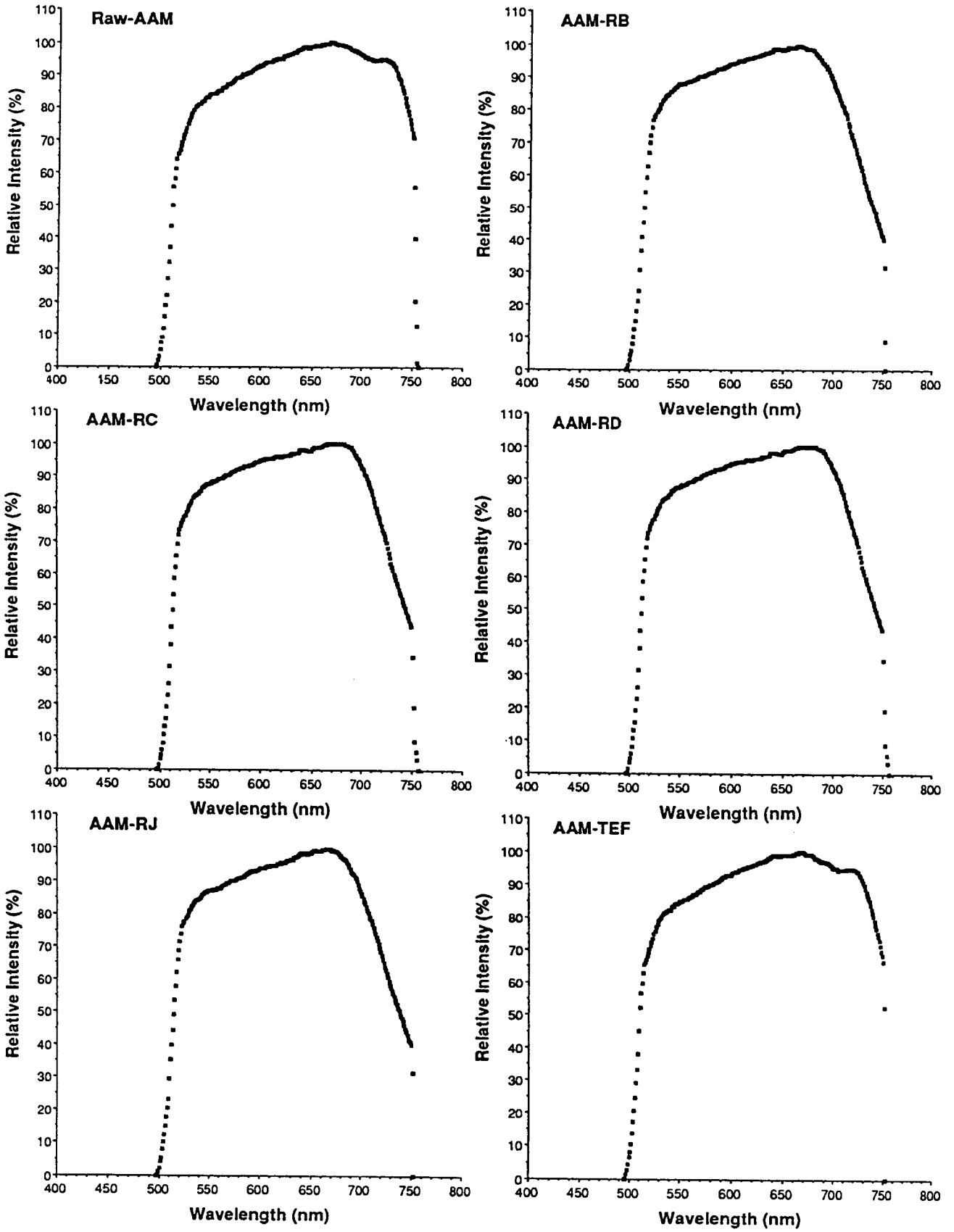

Figure 28. Fluorescence Spectra of Raw AAM-1 Asphalt and Mastics Using Blue-Light Excitation and Mercury-Arc Illumination in Dry Nitrogen

Table 17. Changes in Asphalt Fluorescence Spectral Intensity Resulting from Interaction with Different Aggregates: Only Peak Intensity Differences > 5%

Asphalt & Aggregate Codes	Area #1			Area #2		
	Peak, nm	Relative Intensity, %	Percent of Spectrum	Peak, nm	Relative Intensity, %	Percent of Spectrum
AAA-1, RB	509	21.6	1.02	729	32.8	6.08
AAA-1, RC	509	18.8	0.86	730	26.2	4.18
AAA-1, RD	509	19.0	0.83	730	28.6	4.60
AAA-1, RJ	509	21.6	1.02	730	30.6	5.38
AAA-1, Teflon	-- none --					
ABD, RB	539	-6.6	1.14	666	17.7	10.35
ABD, RC	539	-7.2	1.21	665	16.7	10.51
ABD, RD	536	-7.3	1.23	665	19.7	12.82
ABD, RJ	532	-7.5	1.25	667	19.2	12.09
ABD, Teflon	-- none --					
AAG-1, RB	553	-15.2	1.77	705	23.8	12.53
AAG-1, RC	553	-15.6	1.66	705	25.0	13.64
AAG-1, RD	553	-15.0	1.56	703	24.8	13.82
AAG-1, RJ	553	-15.2	1.36	705	26.0	14.76
AAM-1, RB	522	-17.1	5.67	736	49.1	14.28
AAM-1, RC	512	12.2	0.57	736	31.4	4.98
AAM-1, RD	512	18.4	0.86	737	35.2	6.68
AAM-1, RJ	512	15.8	0.75	736	36.4	6.98
AAM-1, Teflon	--	--	--	752	39.6	0.69

As was shown from fluorescence intensity measurements, spectral fluorescence of the asphalt binder was not greatly influenced by the addition of teflon. These results suggest that the fluorescence properties of asphalts may be influenced partially be dilution, but that the larger component of change appeared to result from the interaction of asphalt and inorganic aggregates.

Conclusions

Preliminary findings of our investigation with asphalt-aggregate mixtures showed that there was a very rapid decrease in fluorescence intensity and a narrowing of the spectral distribution which was comparable to the effects observed from asphalt aging (oxidation). This decrease in intensity was observed within 17h of mastic preparation. Additional curing/aging time of the mastics at room temperature resulted in a further significant decrease in intensity values. However, we were unable to detect any significant influence of the different aggregates on the fluorescence properties of the asphalt binder. Instead, the asphalts used appeared to exert a greater influence on the final fluorescence properties of the mastics. Further, the use of teflon in mastic preparation had little influence on peak wavelength, spectral distribution or fluorescence intensity, thus suggesting that effects of dilution are minimal and that an active surface is necessary to alter asphalt fluorescence properties. These findings seem to run counter to those of other SHRP contractors that have found rather large differences in the adsorptive properties of various aggregates (2). However, our findings may be influenced by the sample preparation techniques or by aggregate particle size.

References

1. Davis, A. and Mitchell, G.D. (1990). Fluorometric Characterization of Asphalts, Phase II Report, SHRP 88-AIIR-04.

2. Jeon, Y.W. and Curtis, C.W. (1990). The Adsorption of Asphalt Functionalities on Aggregate Surfaces, Prepared for SHRP under SHRP A-003B, Task 1.5a, Work Element a1.1, SHRP - A/IR - 90 -014.

RECOMMENDATIONS AND FUTURE WORK

Among the accomplishments of this research project was the development of a simple fluorometric technique based on optical microscopy to obtain repeatable and unique fluorescence intensity values from raw asphalts as well as from asphalt/aggregate mixtures. From this technique, relationships were established between fluorescence intensity and asphalt viscosity resulting from industrial processing (air-blowing), molecular structuring and setting characteristics, and laboratory aging (thin film oven test and pressure vessel aging). However, there was insufficient time and funding to fully develop the technique for practical field applications. Thus, to develop a better understanding of the chemistry of asphalt fluorescence and to complete the development of the analytical technique, we recommend the following areas for continued research in the area of asphalt fluorescence.

1. Investigation of model compounds and asphalt chemical fractions to develop a better understanding of the chemistry of asphalt fluorescence.

2. Study of the influence of aggregate particle size and the presence of moisture on the fluorescence intensity measurements through the evaluation of mastics.

3. Fluorometric analyses of roadway cores and/or environmentally stressed asphalt pavements.

4. Field trial of asphalt fluorometry applied during construction of new roadways. For practical purposes, a study based principally on Pennsylvania roads over a three-year (or longer) period would be ideal.

APPENDIX A

MICROSCOPE EQUIPMENT

All of the fluorometric and spectral fluorescence work conducted in this investigation was performed using two different Leitz MPV-II research microscopes. The base units and accessories for fluorescence photometry were purchased, built and assembled in-house over a ≈15 year period to serve a broad range of research topics. The following discussion reviews the particular characteristics of the microscope systems used in this project, discusses where improvements could be made specifically for application in asphalt science and technology, and attempts to provide approximate equipment costs for a system that could be used by a Department of Transportation laboratory for monitoring asphalt and pavement quality and deterioration.

A Leitz MPV-II microscope photometer system was used for both the fluorometric analysis of intensity at 600 nm as well as spectral distribution. As shown schematically in Figure A-1, in both systems light energy from either a ultra-high pressure xenon or mercury-arc passed through a heat filter (suppressing red and infrared wavelengths) and then through a series of interference filters which defined the appropriate excitation and measuring wavelengths. Analyses were performed using blue-light excitation with the Ploemopak 2 vertical illuminator fitted with an H2 filter combination (390-490 nm excitation; 510 nm dichromatic beam splitter; 515 nm long-pass barrier filter). The excitation light was reflected by a 510 nm reflection short-pass dichromatic beam splitter and condensed onto the sample through a 50X NPL FLUOTAR air objective. The total magnification of the optical system was 625 times. The light energy (both from fluorescence emission and some reflected excitation light) passed back through the dichromatic beam splitter, and a 515 nm long-pass barrier filter blocked any residual reflected excitation light. From this point, the measuring system becomes significantly different depending upon the desired measurement, i.e., intensity at a single wavelength or spectral distribution.

For measurement of intensity, the fluorescence emission passed through a measurement filter which was centered around 600 nm (570-630 nm). The optical signal(s) were transformed into electronic signals by an EMI 9558 photomultiplier and amplified. Once the photoelectric system was calibrated to a glass standard of stable fluorescence intensity (uranyl glass), a statistically adequate number of intensity readings were accumulated. For the measurement of relative intensity by wavelength (spectra), the fluorescence emissions were passed through a motor-driven Kratos GM200 double-grating monochromator with 20 nm bandwidth, and then to a RCA C31034A water-cooled photomultiplier for measurement. However, both wavelength and intensity must be calibrated over the range of visible light. Also, the spectra need to be corrected with respect to color temperature.

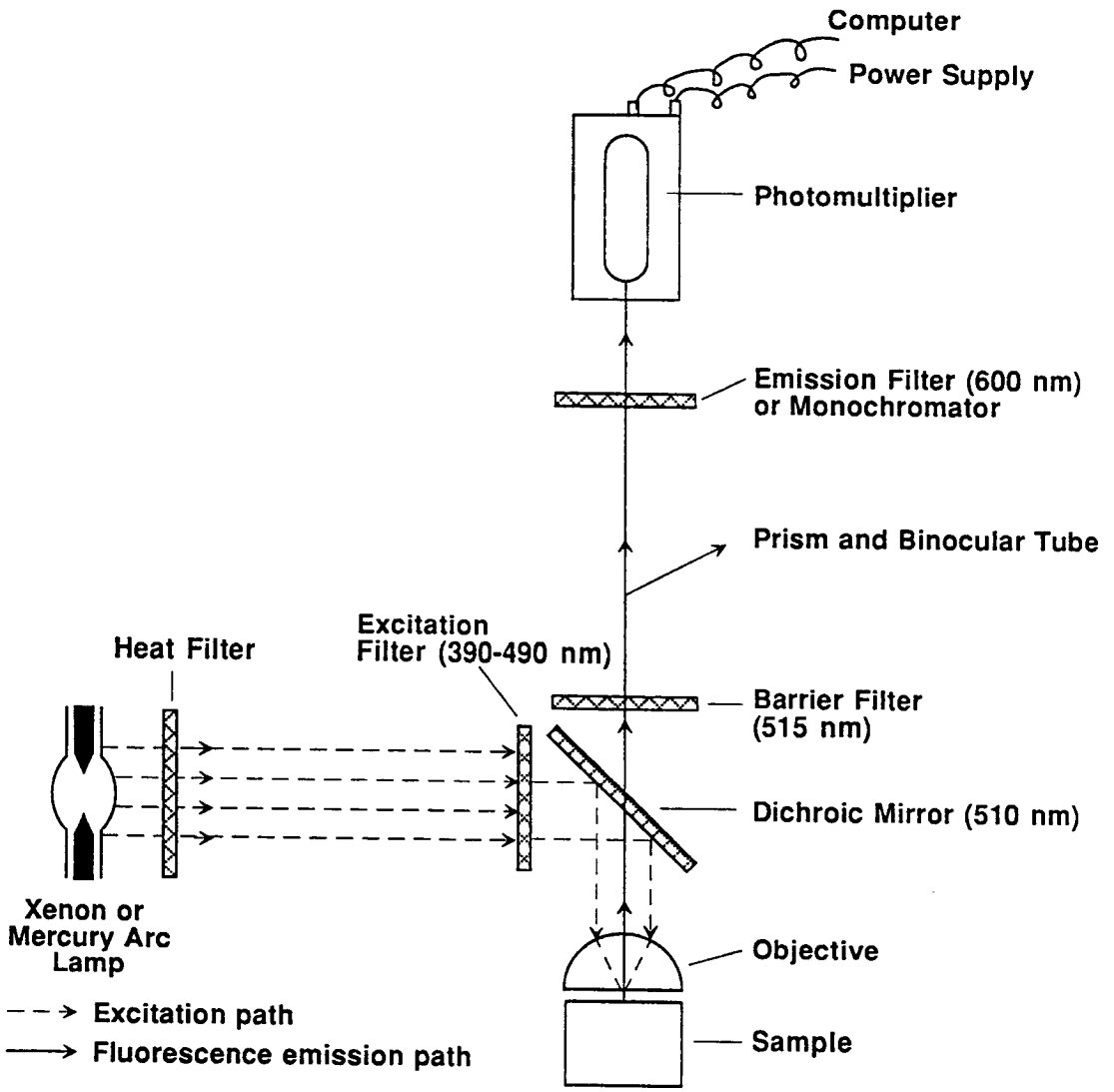

Figure A-1. Schematic of Microscopy System for Fluorescence Microphotometry

Aside from the filtering devices (interference or monochromator) different photomultipliers were employed. Figure A-2 compares the spectral response of the photocathodes from each system and shows that the RCA C31034A gives a more uniform and greater response in the range of visible light than the EMI 9558. However, what this figure fails to show is that the EMI 9558 photomultiplier has a stable dark current which is necessary for quantitative measurements of light intensity. The dark current of the RCA photomultiplier is more variable over time and thus can only provide a relative measure of intensity. This is the reason two different microscope systems were used for the different fluorescence measurements.

Measurement of fluorescence intensity at a single wavelength has many advantages compared with spectral analysis. Microscope systems with the proper requirements can be purchased for less than $60,000 directly from a microscope company. With a relatively small investment of time in writing software to streamline data manipulation, the system could be operational in as little as one month. Operation of the system could easily be handled by a technician (B.S. degree recommended) with a minimum of training. Including calibration of the system for each sample, analysis of a raw asphalt should require about 12 min, whereas pavement samples may each require 35-40 min. The software should report the mean fluorescence intensity and standard deviation.

On the other hand, measurement of spectral fluorescence may require a greater investment of money, time and effort. First, there are a number of microscope systems that can be purchased off the shelf to perform the analysis. Costs for these systems range from $70,000 and up. Secondly, there will be a much larger investment in time to write software that will adequately handle wavelength calibration, generation of color temperature correction algorithms, data collection and manipulation and graphical representation. Operation of the system should be handled by a dedicated professional (M.S. or Ph.D. degree). Calibration of the instrument may require 30 min at the beginning of each session and should be checked on a regular basis. Collection of spectral data (5 different areas) may require only 10 min per sample. Once the data manipulation software has been written, the normalized mean value of relative intensity at each wavelength should be plotted and used for comparative evaluation.

Based on these relative comparisons and the quality of data obtained from fluorometric analysis discussed in this report, we suggest that the fluorescence microscopy system developed for intensity measurements be employed for asphalt characterization.

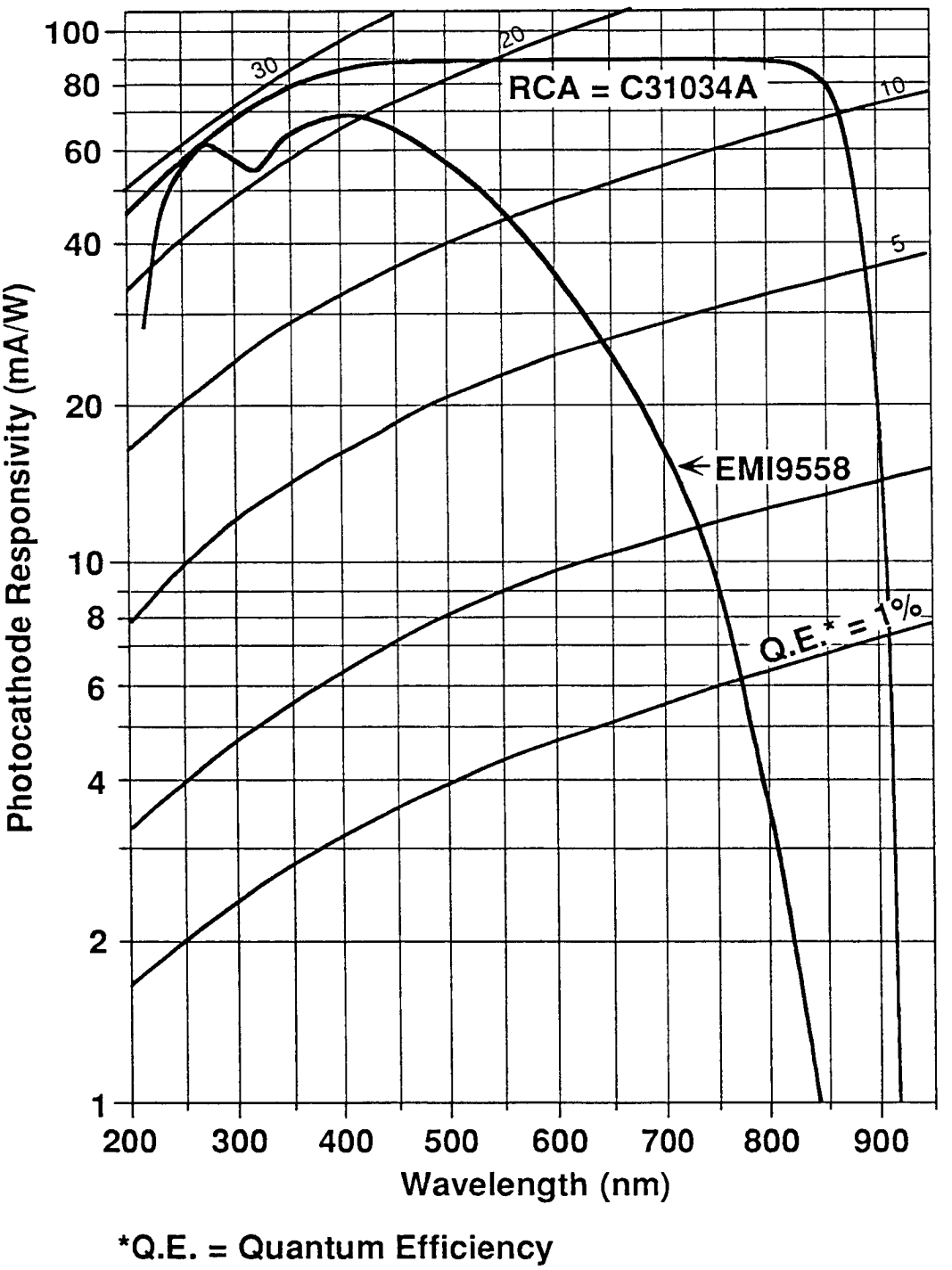

Figure A-2. Responsivity of Photomultipliers, RCA-C31034A Used for Spectral Fluorescence and EMI9558 Used for Fluorometric Analyses of Asphalt

Asphalt Advisory Committee

Chairman
Thomas D. Moreland
Moreland Altobelli Associates, Inc.

Vice Chairman
Gale C. Page
Florida Department of Transportation

Members

Peter A. Bellin
Niedersachsisches Landesamt fur Strassenbau

Dale Decker
National Asphalt Paving Association

Eric Harm
Illinois Department of Transportation

Charles Hughes
Virginia Highway & Transportation Research Council

Robert G. Jenkins
University of Cincinnati

Anthony J. Kriech
Heritage Group Company

Richard Langlois
Universite Laval

Richard C. Meininger
National Aggregates Association

Nicholas Nahas
EXXON Chemical Co.

Charles F. Potts
APAC, Inc.

Ron Reese
California Department of Transportation

Donald E. Shaw
Georgia-Pacific Corporation

Scott Shuler
The Asphalt Institute

Harold E. Smith
City of Des Moines

Thomas J. Snyder
Marathon Oil Company

Richard H. Sullivan
Minnesota Department of Transportation

Haleem A. Tahir
American Association of State Highway and Transportation Officials

Jack Telford
Oklahoma Department of Transportation

Liaisons

Avery D. Adcock
United States Air Force

Ted Ferragut
Federal Highway Administration

Donald G. Fohs
Federal Highway Administration

Fredrick D. Hejl
Transportation Research Board

Aston McLaughlin
Federal Aviation Administration

Bill Weseman
Federal Highway Administration